

ENVIRONMENTAL IMPACT MODELING of The TANGGUH LNG EXPANSION PROJECT

Prepared for

BP Berau Ltd.
October 9th, 2013

Prepared by

Environmental Resources Management
75 Valley Stream Parkway, Suite 200, Malvern, PA 19355

The World's Leading Sustainability Consultancy



TABLE OF CONTENTS

1	EXECUTIVE SUMMARY.....	1-1
2	DESCRIPTION OF STUDY AREA.....	2-1
3	SCOPE OF WORK.....	3-1
4	APPROACH.....	4-1
4.1	MODELLING METHODOLOGY	4-1
	4.1.1 Hydrodynamic Modelling.....	4-3
	4.1.2 Combined Wastewater and Hydrotest Water Discharge Modelling.....	4-4
	4.1.3 Cumulative Drilling Mud and Drill Cuttings Transport and Fate.....	4-4
	4.1.4 Dredge Material Disposal	4-5
4.2	GEMSS SUITE DESCRIPTION	4-5
	4.2.1 GEMSS-HDM.....	4-7
	4.2.2 GEMSS-UDC.....	4-8
	4.2.3 GEMSS-GIFT.....	4-9
4.3	CORMIX DESCRIPTION.....	4-9
4.4	ADDAMS SUITE DESCRIPTION	4-10
	4.4.1 DREDGE.....	4-10
	4.4.2 STFATE.....	4-10
5	HYDRODYNAMIC MODELLING.....	5-1
	5.1 SPATIAL DATA.....	5-1
	5.2 BOUNDARY DATA	5-3
	5.3 SCENARIO DESIGN.....	5-9
	5.4 MODEL CONFIRMATION	5-10
	5.5 GIFT MODEL SUBGRID	5-13
6	COMINGLED WASTEWATER DISCHARGE MODELLING.....	6-1
	6.1 SCENARIO DESIGN.....	6-1
	6.2 DISCHARGE INFORMATION	6-1
	6.3 NEAR - FIELD MODELLING.....	6-2
	6.4 FAR - FIELD MODELLING.....	6-7

	6.5	CONCLUSION	6-15
7		HYDROTEST WATER DISCHARGE MODELLING	7-1
	7.1	SCENARIO DESIGN.....	7-1
	7.2	DISCHARGE INFORMATION	7-1
	7.3	NEAR - FIELD MODELLING.....	7-3
	7.4	FAR - FIELD MODELLING.....	7-8
	7.5	CONCLUSION	7-14
8		COMINGLED WASTEWATER AND HYDROTEST WATER DISCHARGE MODELLING	8-1
	8.1	SCENARIO DESIGN.....	8-1
	8.2	RELEASE INFORMATION.....	8-1
	8.3	NEAR - FIELD MODELLING.....	8-1
	8.4	FAR - FIELD MODELLING.....	8-4
	8.5	CONCLUSION	8-7
9		DREDGE MODELLING	9-1
	9.1	ASSESSMENT CRITERIA	9-1
	9.2	SCENARIO DESIGN.....	9-2
	9.3	DREDGING AND SEDIMENT DATA.....	9-2
	9.4	NEAR - FIELD MODELLING.....	9-5
	9.5	FAR - FIELD MODELLING.....	9-9
	9.6	CONCLUSION	9-13
10		DREDGE DISPOSAL MODELLING	10-1
	10.1	SCENARIO DESIGN.....	10-1
	10.2	DISPOSAL AND SEDIMENT DATA.....	10-1
	10.3	NEAR - FIELD MODELLING.....	10-3
	10.4	FAR - FIELD MODELLING.....	10-15
	10.5	CONCLUSION	10-19
11		DRILLING MUD AND DRILL CUTTINGS MODELLING.....	11-1
	11.1	SCENARIO DESIGN.....	11-1
	11.2	DRILLING MUD AND DRILL CUTTINGS DATA	11-2
	11.3	FAR - FIELD MODELLING.....	11-4

11.3.1	Drilling at ROA	11-5
11.3.2	Drilling at TTB.....	11-9
11.3.3	Drilling at WDA.....	11-12
11.3.4	Drilling at UBA.....	11-16
11.4	CONCLUSION	11-20
12	ACRONYMS.....	12-1
13	REFERENCES.....	13-1

LIST OF TABLES

Table 2.1	Statistical Summaries of Temperature and Salinity Data Described in Section 5.2.....	2-4
Table 4.1	Inventory of Modelling Scenarios	4-2
Table 6.1	Individual Wastestreams and Their Flow Rate that form the Comingled Discharge.....	6-1
Table 6.2	Assumed Comingled Discharge Concentrations and Ambient Standard Concentrations	6-2
Table 6.3	The Predicted Downstream Distances from the Discharge Point Where Water Quality Standards are Achieved and the Corresponding Dilution Factors - Comingled Discharge from Jetty 1	6-3
Table 6.4	The Predicted Downstream Distances from the Discharge Point Where Water Quality Standards are Achieved and the Corresponding Dilution Factors - Comingled Discharge from Jetty 2	6-3
Table 6.5	Maximum Predicted Dry Season Ambient Concentrations Resulting from Comingled Discharge for Jetty 1	6-10
Table 6.6	Maximum Predicted Wet Season Ambient Concentrations Resulting from Comingled Discharge for Jetty 1	6-10
Table 6.7	Maximum Predicted Dry Season Ambient Concentrations Resulting from Comingled Discharge for Jetty 2	6-11
Table 6.8	Maximum Predicted Wet Season Ambient Concentrations Resulting from Comingled Discharge for Jetty 2	6-12
Table 6.9	Maximum Predicted Ambient Concentrations Resulting from Comingled Discharge using Median Discharge Concentrations.....	6-13
Table 6.10	Maximum Predicted Ambient Concentrations Resulting from Comingled Discharge Jetty 1 Depth Sensitivity	6-14
Table 7.1	Hydrotest Water Discharge Locations.....	7-2
Table 7.2	Hydrotest Water Discharge Concentrations	7-3
Table 7.3	Maximum Predicted Ambient Concentrations Resulting from Hydrotest Discharges	7-14
Table 8.1	Maximum Predicted Ambient Concentrations Resulting from Combined Hydrotest and Comingled Discharges at 50m and 100m.....	8-7
Table 9.1	Scenario List.....	9-2
Table 9.2	Discharge Characteristics.....	9-4

Table 9.3	Dredge Material Particle Size Distribution	9-4
Table 9.4	Dredge Material Density.....	9-5
Table 9.5	Input Parameters.....	9-5
Table 9.6	Velocity Averages for Four Tide Simulations.....	9-6
Table 9.7	Summary of Predicted Results for Dredging Operation Scenarios	9-14
Table 10.1	Scenario of Dredge Material Disposal	10-1
Table 10.2	Discharge Characteristics.....	10-2
Table 10.3	Current Components at a Depth of 10 ft at the East Disposal Site	10-3
Table 10.4	Dimensions and Position of the Silt and Clay Clouds on the Bottom.....	10-4
Table 10.5	Summary of Predicted Results for Dredging Operation Scenarios	10-19
Table 11.1	Scenario List.....	11-2
Table 11.2	Discharge Characteristics.....	11-3
Table 11.3	Drill Cuttings and Muds Particle Size Distribution.....	11-4
Table 11.4	Drill Cuttings and Muds Densities.....	11-4
Table 11.5	Summary of Predicted Results for All Drilling Operation Scenarios....	11-20

LIST OF FIGURES

Figure 2.1	Map of Region around Tangguh LNG	2-1
Figure 2.2	Wind Roses Determined from Measurements Taken at Tanah Merah ..	2-3
Figure 2.3	Scatter Graph of Current Speed (cm/s) and Direction Observed at the Ocean Tower Site	2-5
Figure 2.4	Time Series of Current Speed and Direction Observed at the Ocean Tower Site.....	2-6
Figure 3.1	Map of Berau/ Bintuni Bay with Tangguh LNG Plant and Proposed Drilling, Hydrotest Discharge, and Dredge Disposal Sites Included in the Present Modelling	3-2
Figure 3.2	Map of Tangguh LNG Plant with Port Structures, Outfall Locations, and Dredge Location Included in Modelling.....	3-3
Figure 4.1	GEMSS Modules: First Set.....	4-6
Figure 4.2	GEMSS Modules: Second Set.....	4-7
Figure 5.1	Hydrodynamic Model Grid with Bottom Elevations for Berau/ Bintuni Bay	5-2
Figure 5.2	Hydrodynamic Model Grid with Bottom Elevations in the Vicinity of the Tangguh LNG Terminal.....	5-3
Figure 5.3	Tidally-driven Elevation Applied at the Model’s Western Boundary in the Dry and Wet Periods.....	5-4
Figure 5.4	Wind Roses Determined from Measurements Taken at Tanah Merah in 2011 during the Dry (Left) and Wet (Right) Model Periods	5-5
Figure 5.5	Dry Bulb Air Temperature, Dew Point Temperature, Air Pressure, Relative Humidity, and Solar Radiation at Tanah Merah during the Dry Model Period.....	5-6
Figure 5.6	Dry Bulb Air Temperature, Dew Point Temperature, Air Pressure, Relative Humidity, and Solar Radiation at Tanah Merah during the Wet Model Period	5-7
Figure 5.7	Vertical Profile Station Locations	5-8
Figure 5.8	Profiles of Temperature from Dry and Wet Seasons for Eight Stations Used for Model Input	5-8
Figure 5.9	Profiles of Salinity from Dry and Wet Seasons for Eight Stations used for Model Input.....	5-9

Figure 5.10	Water Surface Elevation Comparison between Model and Data for Dry Scenario.....	5-10
Figure 5.11	Water Surface Elevation Comparison between Model and Data for Wet Scenario.....	5-11
Figure 5.12	Salinity Profile Confirmation with Data for Wet Period	5-12
Figure 5.13	Temperature Profile Confirmation with Data for Wet Period.....	5-12
Figure 5.14	Salinity Profile Confirmation with Data for Dry Period.....	5-13
Figure 5.15	Temperature Profile Confirmation with Data for Dry Period	5-13
Figure 6.1	Dilution Factor with Downstream Distance - Comingled Discharge from Jetty 1 at High Tide.....	6-4
Figure 6.2	Dilution Factor with Downstream Distance - Comingled Discharge from Jetty 1 at Low Tide.....	6-4
Figure 6.3	Dilution Factor with Downstream Distance - Comingled Discharge from Jetty 2 at High Tide.....	6-5
Figure 6.4	Dilution Factor with Downstream Distance - Comingled Discharge from Jetty 2 at Low Tide.....	6-5
Figure 6.5	Dry Season Contour Plot of Comingled Jetty 1 Discharge Minimum Dilution Factor.....	6-7
Figure 6.6	Wet Season Contour Plot of Comingled Jetty 1 Discharge Minimum Dilution Factor.....	6-8
Figure 6.7	Dry Season Contour Plot of Comingled Jetty 2 Discharge Minimum Dilution Factor.....	6-9
Figure 6.8	Wet Season Contour Plot of Comingled Jetty 2 Discharge Minimum Dilution Factor.....	6-9
Figure 6.9	Contour Plot of Comingled Jetty 1 Discharge Minimum Dilution Factor Sensitivity (-6 m Discharge).....	6-14
Figure 7.1	Dry Period Surface Current Speed at Jetty 1 with Discharge Durations Shown.....	7-2
Figure 7.2	Wet Period Surface Current Speed at Jetty 1 with Discharge Durations Shown.....	7-2
Figure 7.3	Dilution Factor with Downstream Distance - Hydrotest Water Discharge from ROA at High Tide	7-4
Figure 7.4	Dilution Factor with Downstream Distance - Hydrotest Water Discharge from ROA at Low Tide	7-5

Figure 7.5	Dilution Factor with Downstream Distance – Hydrotest Water Discharge from WDA at High Tide	7-5
Figure 7.6	Dilution Factor with Downstream Distance – Hydrotest Water Discharge from WDA at Low Tide	7-6
Figure 7.7	Dilution Factor with Downstream Distance – Hydrotest Water Discharge from VRF at High Tide	7-6
Figure 7.8	Dilution Factor with Downstream Distance – Hydrotest Water Discharge from VRF at Low Tide.....	7-7
Figure 7.9	Dilution Factor with Downstream Distance – Hydrotest Water Discharge from UBA at High Tide.....	7-7
Figure 7.10	Dilution Factor with Downstream Distance – Hydrotest Water Discharge from UBA at Low Tide.....	7-8
Figure 7.11	Dry Season Contour Plot of Hydrotest ROA Discharge Minimum Dilution Factor	7-9
Figure 7.12	Wet Season Contour Plot of Hydrotest ROA Discharge Minimum Dilution Factor	7-10
Figure 7.13	Dry Season Contour Plot of Hydrotest WDA Discharge Minimum Dilution Factor	7-11
Figure 7.14	Wet Season Contour Plot of Hydrotest WDA Discharge Minimum Dilution Factor	7-11
Figure 7.15	Dry Season Contour Plot of Hydrotest VRF Discharge Minimum Dilution Factor	7-12
Figure 7.16	Wet Season Contour Plot of Hydrotest VRF Discharge Minimum Dilution Factor	7-12
Figure 7.17	Dry Season Contour Plot of Hydrotest UBA Discharge Minimum Dilution Factor	7-13
Figure 7.18	Wet Season Contour Plot of Hydrotest UBA Discharge Minimum Dilution Factor	7-13
Figure 8.1	Dilution Factor with Downstream Distance – Hydrotest Water Discharge from Jetty 1 at High Tide	8-2
Figure 8.2	Dilution Factor with Downstream Distance –Hydrotest Water Discharge from Jetty 1 at Low Tide	8-2
Figure 8.3	Dilution Factor with Downstream Distance –Hydrotest Water Discharge from Jetty 2 at High Tide	8-3
Figure 8.4	Dilution Factor with Downstream Distance –Hydrotest Water Discharge from Jetty 2 at Low Tide	8-3

Figure 8.5	Dry Season Contour Plot of Combined Hydrotest and Comingled Jetty 1 Discharge Minimum Dilution Factor	8-5
Figure 8.6	Wet Season Contour Plot of Combined Hydrotest and Comingled Jetty 1 Discharge Minimum Dilution Factor	8-5
Figure 8.7	Dry Season Contour Plot of Combined Hydrotest and Comingled Jetty 2 Discharge Minimum Dilution Factor	8-6
Figure 8.8	Wet Season Contour Plot of Combined Hydrotest and Comingled Jetty 2 Discharge Minimum Dilution Factor	8-7
Figure 9.1	Dredge Grid with Subgrids to Represent Complex Shorelines and Structures. Structure Shown in this Grid is the Bulk Offloading Facility.....	9-3
Figure 9.2	Sample Screenshots of the Adaptive TSS Grid for Two Different Times	9-4
Figure 9.3	Centerline TSS Concentration Versus Downstream Distance in Each Simulation.....	9-7
Figure 9.4	TSS Concentration (mg/L) Contours for High Tide	9-7
Figure 9.5	TSS Concentration (mg/L) Contours for High Slack Tide	9-8
Figure 9.6	TSS Concentration (mg/L) Contours for Low Tide	9-8
Figure 9.7	TSS Concentration (mg/L) Contours for Low Slack Tide	9-9
Figure 9.8	Maximum Incremental TSS Concentrations during Dredging at BOF under Dry Season Conditions.....	9-10
Figure 9.9	Maximum Sedimentation Rate during Dredging at BOF under Dry Season Conditions	9-11
Figure 9.10	Maximum Sediment Thickness during Dredging at BOF under Dry Season Conditions	9-11
Figure 9.11	Maximum Incremental TSS Concentration during Dredging at BOF Under Wet Season Conditions	9-12
Figure 9.12	Maximum Sedimentation Rate during Dredging at BOF under Wet Season Conditions	9-12
Figure 9.13	Maximum Sediment Thickness during Dredging at BOF under Wet Season Conditions	9-13
Figure 10.1	Dredge Grid with Used to Model the Fate and Transport of Dredge Disposal	10-2
Figure 10.2	Maximum Seabed Deposition Thickness at the High Tide	10-5
Figure 10.3	Maximum Seabed Deposition Thickness at the High Slack Tide.....	10-5

Figure 10.4	Maximum Seabed Deposition Thickness at the Low Tide	10-6
Figure 10.5	Maximum Seabed Deposition Thickness at the Low Slack Tide	10-6
Figure 10.6	Plan View of the Maximum Silt and Clay Particle Concentrations (mg/L) at the Sea Bottom at Hours 1 and 4 Resulting from a Single Release - High Tide Stage	10-8
Figure 10.7	Plan View of the Maximum Silt and Clay Particle Concentrations (mg/L) at the Sea Bottom at Hours 1 and 4 Resulting from a Single Release - High Slack Tide Stage	10-10
Figure 10.8	Plan View of the Maximum Silt and Clay Particle Concentrations (mg/L) at the Sea Bottom at Hours 1 and 4 Resulting from a Single Release - Low Tide Stage	10-12
Figure 10.9	Plan View of the Maximum Silt and Clay Particle Concentrations (mg/L) at the Sea Bottom at Hours 1 and 4 Resulting from a Single Release - Low Slack Tide Stage	10-14
Figure 10.10	Maximum Incremental TSS during Dredge Disposal at the East Disposal Site under Dry Season Conditions	10-16
Figure 10.11	Maximum Sedimentation Rate during Dredge Disposal at the East Disposal Site under Dry Season Conditions	10-16
Figure 10.12	Maximum Sediment Thickness during Dredge Disposal at the East Disposal Site under Dry Season Conditions	10-17
Figure 10.13	Maximum Incremental TSS during Dredge Disposal at the East Disposal Site under Wet Season Conditions	10-17
Figure 10.14	Maximum Sedimentation Rate during Dredge Disposal at the East Disposal Site under Wet Season Conditions	10-18
Figure 10.15	Maximum Sediment Thickness during Dredge Disposal at the East Disposal Site under Wet Season Conditions	10-18
Figure 11.1	Sedimentation and Depositional Thickness Grid	11-3
Figure 11.2	Maximum Incremental TSS Concentrations during Drilling at ROA under Wet Season Conditions	11-6
Figure 11.3	Maximum Sedimentation Rate during Drilling at ROA under Wet Season Conditions	11-6
Figure 11.4	Maximum Sediment Thickness during Drilling at ROA under Wet Season Conditions	11-7
Figure 11.5	Maximum Incremental TSS Concentrations during Drilling at ROA under Dry Season Conditions	11-7

Figure 11.6	Maximum Sedimentation Rate during Drilling at ROA under Dry Season Conditions	11-8
Figure 11.7	Maximum Sediment Thickness during Drilling at ROA under Dry Season Conditions	11-8
Figure 11.8	Maximum Incremental TSS Concentrations during Drilling at TTB under Wet Season Conditions	11-9
Figure 11.9	Maximum Sedimentation Rate during Drilling at TTB under Wet Season Conditions	11-10
Figure 11.10	Maximum Sediment Thickness during Drilling at TTB under Wet Season Conditions	11-10
Figure 11.11	Maximum Incremental TSS Concentrations during Drilling at TTB under Dry Season Conditions	11-11
Figure 11.12	Maximum Sedimentation Rate during Drilling at TTB under Dry Season Conditions	11-11
Figure 11.13	Maximum Sediment Thickness during Drilling at TTB under Dry Season Conditions	11-12
Figure 11.14	Maximum Incremental TSS Concentrations during Drilling at WDA under Wet Season Conditions	11-13
Figure 11.15	Maximum Sedimentation Rate during Drilling at WDA under Wet Season Conditions	11-14
Figure 11.16	Maximum Sediment Thickness during Drilling at WDA under Wet Season Conditions	11-14
Figure 11.17	Maximum Incremental TSS Concentrations during Drilling at WDA under Dry Season Conditions	11-15
Figure 11.18	Maximum Sedimentation Rate during Drilling at WDA under Dry Season Conditions	11-15
Figure 11.19	Maximum Sediment Thickness during Drilling at WDA under Dry Season Conditions	11-16
Figure 11.20	Maximum Incremental TSS Concentrations during Drilling at UBA under Wet Season Conditions	11-17
Figure 11.21	Maximum Sedimentation Rate during Drilling at UBA under Wet Season Conditions	11-17
Figure 11.22	Maximum Sediment Thickness during Drilling at UBA under Wet Season Conditions	11-18
Figure 11.23	Maximum Incremental TSS Concentrations during Drilling at UBA under Dry Season Conditions	11-18

Figure 11.24 Maximum Sedimentation Rate during Drilling at UBA under Dry Season Conditions 11-19

Figure 11.25 Maximum Sediment Thickness during Drilling at UBA under Dry Season Conditions 11-19

Figure 11.26 Maximum TSS Concentration at UBA under Wet Season Drilling..... 11-21

BP Indonesia has assigned ERM to conduct a study on the environmental impact of the Tangguh LNG Expansion Project in Teluk Bintuni and Fakfak District, West Papua Province. BP and its business partners (“Tangguh LNG”) plans to expand its operations with development of LNG Train 3 and future development of which includes LNG Train and its supporting facilities.

Tangguh LNG facility is located on the southern shore of Bintuni Bay waters in Teluk Bintuni Regency, West Papua Province. This report covers the modelling studies conducted as part of the overall environmental impact study to evaluate the fate and transport of the discharge of a wide range of surface water and their impact on aquatic and benthic populations in Bintuni Bay waters.

The evaluation of impacts on surface waters was done using a comprehensive modelling approach which relies on a single modelling system, GEMSS®. Various modules in GEMSS were used to estimate the transport and fate of combined wastewater, hydrotest water, drill muds and cuttings, and suspended sediment from dredging and dredged material disposal. Cumulative impacts throughout Bintuni Bay were addressed by using both near- and far-field calculations.

Various contaminants of concern from the combined waste stream were evaluated through comparison to ambient and near-field standards taking baseline conditions into account. The results of the modelling indicated that the waste stream has the potential to violate ambient water quality standards for some constituents including ammonia, chromium, copper, DO, lead, and zinc. However, for chromium, copper and lead, this prediction was primarily an artefact of the high limit detection of the waste stream sampling data. Additionally, extreme conservatism was applied by choosing maximum possible discharge concentrations combined with no water loss due to decay or consumption. It was found that lower concentrations can be achieved by moving the outfall to Jetty 2. Various other options such as moving the discharge away from the seabed to mid-depth or away from the shore into deeper waters can achieve similar reductions. Overall the comingled release has low potential of causing any impacts to the aquatic community. Ambient standards are either met within a few hundred meters of the discharge or can be met by adopting one of the suggested alternatives.

Release of hydrotest water treated with biocide, oxygen scavenger, and fluorescein tracer was evaluated using a similar modelling approach. Since no ambient standards exists for these chemicals, qualitative evaluation based on predicted concentrations and the extent of the plume was done. The modelling indicated that hydrotest water release will result in very low concentrations of chemical additives. It was found that the timing (i.e. tidal stage) of the discharge has a large effect on the trajectory of the plume suggesting that, if potential receptors exists nearby, timing the discharge could mitigate impacts to these receptors.

Dredging planned around the various marine facilities (combo dock, bulk offloading facility and Jetty 2) was modelled to evaluate the resulting incremental TSS, sedimentation rate and the sediment thickness. Dredging operations at the bulk offloading facility, which requires the removal of the largest volume of sediment, was selected for analysis along with the related disposal of further offshore operations. The results of the modelling indicated that the deposition of dredge operation-related sediments only occurs in the vicinity of the release location, mostly within 500 m of dredge location and within 10 km of the disposal location. The maximum incremental TSS was predicted to be only 11.8 mg/L for dredging operation and 5.5 mg/L for disposal. The maximum TSS baseline during dry period was 27 mg/L which when added to the maximum incremental TSS results in a TSS value of 38.8 mg/L and 32.5 mg/L, well below the ambient seawater quality standard for mangrove-lined water bodies of 80 mg/L. These predicted results show that the proposed dredging and disposal operations are unlikely to result in exceedance of applicable environmental standards or to create any significant impacts.

The drilling activities related to the proposed integrated activity of the Tangguh LNG Expansion Project were modelled to estimate the possible increase in TSS and sedimentation due to drilling at four well sites (Wiriagar, Roabiba, Ofaweri and Vorwata). The modelling indicated that the deposition of drill cuttings and muds only occurs in the vicinity of the drilling location, mostly within 150 m. The maximum incremental TSS was predicted to be only 1.9 mg/L. The maximum baseline TSS during the dry period is 27 mg/L which when added to the incremental maximum TSS due to drilling results in a TSS value of 28.9 mg/L, again well below the ambient seawater quality standard for mangrove-lined water bodies of 80 mg/L. These predicted results show that the proposed drilling operations are unlikely to result in exceedance of applicable environmental standards or to create any significant impacts.

Overall, the Tangguh LNG Expansion Project has low likelihood of causing any impact to the aquatic and benthic community within Bintuni Bay. The modelling study presents some constituents that may be of concern. Suggested mitigating measures and additional sampling can alleviate these concerns.

DESCRIPTION OF STUDY AREA

The Tangguh LNG facility is located at 2° 26' S, 133° 8' E at Tanah Merah village on the northshore of the Bomberai Peninsula of West Papua (**Figure 2.1**). The facility is at the southern edge of the connection between Berau Bay (to the west) and Bintuni Bay (to the east). Background descriptions of the region around the facility relevant to hydrodynamic, discharge, drill, and dredge modelling have been provided in previous reports. The most complete description is in the Tangguh LNG ANDAL report (henceforth referred to as ANDAL) prepared by Pertamina and BP during the facility planning phase (Pertamina, 2002). Other relevant reports include “Summary Environmental Impact Assessment: Tangguh LNG Project in Indonesia” (Asian Development Bank, 2005) and “Drill Cutting and Mud Dispersion Simulation: Final Report” (ITB, 2012).

While there is year-to-year variability (and the possibility of trends) in some of the processes affecting the hydrodynamics near the facility, hydrodynamics in Berau/Bintuni Bay is primarily determined by cyclic processes: tides and seasonal monsoon winds, rainfall, and stream runoff. The information provided in the previous reports is still relevant, and can be relied upon providing the summary description of the study area. While some independent published research relevant to hydrodynamics is available for the broader region around western New Guinea, none is available for Berau/Bintuni Bay; the reports related to the Tangguh development are the best sources because of the site-specific nature of these studies.

The following is a summary of the background information available in the Tangguh development reports.



Figure 2.1 Map of Region around Tangguh LNG

From ANDAL

Berau Bay opens up to the Ceram Sea at its western end at 132° 19' E. At this point the north-south width is 42 km. The bay narrows toward the east, and the shortest distance across the bay is 22 km at 133° 13' E. Berau/Bintuni Bay is elongated in the east-west direction, is 164 km long at 2° 20' S, and separates the Bird's Head Peninsula from the rest of West Papua. The deepest part of the bay is along a SW-NE axis where the bottom depth east of 132° 19' E reaches 80 m (see **Figure 5.1**). Near Tangguh LNG, the deeper bottom depths are on the north side of the bay.

The area surrounding the bay can be divided into three physiographic regions: North Plain (Bird's Head Peninsula), Bomberai Plain (Peninsula), and Onin Peninsula. The north shore has extensive swamps. The Bomberai Plain (also known as the South Plain) consists of low-lying coastal alluvial plain and savannah with interspersed low-lying bedrock hills. South of Tangguh LNG, the terrain is flat to gently undulating, with several low east-west trending ridges extending to 50 m above sea level. Farther east, extending around the eastern and southern perimeter of Bintuni Bay, swamps are present on a variety of islands and promontories, and are separated by estuarine channels. The Onin Peninsula has steep slopes close to Berau Bay and rugged peaks with elevations reaching 1619 m.

Numerous rivers flow into the bay from the northern, eastern, and southern directions. The Kamundan, Weriagar, Sebyar, and Tembuni are the four major rivers that enter the north side of the bay; they have annual average flow rates of 380, 175, 355, and 185 m³/s, respectively. The Bedidi and Bomberai are the two major rivers that enter the south side of the bay; they each have annual average flow rates of about 100 m³/s. The main rivers near the facility are the Manggosa, which forms the eastern boundary of the Tangguh LNG site, and the Saengga, which parallels the western LNG boundary, about 1.5 km to the west. Drainage from the Tangguh LNG facility is predominantly to the Saengga via several intermittent, westward-flowing streams.

West Papua has a tropical climate characterized by high temperature and humidity throughout the year. There are seasonal monsoons; the southeast (SE) monsoon (dry season) extends from June to October, and the northwest (NW) monsoon (wet season) extends from December to March. During the last decade at Tanah Merah dry season winds have been from the north (350° most probable) and during the wet season have been from the east (90° most probable) (**Figure 2.2**). The monsoon winds are the main contributors to winds during the entire year. There is some diurnal variation in the winds at the coastline. During the NW monsoon, the monsoon winds are stronger from late evening to early morning, while in the afternoon they reverse and are light. During the SE monsoon, the winds are stronger in the afternoon, while in the morning they reverse and are light. July and August (dry season) tend to be the coolest months, and November to March (wet season) tend to be the warmest months. Temperature variations in the region depend more on altitude than on geographical location. There

is considerable year-to-year variation in precipitation. Rainfall totals exceed 3,000 mm in an average year, distributed among all months, with February the wettest, and August–September the driest (Asian Development Bank, 2005). It is difficult to verify the seasonality of rainfall in Berau/Bintuni Bay as precipitation data from the bay are not immediately available. Seasonal variations in the nearshore environment are expected to occur as a result of differences in rainfall and river runoff between the dry and wet seasons.

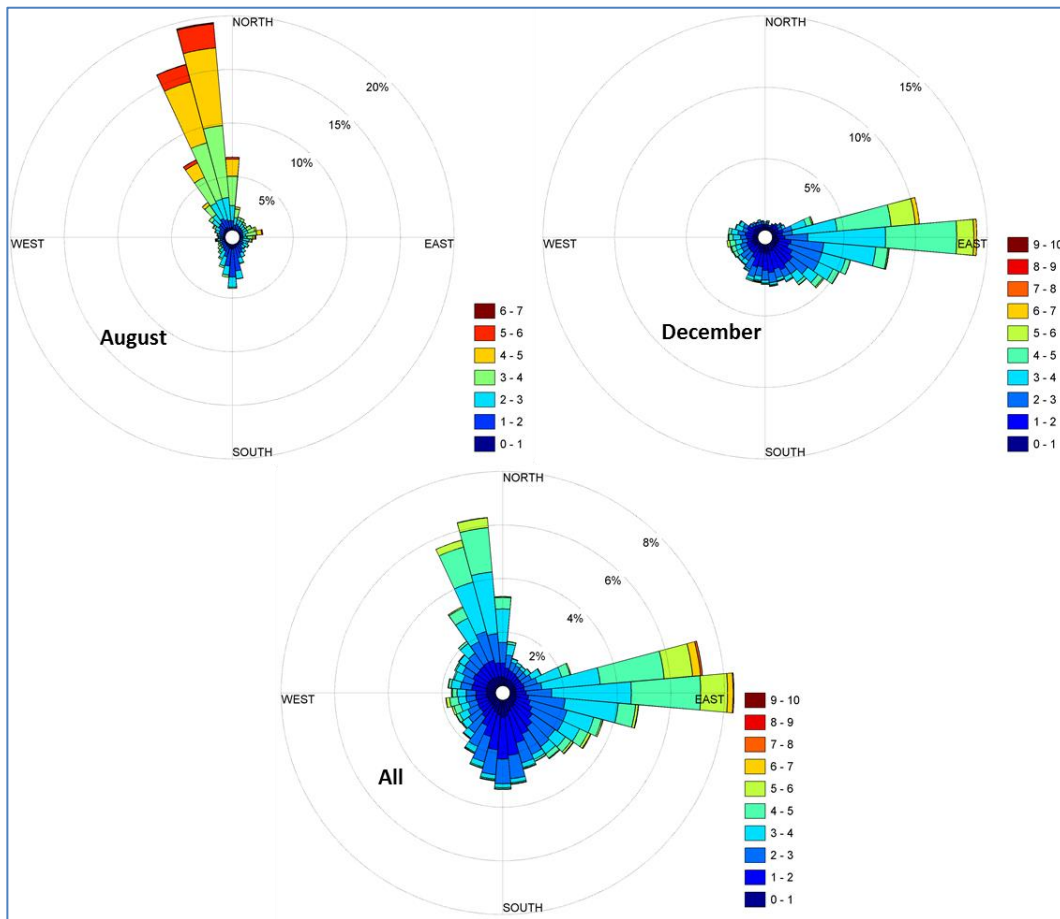


Figure 2.2 Wind Roses Determined from Measurements Taken at Tanah Merah

Data collected from 2002–2011 during August (left), December (centre), and all months (right). Colours indicate wind speed ranges in units of m/s and wind blows from directions shown.

Because Berau/Bintuni Bay is confined on three sides with a limited connection to the Ceram Sea and receives significant freshwater river input, it functions as an estuary. Estuaries are characterized by salinity gradients in the longitudinal or vertical directions with flow fields dominated by tides, wind, and freshwater inflows. In addition, estuaries typically have upstream shallow regions that grade to deep ocean boundary cross-sections.

Profiles of temperature (T) and salinity (S) acquired in 2012–2013 (described in Section 5.2) provide some recent information about the range of these properties in the bay. Water temperatures are higher during the wet season, when air temperature, rainfall, and river runoff are greater (**Table 2.1**). Temperature has noticeable depth dependence in both the dry and wet seasons, extending deeper in the wet season (**Figure 5.8**). The wet season has fresher water, especially in the eastern bay and close to rivers (**Table 2.1**). The depth dependence of salinity is more prominent during the wet season, and the fresh water contribution most evident at the shallowest depths (**Figure 5.9**).

Table 2.1 *Statistical Summaries of Temperature and Salinity Data Described in Section 5.2*

	Dry Season	Wet Season
Minimum T (°C)	27.2	29.3
25 th Percentile T (°C)	28.2	30.1
50 th Percentile T (°C)	28.4	30.2
75 th Percentile T (°C)	28.6	30.3
Maximum T (°C)	31.0	32.4
Minimum S	19.4	19.1
25 th Percentile S	29.6	27.6
50 th Percentile S	29.9	28.9
75 th Percentile S	30.5	30.1
Maximum S	32.1	31.9

Currents in Berau/Bintuni Bay are dominated by tides, as can clearly be seen at the Tangguh LNG facility (**Figure 2.3** and **Figure 2.4**). Here the largest mid-water depth speed is 1.6–1.8 m/s and the current direction is along-shore. The tidal currents are largely semidiurnal (two highs and two lows per day), but are modified by diurnal contributions. The largest tidal constituents are M_2 , S_2 , and N_2 and K_1 and O_1 . In deeper water in the central bay, currents are strongest near the surface and decrease toward the bottom, and seasonal variations are small compared to the tides (ANDAL).

Surface waves in Berau/Bintuni Bay display directions consistent with those of the monsoon winds. The wave extremes are not great compared to other parts of the world. A significant wave height of 1 m has a non-exceedance probability of 99.7% (ITB, 2012). Most of Berau/Bintuni Bay is well protected from large deep water ocean swells because of the limited exposure to the Ceram Sea and the open ocean.

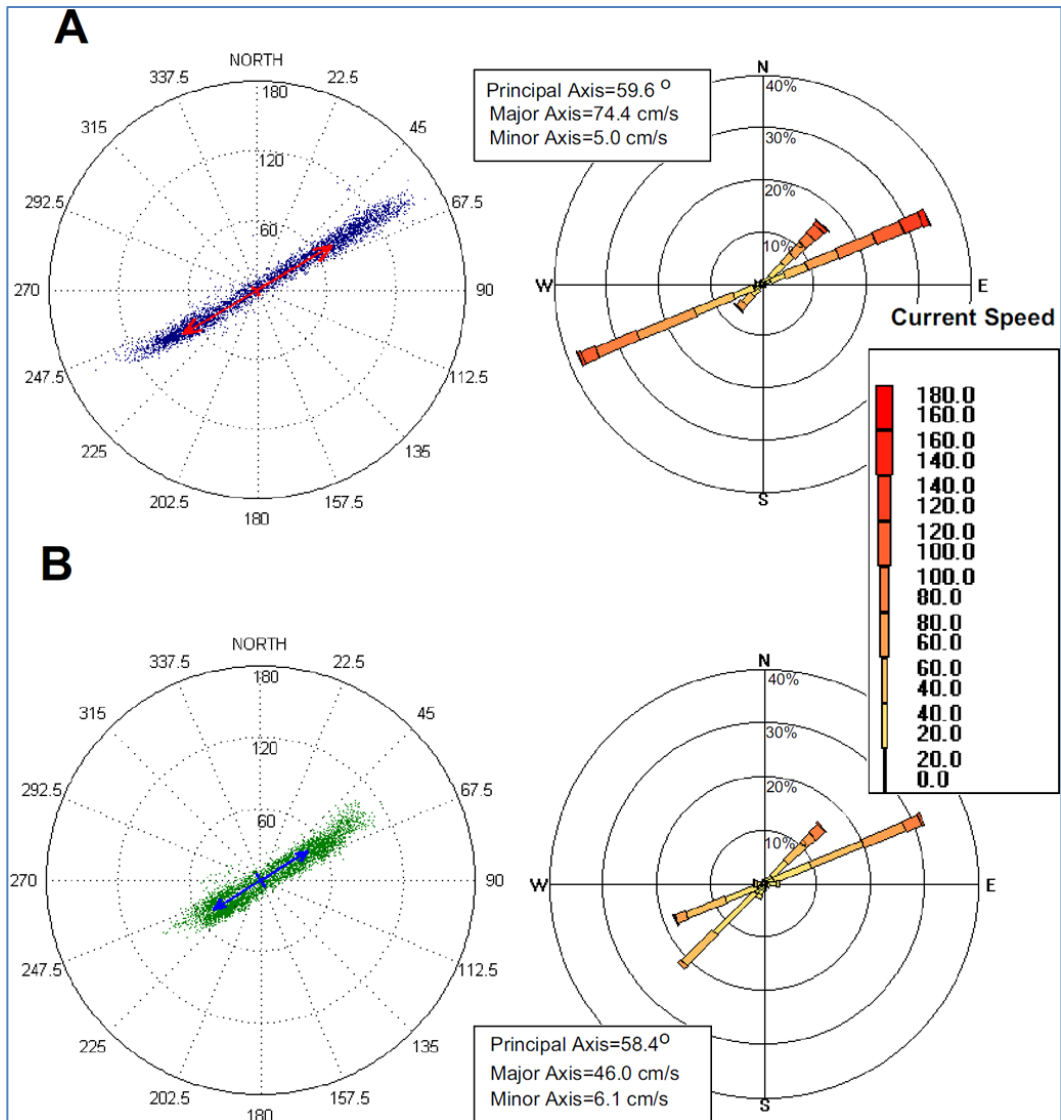


Figure 2.3 Scatter Graph of Current Speed (cm/s) and Direction Observed at the Ocean Tower Site

Data collected near Tanah Merah from 1999-12-07 to 2000-03-03 at A) mid-water (5.5 m above seabed) and B) near-bottom (0.5 m above seabed). From ANDAL.

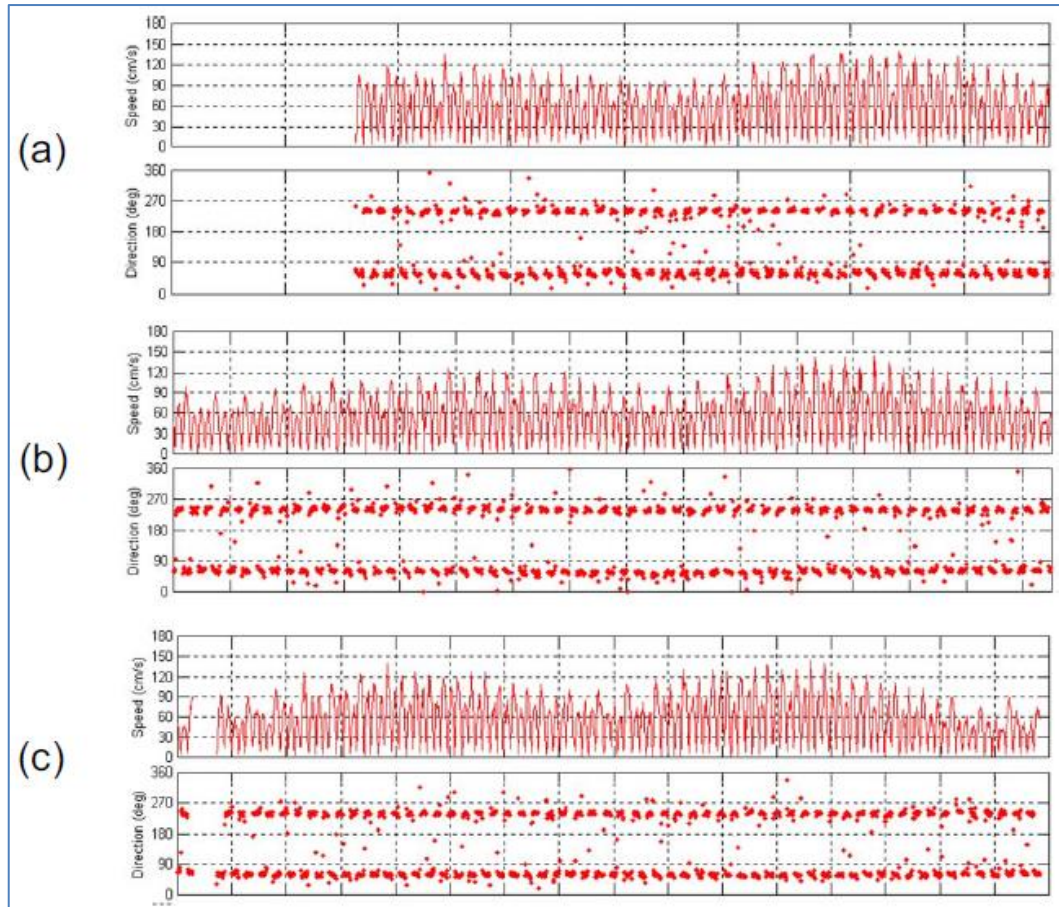


Figure 2.4 *Time Series of Current Speed and Direction Observed at the Ocean Tower Site*

Data collected at mid-water (5.5 m above seabed) from a) 1999-12-07 to 1999-12-31, b) 2000-01-01 to 2000-01-31, and c) 2000-02-01 to 2000-03-03. From ANDAL.

SCOPE OF WORK

The scope of the work presented here includes several modelling studies to characterize the environmental effects on surface waters from the Tangguh LNG Expansion Project in Bintuni Bay. The activities associated with the expansion that are assessed through modelling include:

- Comingled discharges from the LNG facility
- Pipeline hydrotest water discharges
- LNG port dredging and dredged material disposal
- Drilling mud and cuttings discharges

The LNG facility discharges include the combined waste stream from several sources including:

- Produced water
- Desalinization water (brine water reject)
- Treated sewage
- Treatment pit water
 - Neutralization pit
 - Oily pit

Various contaminants of concern from the combined waste stream are modelled and evaluated through comparison to ambient and near-field standards taking baseline conditions into account. Contaminants selected for comparison are those which have existing seawater ambient or near-field water quality standards and have measured waste stream concentrations that exceed applicable standards. Additionally, the LNG plant discharges are evaluated at two locations within the terminal port to assess optimal outfall operation. **Figure 3.2** shows the LNG terminal port structures and the location of the two proposed outfalls.

Hydrotesting involves flushing the pipelines with freshwater treated with biocide, oxygen scavenger, and fluorescein tracer. Discharges of hydrotest water are evaluated by modelling these additives to estimate ambient concentrations. While no ambient standards currently exist for these chemicals, qualitative evaluation will be based on estimated concentrations and the extent of the concentration field. Discharge from four offshore development locations (two platforms in the initial stage development and two platforms in the future development) as well as from the two marine facilities locations (comingled with the LNG discharge) are modelled. **Figure 3.1** shows the four offshore locations (UBA, ROA, WDA, and VRF) and **Figure 3.2** shows two outfalls locations at the marine facilities.

Initial and maintenance dredging around various port facilities are part of the Tangguh LNG Expansion Project. These include the existing Combo Dock and BOF as well as the proposed LNG jetty (Jetty 2). Solids released to the water as a consequence of dredge resuspension are modelled for one representative location. Evaluation is based on comparison of predicted TSS, including baseline TSS, to ambient standards. The depositional footprint on the sediment bed is also calculated. **Figure 3.2** shows the location around the BOF used for dredge modelling.

Disposal of this dredge material is planned to occur at two sites in deeper areas offshore. Solids released to the water as a consequence of dredge disposal are modelled for one representative disposal location. Similar to dredge modelling, evaluation is based on comparison of predicted TSS to ambient standards and the extent of the depositional footprint. **Figure 3.1** shows the East Disposal Site used in modelling.

Wells at numerous sites within Bintuni Bay are being considered as part of Tangguh LNG Expansion Project. These include sites within the Wiriagar, Roabiba, Ofaweri, Vorwata, and Ubadari Fields as well as Teteruga Prospect. Four of these sites are modelled to predict the TSS and bed depositional footprint of drill cuttings and drilling mud. Modelling covers the full duration of drilling activities at each well. **Figure 3.1** shows the four wells (UBA, WDA, ROA, and TTB) considered in the drill cuttings and mud modelling.

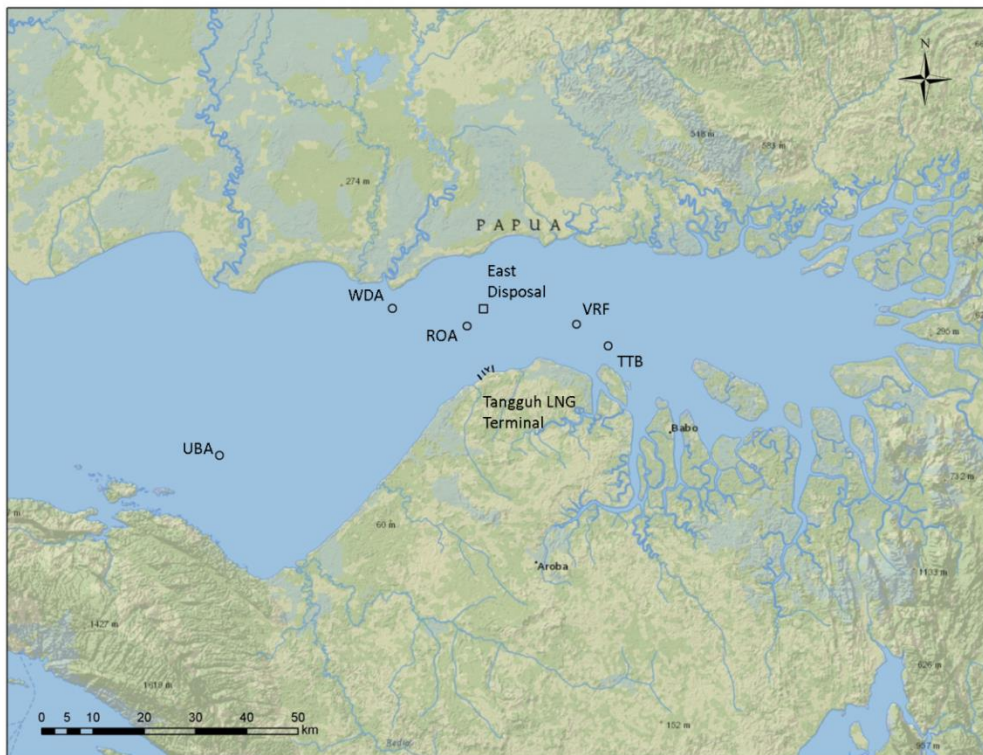


Figure 3.1 Map of Berau/Bintuni Bay with Tangguh LNG Plant and Proposed Drilling, Hydrotest Discharge, and Dredge Disposal Sites Included in the Present Modelling

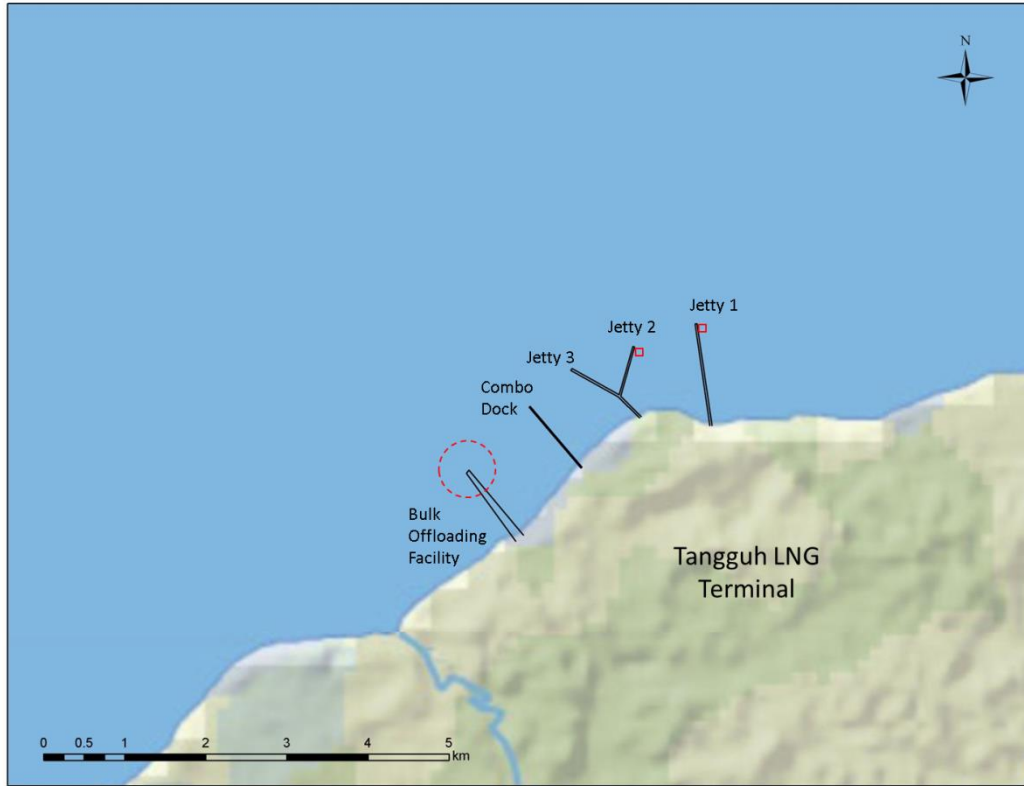


Figure 3.2 *Map of Tangguh LNG Plant with Port Structures, Outfall Locations, and Dredge Location Included in Modelling*

4 APPROACH

4.1 MODELLING METHODOLOGY

Environmental effects on surface waters from the expansion of the Tangguh LNG facility in Bintuni Bay are assessed using a comprehensive modelling approach. In the comprehensive modelling approach, GEMSS®, the Generalized Environmental Modelling System for Surface waters, is used to calculate flow fields throughout Bintuni Bay. These flow fields are then used to estimate the transport and fate of combined wastewater, hydrotest water, drill muds and cuttings, and suspended sediment from dredging and dredged material disposal.

Cumulative impacts are addressed by using both near- and far-field calculations to estimate effects throughout Berau/Bintuni Bay. Near-field models allow high-resolution estimates of the discharge plume on a scale of 100-200 m. Far-field models provide estimates of the overall extent of the discharge throughout the Bay and represent concentrations after the initial plume dilution.

The far-field models are the GEMSS suite of hydrodynamic (GEMSS-HDM), user defined (GEMSS-UDC), and sediment transport (GEMSS-GIFT) modules. The modelling is conducted for two climatological / oceanographic seasons. The wet season represents June to October and the dry season represents December to March. For each season, simulations cover a single, 28-day tidal cycle to capture both spring and neap tides. Two periods from the historical data record are used in the modelling to represent these seasonal conditions. Flow fields calculated by the GEMSS-HDM hydrodynamics module are used directly in GEMSS-UDC and GEMSS-GIFT modules.

The models used for the near-field calculations are CORMIX (US EPA's dilution model) and ADDAMS (US Army Corps of Engineers suite of dredge impact models). These models are steady-state models and are used in this modelling study to simulate high and low tide conditions. Hydrodynamic results (depth, velocity, temperature, and salinity) for these conditions are extracted from the flow field generated by the GEMSS-HDM for use in the near-field models.

The effects of various direct discharges are estimated by calculating the contribution of the discharge to the water column concentrations. For the wastewater and hydrotest water discharges, this concentration is calculated by using the dilution computed by the model. These dilution factors are applied to the various discharge concentrations to estimate the incremental contribution to ambient concentrations. As many of the applicable standards only apply to ambient conditions (ambient standards), these incremental contributions are added to baseline concentrations to estimate total ambient concentrations. The equation used to calculate the ambient concentrations is given by:

$$C = C_{baseline} + \frac{(C_{discharge} - C_{baseline})}{Dilution\ Factor}$$

As can be seen from this equation, the minimum dilution factor will yield the maximum ambient concentration. Maximum measured discharge concentrations and zero decay rates are used to provide a high level of conservatism. Many of the constituents modelled here are known to decay at a rapid rate.

The effects of dredging and drilling activities are assessed by predicting the TSS and sediment bed footprint (i.e., the extent and thickness) of deposited material.

The modelling methodologies and datasets necessary for each modelling effort are described in the following sections. A tabulation of all model scenarios is provided in **Table 4.1**. As noted earlier, flow fields for each model and scenario are computed using the overall hydrodynamic model, GEMSS-HDM.

Table 4.1 *Inventory of Modelling Scenarios*

Modeling Component	Model	Location	Season	Tide
Far-Field				
Comingled Release	GEMSS-UDC	Jetty 1	Dry	NA
		Jetty 1	Wet	NA
		Jetty 2	Dry	NA
		Jetty 2	Wet	NA
Comingled Release + Hydrotest		Jetty 1	Dry	NA
		Jetty 2	Dry	NA
		Jetty 1	Wet	NA
		Jetty 2	Wet	NA
Hydrotest		ROA	Dry	NA
		VRF	Dry	NA
		WDA	Dry	NA
		UBA	Dry	NA
		ROA	Wet	NA
		VRF	Wet	NA
	WDA	Wet	NA	
	UBA	Wet	NA	
Comingled Release + Sensitivity	Worst	Worst	NA	
Dredging + Disposal	GEMSS-GIFT	BOF	Dry	NA
		BOF	Wet	NA
		East Disposal	Dry	NA
		East Disposal	Wet	NA

Modeling Component	Model	Location	Season	Tide
Drilling		ROA	Dry	NA
		ROA	Wet	NA
		UBA	Dry	NA
		UBA	Wet	NA
		TTB	Dry	NA
		TTB	Wet	NA
		WDA	Dry	NA
		WDA	Wet	NA
Near-Field				
Comingled Release	CORMIX	Jetty 1	NA	High
		Jetty 1	NA	Low
		Jetty 2	NA	High
		Jetty 2	NA	Low
Hydrotest		WDA	NA	High
		WDA	NA	Low
		ROA	NA	High
		ROA	NA	Low
		VRF	NA	High
		VRF	NA	Low
		OFA	NA	High
		OFA	NA	Low
Comingled Release + Sensitivity		Worst	NA	Worst
Dredging + Disposal	DREDGE	BOF	NA	High
		BOF	NA	High Slack
		BOF	NA	Low
		BOF	NA	Low Slack
	STFATE	East Disposal	NA	High
		East Disposal	NA	High Slack
		East Disposal	NA	Low
		East Disposal	NA	Low Slack

4.1.1 *Hydrodynamic Modelling*

Model inputs common to the various impact modelling tasks are gathered and formatted for use in GEMSS®. These inputs include bathymetry, coastal maps, tides, any freshwater or existing industrial discharges, climatological and meteorological conditions, and any current meter records. A hydrodynamic model is developed using GEMSS and the assembled datasets that represent conditions throughout the two periods selected for simulation.

A limited set of current meter and water surface elevation records in Berau/Bintuni Bay from 2011 are available for model confirmation, accomplished by performing a comparison to the model results.

4.1.2 Combined Wastewater and Hydrotest Water Discharge Modelling

Near-field Model Applications

Hydrodynamic conditions for two tidal conditions are extracted from the 28-day simulations to apply to the near-field models. The near-field dilution model, CORMIX, is used to estimate the dilution in the vicinity of the discharge.

Far-field Model Applications

The fate and transport of combined wastewater and hydrotest discharges are estimated using the user-defined constituent (UDC) module of GEMSS. The module allows specific substances to be modelled using the general concentration variables already coded into the model. Far-field dilution is estimated for various discharges for the two seasonal periods. The combined wastewater discharge is considered to be continuous and is simulated over the entire 28-day tidal cycle. Hydrotest discharges are limited in duration and are simulated for a 3-day portion of the full cycle. This 3-day period is selected to correspond to a period of low velocities in order to yield conservative estimates. Constituents that are discharged that have ambient water quality standards are assessed with respect to concentrations above background levels.

4.1.3 Cumulative Drilling Mud and Drill Cuttings Transport and Fate

The intention of the drill cuttings modelling is to determine the water column TSS concentrations and the bottom accumulation of the drill cuttings (the “footprint”) in order to assess potential impacts to aquatic and benthic organisms. The drill cuttings model uses the sediment fate and transport module, GIFT, which simulates the fate of particulate material discharged during well drilling. This three-dimensional particle-based model uses Lagrangian algorithms in conjunction with currents generated by GEMSS® (or, in other cases, from measured or globally modelled currents) to estimate the fate and transport of drill cuttings and muds. The model does not predict the concentrations of oil in synthetic based muds.

Time-varying velocities mapped onto the model grid and computed by the hydrodynamic model are used to disperse drill cuttings and mud, modelled as particles. Movement in the vertical direction includes settling, deposition, and erosion. The combined action of erosion and deposition results in net accumulation of drill cuttings on the seabed.

4.1.4 *Dredge Material Disposal*

Near-field Model Applications

Hydrodynamic conditions for two tidal conditions are extracted from the 28-day simulations to apply to the near-field models. Near-field models from the ADDAMS suite of models (DREDGE and STFATE) are used to estimate sediment resuspension near the dredging site and dredge disposal location.

Far-field Model Applications

Potential environmental impacts are assessed for dredging and dredge disposal during which sediment is released into the water column. For dredging, sediment is released during seabed disturbance and leakage from the dredging equipment; for dredge disposal, sediment is introduced at the surface and smaller particles will disperse as the heavier particles fall to the bottom. The assessment includes estimates of sedimentation rates, TSS, and thickness of sediments added to the sea floor. Modelling is performed using the currents established in the hydrodynamic modelling task and the GIFT module for the two seasonal periods selected.

4.2 *GEMSS SUITE DESCRIPTION*

GEMSS® is an integrated system of 3-D hydrodynamic and transport models embedded in a Geographic Information System (GIS). GEMSS includes an environmental data system, grid generator and editor, control file generator, 2-D and 3-D post processing viewers and additional tools such as meteorological and time-varying data generators to aid the modelling process. Customization of the suite of hydrodynamic, transport and water quality models to reflect the needs of each application is easily done because of the modular design of GEMSS. A list of modules available within GEMSS are shown in Figure 4.1 and Figure 4.2, and also listed below.

- HydroDynamic and Transport Module - HDM
- Source water Protection zone Module - SPM
- Water Quality Module - WQM
 - WQDPM -EPA's EUTRO5 as modified for dissolved and particulate organic matter
 - WQCBM - Carbon based kinetics with sediment diagenesis
 - WQICM - USACE's CE-QUAL-ICM kinetics with sediment diagenesis
 - WQW2M - USACE's CE-QUAL-W2 water quality kinetics
- Chlorine Kinetics Module - CKM
- Atmospheric Diffusion Module - ADM
- Gas Transfer Module - GTM

- Sediment Transport Module - STM
- Toxic Module - TOX
- Particle Tracking Module - PTM
- Thermal Analysis Module - TAM
- Generalized Bacterial Module - GBM
- Generalized Algal Module - GAM
- User Definable Constituents Module - UDM
- Entrainment Module - ENM
- Macrophytes Module - MPM
- Empirical Transport Module - ENETM
- Equivalent Adult Module - ENEAM
- Generalized Integrated Fate and Transport - GIFT
- Chemical and Oil Spill Impact Module - COSIM

GEMSS modules used in the present study are GEMSS-HDM, GEMSS-GIFT and GEMSS-UDC.

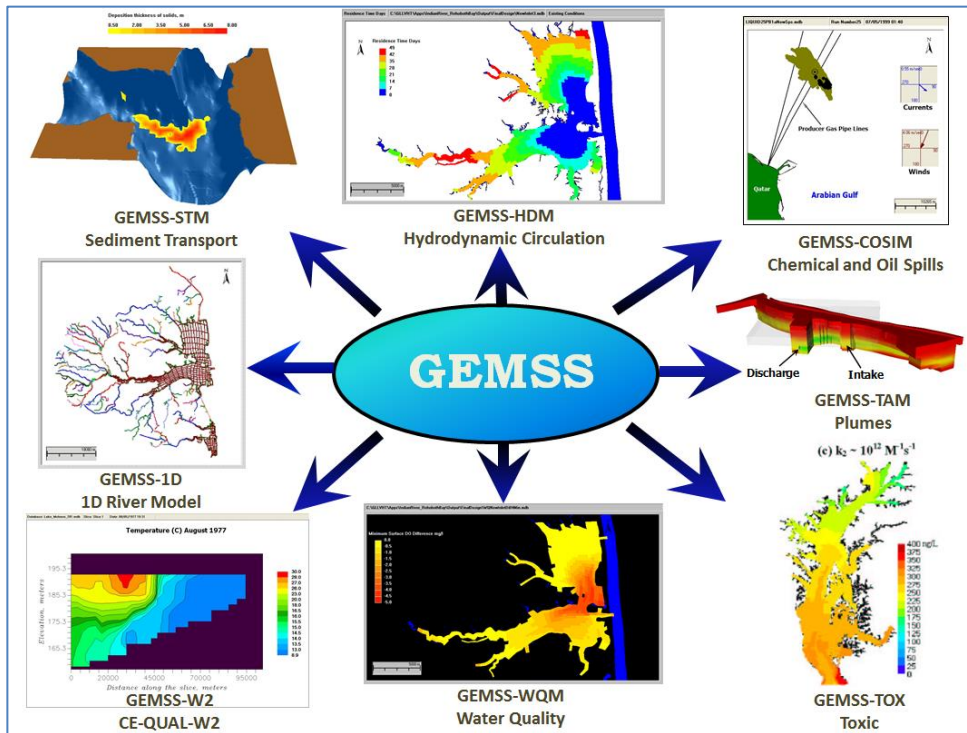


Figure 4.1 GEMSS Modules: First Set

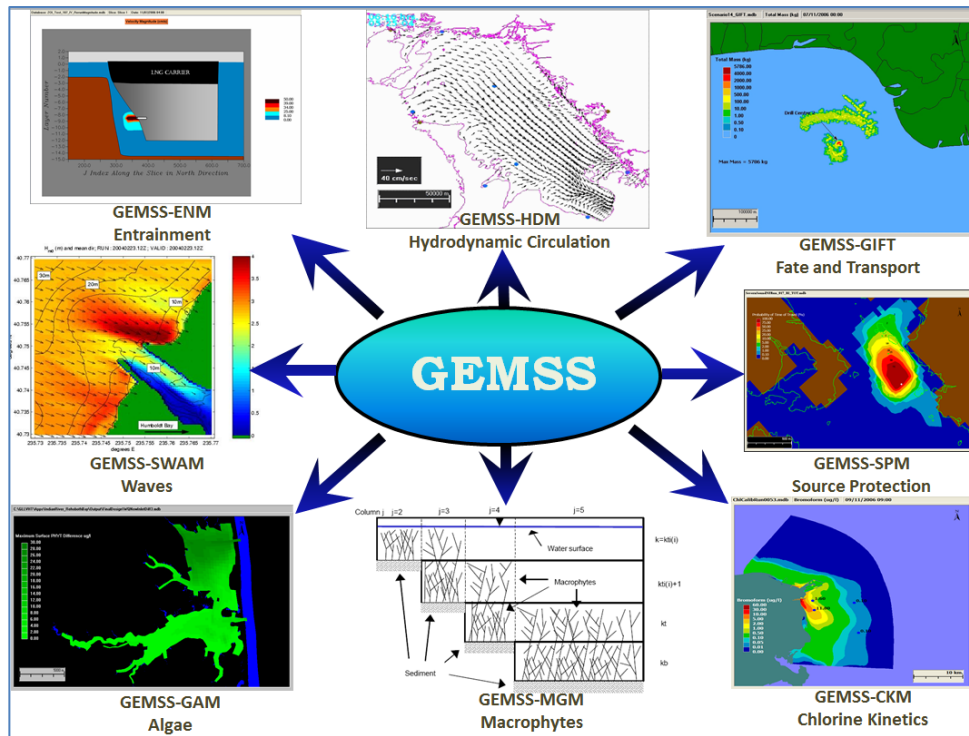


Figure 4.2 GEMSS Modules: Second Set

4.2.1 GEMSS-HDM

GEMSS®-HDM is a state-of-the-art three-dimensional numerical model that computes time-varying velocities, water surface elevations, salinity and temperature in rivers, lakes, reservoirs, estuaries, and coastal water bodies. Prior to 2000, GEMSS-HDM was referred to as GLLVHT (Generalized Longitudinal-Lateral-Vertical Hydrodynamics and Transport).

The theoretical basis of the hydrodynamic kernel of GEMSS is the three-dimensional Generalized, Longitudinal-Lateral-Vertical Hydrodynamic and Transport (GLLVHT) model which was first presented in Edinger and Buchak (1980) and subsequently in Edinger and Buchak (1985). The GLLVHT computation has been peer reviewed and published (Edinger and Buchak, 1995; Edinger, et al., 1994 and 1997; Edinger and Kolluru, 1999). The kernel is an extension of the well-known longitudinal-vertical transport model written by Buchak and Edinger (1984) that forms the hydrodynamic and transport basis of the Corps of Engineers' water quality model CE-QUAL-W2 (U. S. Army Engineer Waterways Experiment Station, 1986). Improvements to the transport scheme, construction of the constituent modules, incorporation of supporting software tools, GIS interoperability, visualization tools, graphical user interface (GUI), and post-processors have been developed by Kolluru et al. (1998; 1999; 2003a; 2003b) and by Prakash and Kolluru (2006).

GEMSS capabilities have been inventories by professional organizations, e.g., HGL and Aqua Terra, 1999 and Water Environment Federation (2001).

GEMSS development continues as additional applications are completed. A second hydrodynamic kernel, POM, has been added to supplement GLLVHT. In addition, new constituent modules have been developed and tested, including source water protection (Kolluru and Prakash, 2012), watershed nutrient load allocation (Kolluru et al., 2009), chlorine and chlorine by-products fate and transport (Kolluru et al. 2012); mine pit lake analysis (Vandenberg, et al., 2011; Prakash, et al., 2012), debris fouling at cooling water intakes (Prakash et al., 2012), coliform fate and transport (Tryland et al., 2012) and thermal avoidance calculations (Buchak, et. al., 2012), impact assessment (Fichera, et al., 2013)

GEMSS applications to estuarine and coastal waterbodies have been validated by comparisons to extensive, field-collected datasets. These include currents, temperature and chlorine and chlorine by-products offshore Qatar (Kolluru et al., 2005; Adenekan et al., 2009; Febbo et al., 2012; Kolluru et al., 2003; Kolluru et al., 2012); currents, temperatures and nutrient water quality in Puget Sound (Albersson et al., 2009) in coastal Delaware (Kolluru and Fichera, 2003), and Vistula River in Poland (Kruk et al., 2011); currents and temperatures in the New York Harbor area (Edinger et al., 1997); larval populations in coastal Alaska (Edinger et al., 1994); and, mine tailings ponds (Prakash et al., 2011).

The computations are done on a horizontal and vertical grid that represents the waterbody bounded by the surface, shoreline, and bottom. The water surface elevations are computed simultaneously with the velocity components. The velocity components and water elevations are then fed into the solute transport routines to compute the water quality constituent concentrations. Included in the computations are boundary condition formulations for friction, wind shear, turbulence, inflow, outflow, surface heat exchange, and water quality kinetics. The model can be used to analyse system dynamics and to predict the effects of existing conditions or possible design or management alternatives.

4.2.2 GEMSS-UDC

The User Defined Constituent (UDC) module simulates the fate and transport of generic constituents. These generic constituents are modelled by assuming that transport and fate can be represented satisfactorily in terms of simple decay/growth (zero order or first order) and settling, which can be set to zero. The module allows a user to set up any number of non-interacting generic constituents. The module works with the far-field hydrodynamic module, GEMSS-HDM and can use any of the transport algorithms available in GEMSS including Upwind, QUICKEST and QUICKEST with ULTIMATE.

4.2.3 *GEMSS-GIFT*

GIFT simulates the fate of dissolved and particulate material discharged from dredging barges, mine tailings, drill cuttings and muds, and produced water. This three-dimensional particle-based model uses Lagrangian algorithms in conjunction with currents, specified mass load rates, release times and locations, particle sizes, settling velocities, and shear stress values (Shields number).

Modelling methodology is based on a deterministic mode of simulation. In deterministic single event simulations, the starting date and current speed and direction at each time step are chosen from a database of properties in the selected periods.

Drill cuttings and muds are modelled as particles. Movement in the vertical direction results in the settling and deposition of cuttings on the seabed. The combined action of erosion and deposition, based on particle size distribution and the intensity of release, results in the net accumulation of drill cuttings on the seabed.

4.3 *CORMIX DESCRIPTION*

In this study the United States Environmental Protection Agency's (US EPA) Cornell Mixing Zone Expert System (CORMIX) model Version 7.0. GT was used to estimate the dilution factor, configuration and dimensions of effluent plumes from different discharge configurations and flow rates. CORMIX is an outfall design tool that is also used by regulatory agencies to estimate the size and configuration of proposed and existing mixing zones resulting from wastewater discharges. CORMIX is applied to the region adjacent to the discharge structure in which the effluent plume is recognisable as separate from the ambient water. Its trajectory is dominated by the discharge rate, effluent density, and geometry of the discharge structure.

CORMIX calculations are based on defining the various hydraulic zones the effluent plume traverses when introduced into a receiving water body. The model computes the plume trajectory and dilution rate in each zone by applying calculations based on either an analytical or empirical relationship. These relationships have been validated by the developers and other researchers against laboratory and field studies. CORMIX has been applied to many effluent discharge dilution studies (<http://www.cormix.info/>) and is recognised by the US EPA and other national regulatory agencies as an appropriate model for computing trajectories, dilution rates and consequently mixing zone dimensions.

CORMIX has a couple of limitations. It assumes steady-state conditions and unidirectional, uniform flow in the receiving water body. Secondly, CORMIX has simplified geometric capabilities and assumes an idealised water body with straight sides and a uniform bottom.

4.4 *ADDAMS SUITE DESCRIPTION*

The Automated Dredging and Disposal Alternatives Modelling System (ADDAMS) is distributed by the U.S. Army Corps of Engineers through the Environmental Laboratory, USAE Research and Development Center Waterways Experiment Station. ADDAMS consists of approximately 20 modules to assist in design and evaluation of various aspects of dredging and dredged material disposal operations. Two of these modules, DREDGE and STFATE are used in this study.

4.4.1 *DREDGE*

In order to assess the potential dispersion and deposition of dredged marine sediments, the United States Army Corps of Engineers' (USACE) DREDGE (Hayes and Je, 2008) model was used. This model is a steady-state calculation, developed to estimate impacts from proposed dredging operations. DREDGE computes the rate at which sediments become suspended as the result of hydraulic and mechanical dredging operations, and then computes the resulting suspended sediment plume dimensions and configuration using site-specific information. Details of the DREDGE simulations are presented in this report.

4.4.2 *STFATE*

STFATE (Short-Term FATE) is a module of the Automated Dredging and Disposal Alternatives Management System (ADDAMS) (Schroeder and Palermo, 1990). STFATE (Johnson et al., 1994) was developed from the DIFID model (Disposal from an Instantaneous Discharge) prepared by Koh and Chang (1973). DIFID was used for discrete discharges from barges and hoppers. The model computations apply the assumption that the behaviour of the disposed material can be separated into three phases: convective descent, during which the disposal cloud falls under the influence of gravity and its initial momentum is imparted by gravity; dynamic collapse, occurring when the descending cloud either impacts the bottom or arrives at a level of neutral buoyancy where descent is retarded and horizontal spreading dominates; and passive transport-dispersion, commencing when the material transport and spreading are determined more by ambient currents and turbulence than by the dynamics of the disposal operation. The model simulates the distribution of dredged material in the water column and on the seabed that originated in discrete disposal loads. However, STFATE does not account for density currents (and entrainment of clay/silt particles). Therefore it can be considered conservative in terms of impacts to the water column. The model considers various input parameters including the type of disposal vessel, physical properties of the water body, and material properties.

5 HYDRODYNAMIC MODELLING

5.1 SPATIAL DATA

Spatial data required for modelling includes:

- Delineation of the Berau/Bintuni Bay shoreline and Tangguh LNG port structures
- Locations of the wells, dredge areas, and disposal areas
- Berau/Bintuni Bay bottom elevation (bathymetry)

The coastline of Berau/Bintuni Bay is delineated using nautical charts and satellite imagery. The supratidal extent indicated on the nautical chart provided by the Tangguh LNG serves as the basis for the shoreline. This map is georeferenced using ESRI ArcGIS software and verified using satellite imagery provided by ESRI as part of their online data service. Small adjustments to the shoreline are made in the area of the LNG terminal in order to more closely match imagery.

The port structures that require representation in the hydrodynamic modelling include Jetty 1 (existing), Jetty 2 (proposed), Combo Dock, and BOF. The delineation of these structures is taken from georeferenced CAD drawings provided by the Tangguh LNG (BP 2013a) and are shown in **Figure 3.2**. The jetties and BOF are simulated as barriers in the hydrodynamic model. The Combo Dock only serves as a barrier in the topmost layer of the model. It should be noted that although Jetty 3 is shown in **Figure 3.2**, it is not included in the modelling as this jetty is not proposed for the forthcoming port expansion.

The locations of the wells to be modelled for hydrotest discharge and/or drill cuttings and mud are ROA, WDA, UBA, VRF, and TTB (**Figure 3.1**). Locations of these wells are estimated by georeferencing maps provided by the Tangguh LNG (BP 2013a). The location of the dredging and dredge disposal sites are identified via e-mail communication with the Tangguh LNG (BP 2013b).

The model grid is constructed to conform to the Berau/Bintuni Bay shoreline as well as the port structures. The western end of the model extends nearly to the Ceram Sea near Ogar. The model grid consists of over 11,000 grid cells horizontally with up to 34 layers in the vertical. The model grid is shown in **Figure 5.1**. The grid has variable resolution to allow for finer resolution near the Tangguh LNG Terminal (**Figure 5.2**) relative to offshore areas. The average grid cell dimensions are 1.0 by 1.5 km with 85 by 110 m resolution in the nearshore facilities area.

The bathymetry of the Bay is based on data compiled by URS and provided by the Tangguh LNG. It covers the entire Berau/Bintuni Bay and is a composite of various data sources including 2009 dredging surveys, 2007 surveys by Janhidros, and 2004 surveys of the Combo Dock and Jetty 1 berth. This extensive dataset is mapped to the model grid by averaging (and interpolation as needed). In the area around the LNG Plant, minor adjustments to the grid are made in order to achieve general agreement with the nautical chart. The resulting bathymetry used in the model is shown in **Figure 5.1** with a close-up of the terminal area in **Figure 5.2**.

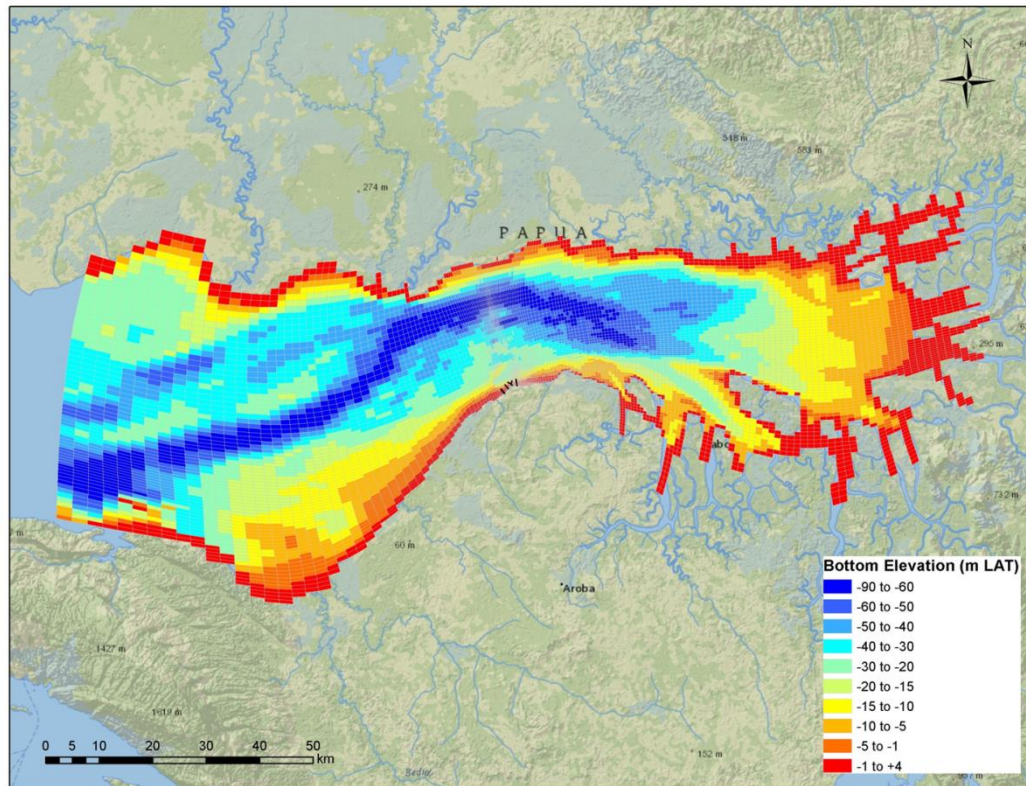


Figure 5.1 *Hydrodynamic Model Grid with Bottom Elevations for Berau/Bintuni Bay*

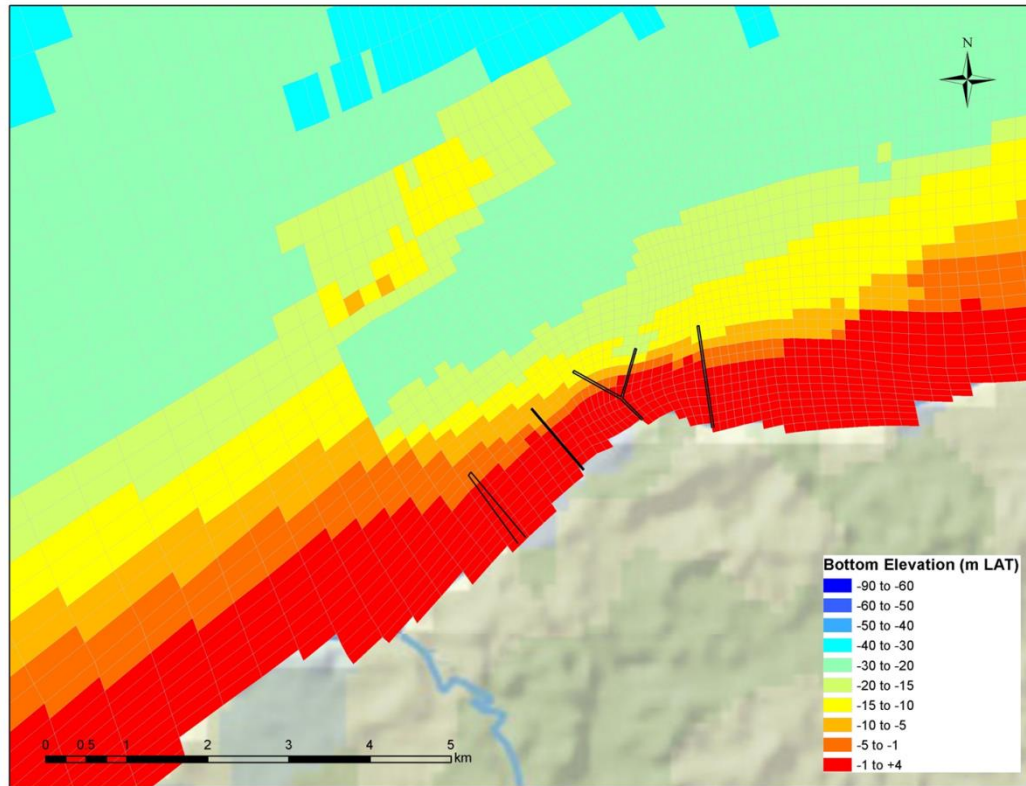


Figure 5.2 *Hydrodynamic Model Grid with Bottom Elevations in the Vicinity of the Tangguh LNG Terminal*

5.2 BOUNDARY DATA

Model Inputs

Data used for hydrodynamic model input include: tidal elevation at the western boundary (where Berau Bay opens to the Ceram Sea), temperature and salinity at the western boundary and throughout the bay, and meteorological data. Boundary data are required for the entire dry (2011-08-12 to 2011-09-15) and wet (2011-12-01 to 2011-12-31) model simulation time periods. A constant freshwater contribution is added during the wet season. The following subsections describe these input data individually.

Tidal Elevation

To run the model, tidal elevation data is needed at the model's western boundary with the Ceram Sea. Recent elevation measurements are only available at the Tangguh LNG berth (2.4260° S, 133.1330° E). These measurements were collected by URS from 2011-07-29 to 2012-02-05. Additionally, predicted tidal elevations, obtained from Oregon State University's tidal prediction software OTPS (OSU Tidal Prediction Software: <http://volkov.oce.orst.edu/tides/otps.html>), were considered. The OTPS software has

the benefit of providing predicted tidal elevations at any user-defined location. However, the OTPS prediction for the Tangguh LNG berth is qualitatively very different from the actual observations, perhaps because of sloshing driven by diurnal winds or Kelvin waves entering from the Ceram Sea. Therefore, the berth tidal measurements are used to determine the elevation at the western boundary. This tidal signal is adjusted in amplitude and phase using the shift in OTPS-predicted amplitude and phase between the berth and the western boundary. The elevation time series applied at the western boundary are shown in **Figure 5.3**. Elevations in this report are relative to LAT, which is 2.15 m below mean sea level at Tangguh LNG.

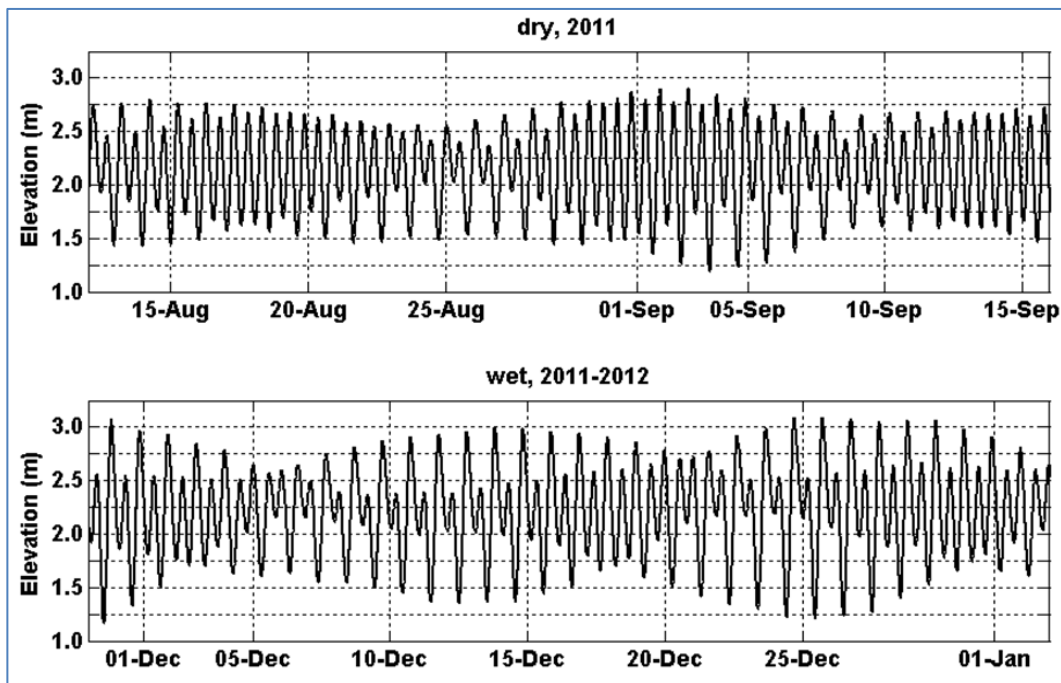


Figure 5.3 Tidally-driven Elevation Applied at the Model's Western Boundary in the Dry and Wet Periods

Meteorological Properties

Meteorological observations were recorded on a hill to the southeast of Tanah Merah and the Tangguh LNG facility at 2.4397° S, 133.1366° E (Meteorological Data Collection Program, 2000). This position on the hill is 44 m above mean sea level. The observations are taken from the anemometer mast, which is an additional 30 m higher, well above the tree line. Observations of wind speed and direction, dry bulb air and dew point temperatures, air pressure, sky cover, and relative humidity are available for the period 2002-01-01 to 2011-12-31. During the dry season model period winds are from the north (350° most probable) and during the wet season model period are from the east (90° most probable) as seen in **Figure 5.4** Error! Reference source not found.. Time series of other meteorological properties are shown in **Figure 5.5** for dry season model period

and **Figure 5.6** for the wet season model period. The meteorological data are used in the model to calculate surface wind stress and heat exchange with the atmosphere.

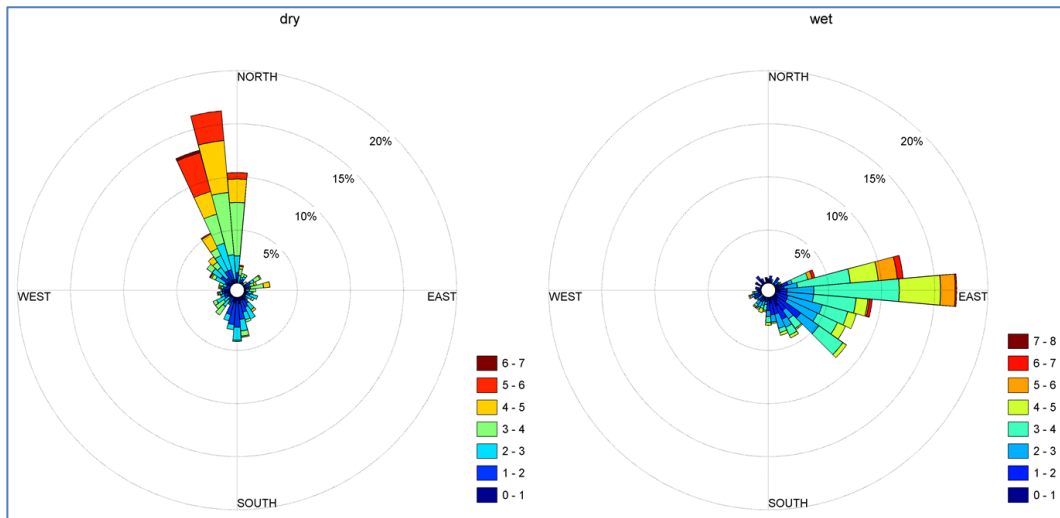


Figure 5.4 *Wind Roses Determined from Measurements Taken at Tanah Merah in 2011 during the Dry (Left) and Wet (Right) Model Periods*

Colors indicate wind speed ranges in units of m/s and wind blows from directions shown

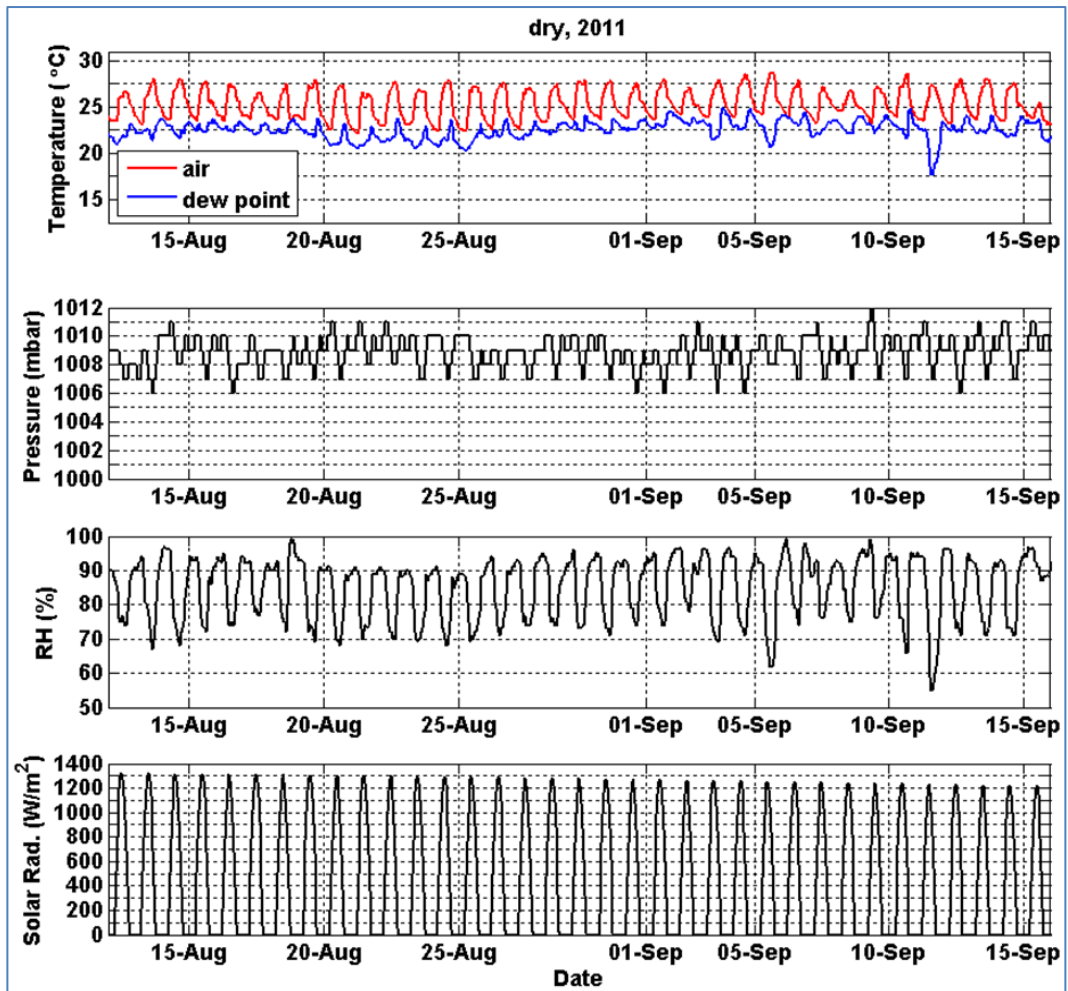


Figure 5.5 Dry Bulb Air Temperature, Dew Point Temperature, Air Pressure, Relative Humidity, and Solar Radiation at Tanah Merah during the Dry Model Period

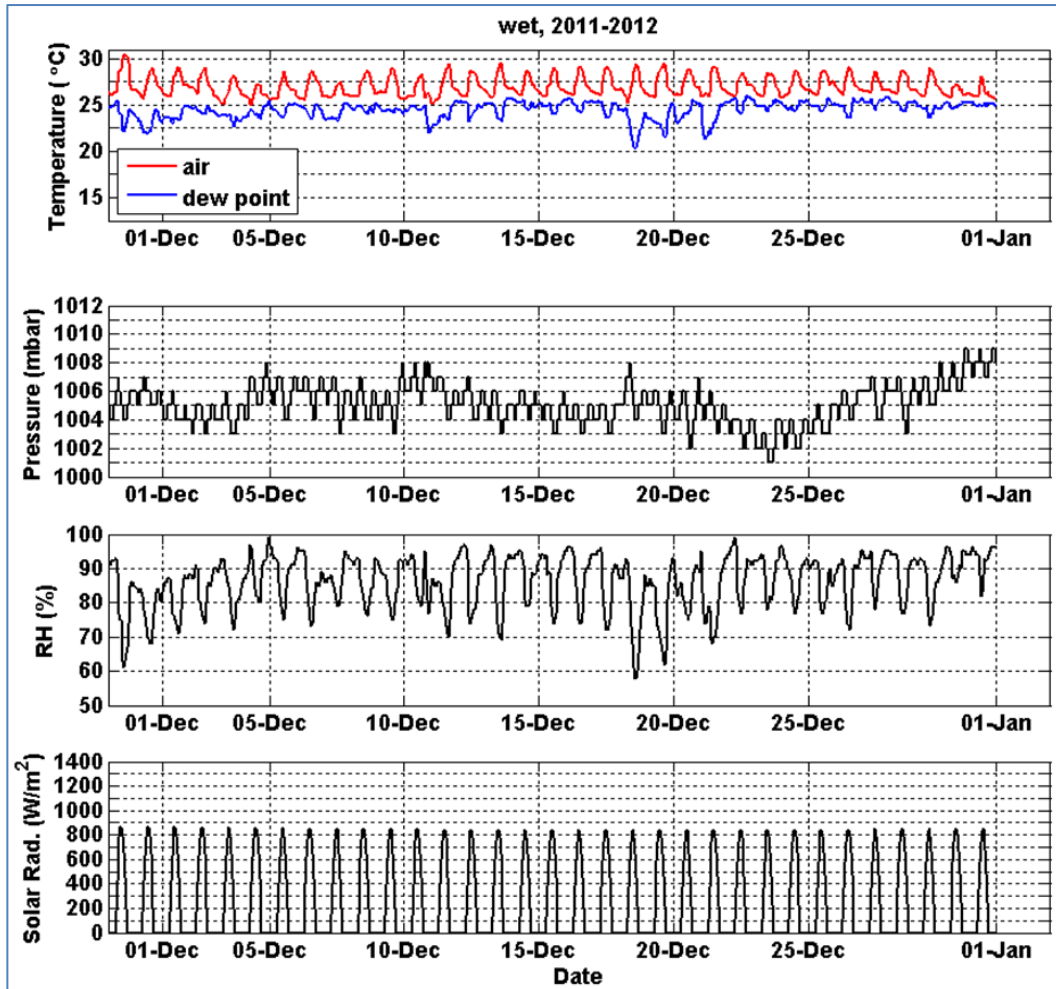


Figure 5.6 Dry Bulb Air Temperature, Dew Point Temperature, Air Pressure, Relative Humidity, and Solar Radiation at Tanah Merah during the Wet Model Period

Temperature and Salinity

Vertical profiles of temperature and salinity were collected at 23 stations from 2012-07-29 to 2012-10-27 during the dry season and at 30 stations from 2013-03-15 to 2013-04-26 during the wet season. Station locations are shown in **Figure 5.7**. Profiles from station OS02 (2.4121° S, 132.5451° E) are used to define the entire western boundary throughout each dry or wet simulation period (black curves in **Figure 5.8** and **Figure 5.9**). In the dry season simulation, the initial temperature and salinity is everywhere set to 28° C and 30 ppt, respectively. In the wet season simulation, the initial temperature is everywhere set to 30° C. The wet season initial salinity is set according to the west-east position within the model domain by using offshore salinity profiles from stations OS02, OS05, OS01, OS08, OS11, OS12, OS13, and OS14 as shown in **Figure 5.9**.



Figure 5.7 Vertical Profile Station Locations

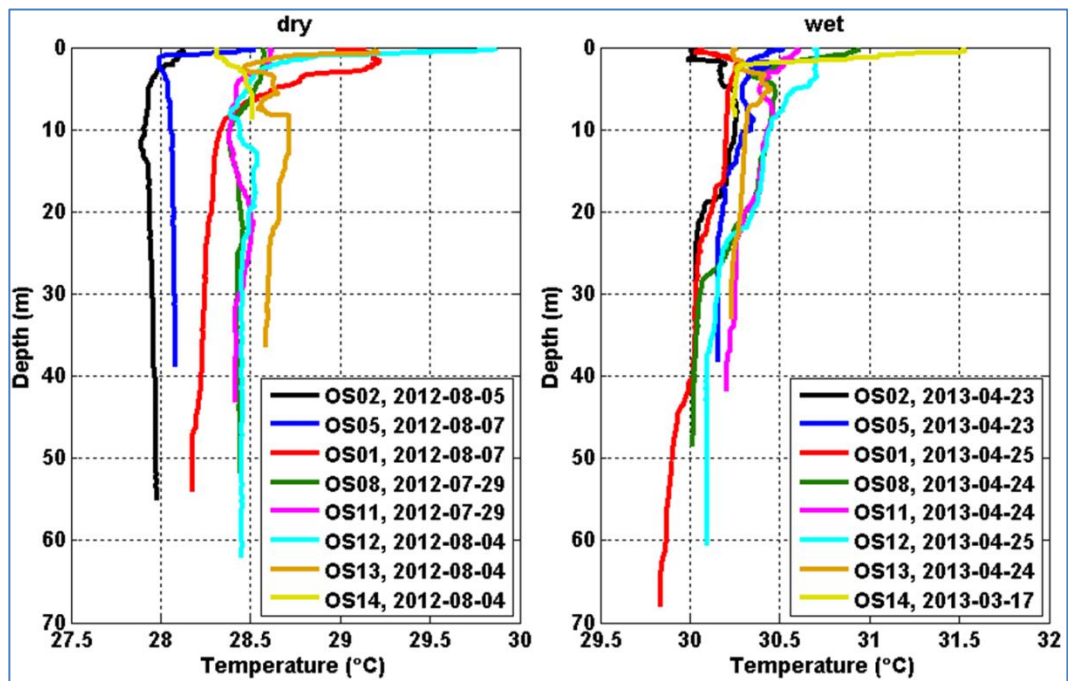


Figure 5.8 Profiles of Temperature from Dry and Wet Seasons for Eight Stations Used for Model Input

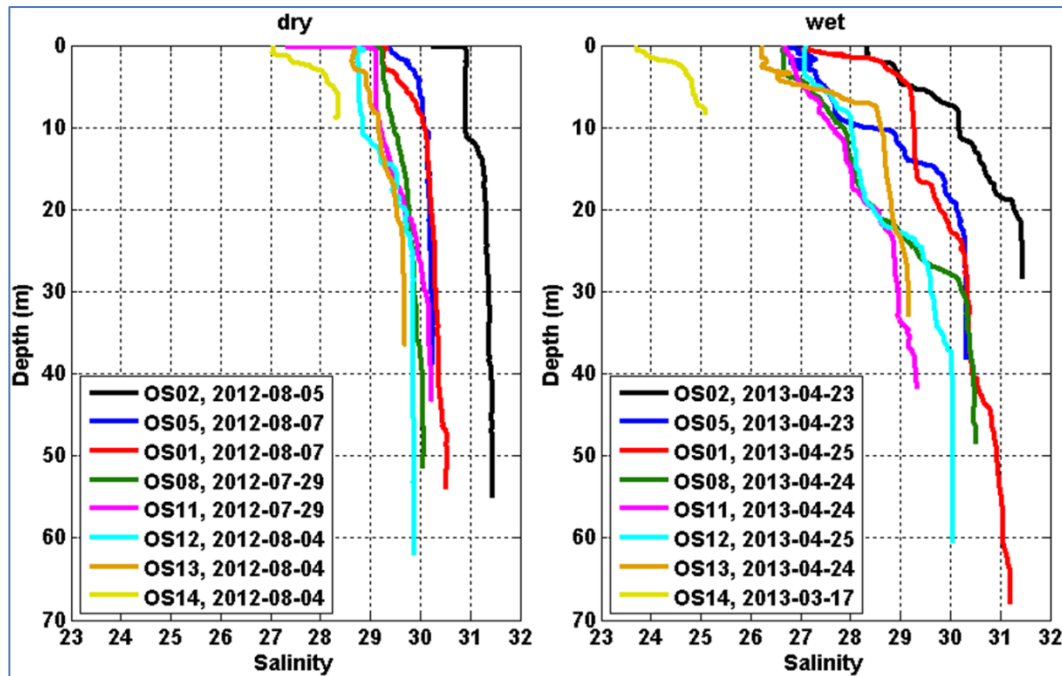


Figure 5.9 Profiles of Salinity from Dry and Wet Seasons for Eight Stations used for Model Input

Freshwater

As seen in **Figure 5.9**, estuarine salinity stratification characteristic is evident during the wet season. This is due to increased freshwater inflow originating from river runoff and rainfall during this time. In order to reproduce this stratification in the model, constant freshwater flow is added to the shallowest 5 m of the model uniformly across all areas east of the Tangguh LNG facility. The total magnitude of this flow is approximately 2300 m³/s and is determined by qualitative comparison of observed and modelled salinity profiles (see Section 5.4). For comparison, the total average annual (wet and dry seasons included) flow of the six major rivers described in Section 1 is 1295 m³/s. The modelled freshwater flow is only applied during wet season simulations.

5.3 SCENARIO DESIGN

There are two distinct climatological seasons in Berau/Bintuni Bay seen from the public climatology data and oceanic observations. The climate in this region can be classified into wet and dry season shown in the historical precipitation record and salinity profiles in Section 5.2. The hydrodynamic characteristics in the wet and dry seasons can be different due to different freshwater flow and salinity profile. These differences create seasonal stratifications and may introduce different circulation patterns in both the upper and lower depths. The difference in circulation and stratification will constrain the transport of various constituents or pollutants in this marine environment. In order to capture the patterns and provide accurate predictions for the

various discharges, the hydrodynamic model is set up with two scenarios: dry and wet scenarios.

The dates for these two scenarios are chosen based on availability and analysis of historical data, which include wind data, tide and current data. The typical winds for the dry and wet period were identified based on ten-year (2002-2011) wind rose analysis, which shows that the dominant winds are from the north and east. With the historical wind rose analysis, the year to be simulated was selected based on the availability of confirmation data. The only year that has elevations, current and meteorology data covering both wet and dry period is 2011. The months for the two periods were selected by revisiting the wind rose analysis for 2011 only. The months that preserve the dominant wind patterns and have the most available data are used for these two scenarios: August (2011-08-12 to 2011-09-15) for dry season and December (2011-12-01 to 2011-12-31) for wet season.

5.4 MODEL CONFIRMATION

Surface elevation

The surface elevation calculated from the model for dry and wet scenarios are compared with the tide gauge observation at the Jetty 1 berth (**Figure 3.2**). The surface elevation confirmations for the dry and wet periods are shown in **Figure 5.10** and **Figure 5.11**, respectively. As seen from the comparisons, the surface elevation from the model matches very well with the data. The mean differences between the model and data are 0.009 and -0.058 m for the dry and wet scenario respectively. The root-mean-square-error (RMSE) between the model and data are 0.207 and 0.255 m for the dry and wet scenario respectively.

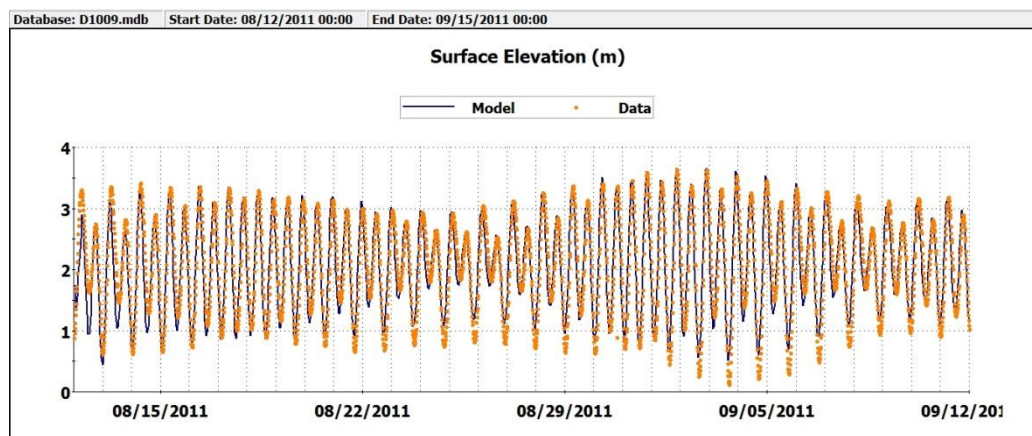


Figure 5.10 Water Surface Elevation Comparison between Model and Data for Dry Scenario

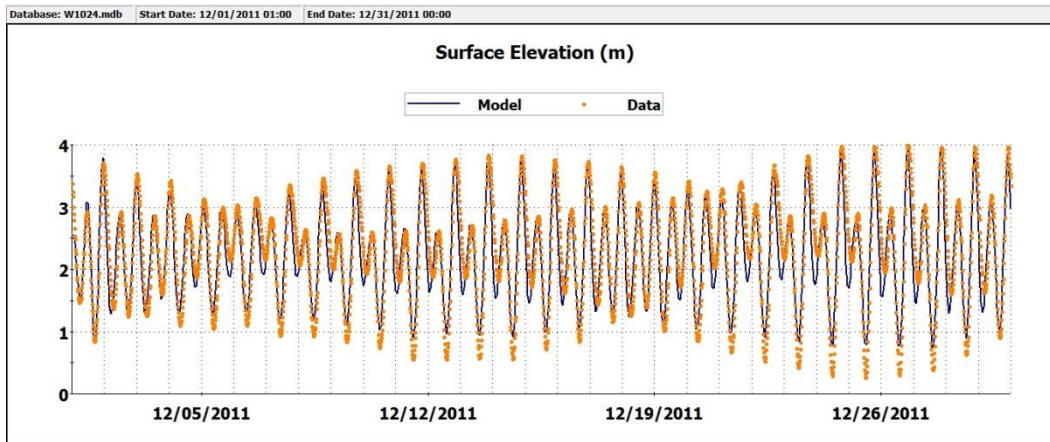


Figure 5.11 *Water Surface Elevation Comparison between Model and Data for Wet Scenario*

Current statistics

Available surface current data are used to confirm currents predicted by the model. There is one current dataset available, near Jetty 1, for the simulation periods (measured by URS). The average magnitude of surface current in the dry scenario is 34.5 cm/s calculated by the model and 51.7 cm/s seen from the data. The minimum current speed is 0.0 cm/s for both model and data. The maximum current simulated in the model is 104.3 cm/s and the data is 116 cm/s. The currents near the LNG facility are strong and dynamic. For the wet period simulation, the predicted current speed ranges between 0.0 cm/s and 90.1 cm/s. The average predicted current speed for the wet period simulation is 35.9 cm/s. The statistics for the data in the same period are: minimum speed is 0.8 cm/s, maximum speed is 137.3 cm/s, and average speed is 57.0 cm/s. The differences between the data and model can be attributed to differences in the bathymetry at the time of data measured and surveyed for the model as well as local disturbances from small scale forces and structures not represented in the model. Smaller predicted current speed in the modelling produces somewhat smaller dispersion of the discharge plume and thus more conservative estimates of maximum ambient concentrations.

Temperature and Salinity Profiles

The initial conditions for temperature are assumed to be vertically uniform for both dry and wet periods. The initial salinity in the dry period is also considered vertically uniform. However, the initial wet period salinity vertical distribution is not uniform because of the large gradients observed. Freshwater is added in the model to reproduce the observed stratification. The salinity set up and freshwater input helps the model to achieve the stratification needed for constituent simulation. Additionally, the first five days of the simulation are considered part of the 'spin-up' model period to allow development of stratification. Although the salinity data was collected at times that are

not included in the simulation, **Figure 5.12** shows that the model qualitatively captures the salinity stratification well for the three representative locations (OS02, OS11 and OS13).

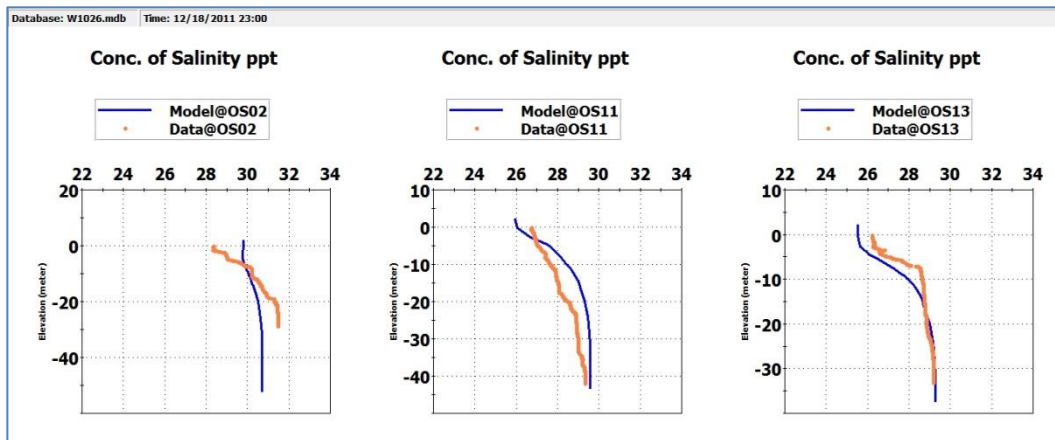


Figure 5.12 Salinity Profile Confirmation with Data for Wet Period

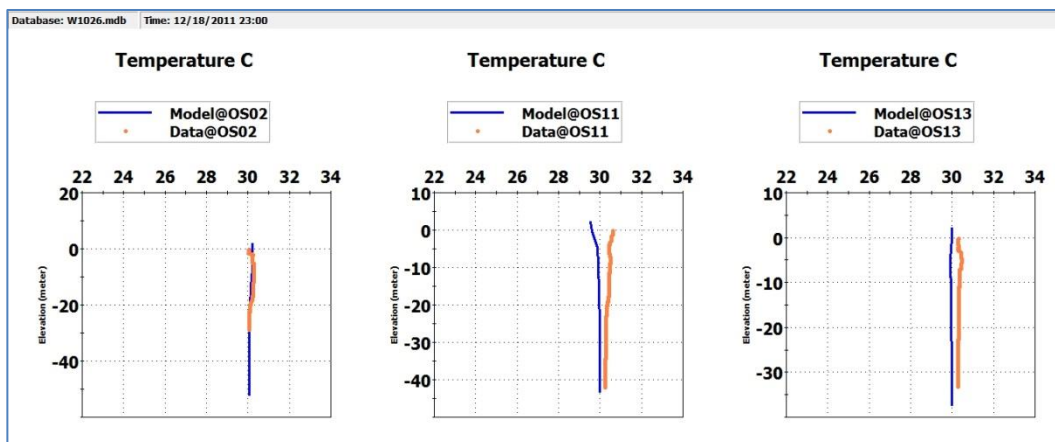


Figure 5.13 Temperature Profile Confirmation with Data for Wet Period

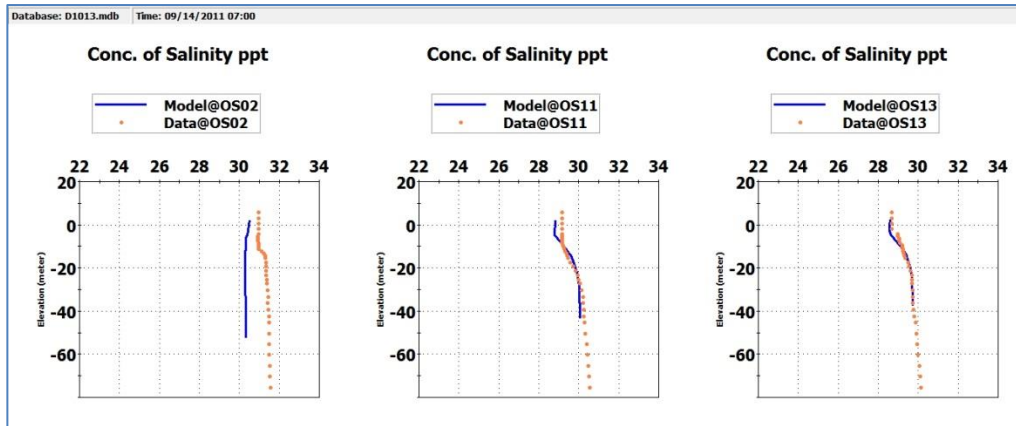


Figure 5.14 Salinity Profile Confirmation with Data for Dry Period

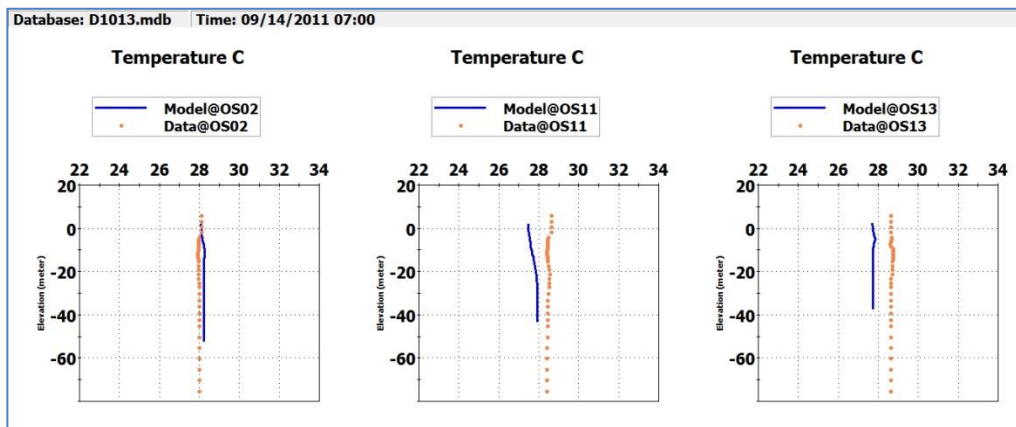


Figure 5.15 Temperature Profile Confirmation with Data for Dry Period

5.5 GIFT MODEL SUBGRID

The output from the hydrodynamic modelling was used to generate a bathymetric data set that was mapped to a grid for the GIFT far field dredging, disposal, and drill cuttings modelling. Different grids were created from this data set for each of the modelling tasks. A discussion of the GIFT grid used in the drill cuttings modelling can be found in Section 0. Discussions of the far field dredge and disposal GIFT modelling can be found in Section 0 and Section 0, respectively.

6 COMINGLED WASTEWATER DISCHARGE MODELLING

6.1 SCENARIO DESIGN

The wastewater discharge from the Tangguh facility represents the comingled waste stream from various activities at the terminal. Two discharge locations are considered: the existing outfall at the far end of Jetty 1 and the proposed outfall at the far end of Jetty 2 (see **Figure 3.2**). Each outfall is considered in turn; the full discharge is applied to the outfall under consideration. For the far-field simulations, each outfall is simulated for both representative wet and dry seasonal conditions as described in Section 5.3. For near-field simulations, each outfall is simulated for two representative tidal conditions, high tide and low tide.

6.2 DISCHARGE INFORMATION

The discharge is assumed to be 1900 m³/hour which represents the total flow for all waste streams rounded up to the nearest hundred. The individual wastestreams and their magnitude that form this comingled discharge are shown in **Table 6.1**. This discharge is considered to be continuous. The discharge depth is at -13 m below LAT at both jetties. At Jetty 1, this depth represents the very bottom of the water column because the bottom elevation is -13.5 m LAT. The Jetty 2 outfall is 3 m above the bed as it is proposed that the berth area will be dredged to -16 m LAT. The outfall pipe is 20" diameter oriented horizontally and assumed directed away from shore.

Table 6.1 Individual Wastestreams and Their Flow Rate that form the Comingled Discharge

Wastestream	Flow (m ³ /hour)
Neutralization pit	142
Oily pit	200
Sewage pit	37
STP load B	55
Produced water	50
Brine return	1368
<i>Total flow rate</i>	<i>1851</i>

Composite wastewater sampling conducted by the Tangguh LNG in December 2012 and March 2013 is the basis for the assumed comingled waste stream concentrations. For all constituents modelled (except DO), the maximum value observed is used. This assumption is conservative in nature as it represents the maximum, not average, wastewater concentrations. Moreover, constituents measured below the detection limit are assumed to have values at the corresponding detection limits. With regard to DO, the ambient standard is a minimum value, not a maximum value; a conservative

discharge concentration of 0.0 mg/L is used. **Table 6.2** provides a summary of the discharge concentrations used as well as whether dilution is necessary to meet ambient standards.

As described in Section 4.1, baseline concentrations are used with modelled discharge concentrations to calculate the total ambient concentrations. As part of the 2012-2013 field survey that measured vertical profiles of temperature and salinity, water samples were collected at the stations shown in **Figure 5.7** and analysed for various constituents. Data from all stations are used to calculate average concentrations representing baseline values for the dry and wet period. These values are also shown in **Table 6.2**.

Table 6.2 Assumed Comingled Discharge Concentrations and Ambient Standard Concentrations

Constituent	Discharge Concentration Used in Modelling	Ambient Standard	Baseline Concentration		Dilution Needed
			Dry Period	Wet Period	
Total Ammonia (mg/L as N)	3.71	0.3	<0.020	<0.020	Yes
Arsenic (mg/L)	0.0064	0.012	0.00098	0.00126	No
BOD5 (mg/L)	10	20	2.1	<2.0	No
Cadmium (mg/L)	<0.005	0.001	0.00020	0.00040	Yes
Chromium-VI (mg/L)	<0.05	0.005	<0.0020	<0.0020	Yes
Copper (mg/L)	0.13	0.008	0.0010	0.0011	Yes
Dissolved Oxygen (mg/L)	0.0	>5.0	5.55	5.49	Yes
Lead (mg/L)	<0.05	0.008	<0.0010	<0.0010	Yes
Mercury (mg/L)	0.00014	0.001	<0.00005	<0.00005	No
Oil and Grease (mg/L)	<1	1	<1.0	<1.0	No
pH	8.57	6.5-8.5	8.06	7.86	Yes
Salinity (ppt)	39.0	34	28.50	25.46	Yes
Sulfide (mg/L)	<0.002	0.01-0.03	<0.0020	<0.0020	No
Temperature (°C)	34	28-32	29.12	30.67	Yes
Total Phenol (mg/L)	<0.001	0.002	<0.0010	<0.0010	No
TSS (mg/L)	176	80	27.74	26.63	Yes
Zinc (mg/L)	1.012	0.05-0.1	0.0071	0.0052	Yes

6.3 NEAR - FIELD MODELLING

The *Environmental, Health and Safety (EHS) Guidelines* provided by the *International Finance Corporation (IFC)* recommend criteria for discharge into seawater. The criterion for maximum temperature increase is 3 °C at the edge of the mixing zone and is adopted in investigating the thermal plume. In the absence of a definition for the mixing zone, 100 m from the discharge point is used in accordance with the *IFC EHS*

Guidelines. The criterion for maximum salinity change is $\pm 5\%$, relative to the ambient value, at 30 m from the discharge point (BP, 2013).

The current speeds extracted from the hydrodynamic model at Jetty 1 are 0.31 m/s at high tide and 0.04 m/s at low tide. The current speeds extracted at Jetty 2 are 0.04 m/s at high tide and 0.05 m/s at low tide. These values are used in the near-field modelling to represent the ambient currents.

The temperature of the comingled wastewater discharge is 34 °C and its salinity is 39 ppt. Based on these values, the effluent density is estimated to be 1023 kg/m³ by using the El-Dessouky and Ettouney (2002) method embedded in CORMIX. The averaged ambient seawater temperature is 29 °C and the seawater salinity is 30 ppt. Based on these values, the seawater density is estimated to be 1018 kg/m³.

The downstream distances where temperature and salinity standards are achieved were determined and the results for all scenarios are provided in **Table 6.3** and **Table 6.4**. The corresponding dilution factors at these locations are also provided in **Table 6.3** and **Table 6.4**. The dilution curves for comingled discharge from Jetties 1 and 2 at high and low tide is presented from **Figure 6.1** to **Figure 6.4**.

Table 6.3 *The Predicted Downstream Distances from the Discharge Point Where Water Quality Standards are Achieved and the Corresponding Dilution Factors - Comingled Discharge from Jetty 1*

Constituent	Ambient Standard	High Tide		Low Tide	
		Distance ¹ (m)	Dilution Factor	Distance ¹ (m)	Dilution Factor
Temperature	$\leq 3^{\circ}\text{C}$ at 100 m	0.3	1.7	0.1	1.7
Salinity	$\pm 5\%$ of ambient salinity at 30 m	3.4	6.0	1.8	6.0

Downstream distance from the discharge point where temperature increase meets 3°C or salinity change achieves $\pm 5\%$ of ambient salinity.

Table 6.4 *The Predicted Downstream Distances from the Discharge Point Where Water Quality Standards are Achieved and the Corresponding Dilution Factors - Comingled Discharge from Jetty 2*

Constituent	Ambient Standard	High Tide		Low Tide	
		Distance ¹ (m)	Dilution Factor	Distance ¹ (m)	Dilution Factor
Temperature	$\leq 3^{\circ}\text{C}$ at 100 m	2.0	1.7	2.0	1.7
Salinity	$\pm 5\%$ of ambient salinity at 30 m	9.9	6.0	9.8	6.0

Downstream distance from the discharge point where temperature increase meets 3°C or salinity change achieves $\pm 5\%$ of ambient salinity.

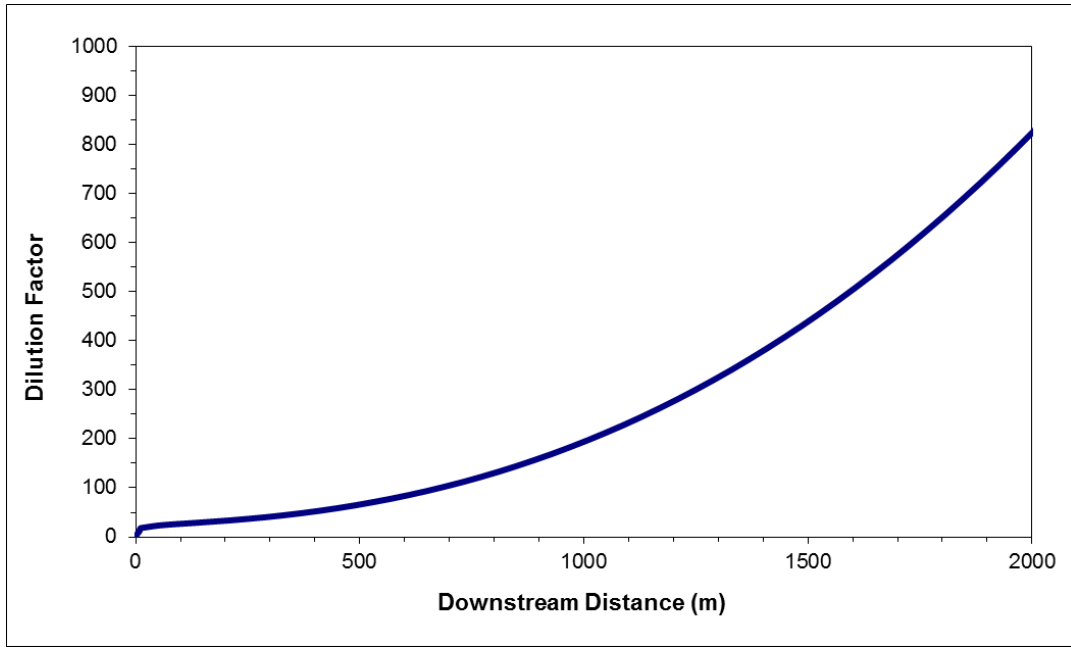


Figure 6.1 Dilution Factor with Downstream Distance - Comingled Discharge from Jetty 1 at High Tide

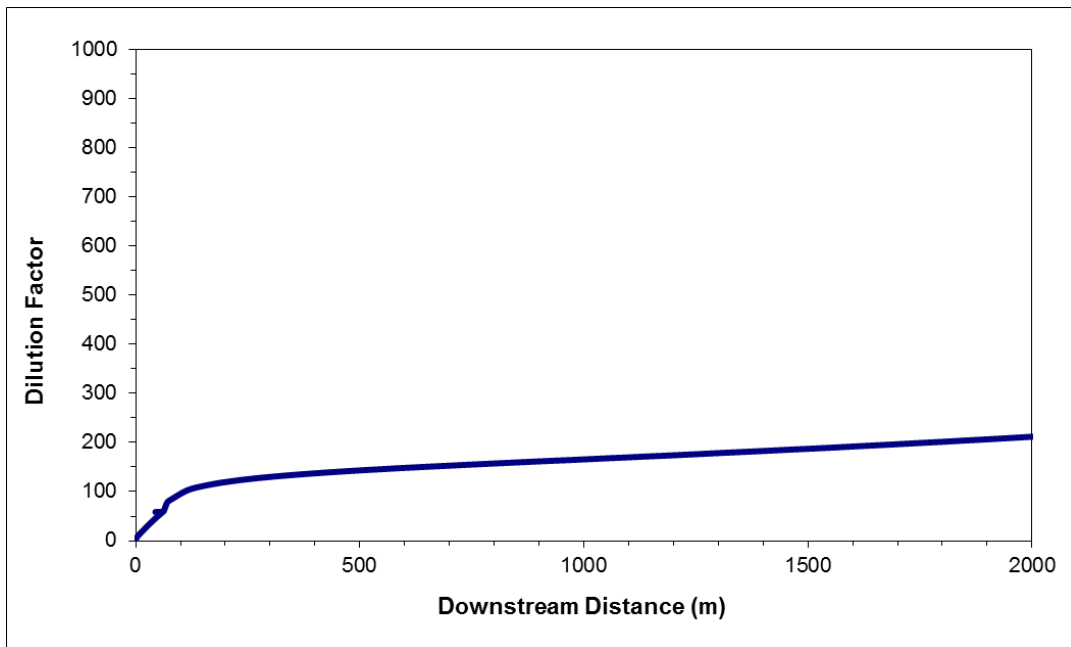


Figure 6.2 Dilution Factor with Downstream Distance - Comingled Discharge from Jetty 1 at Low Tide

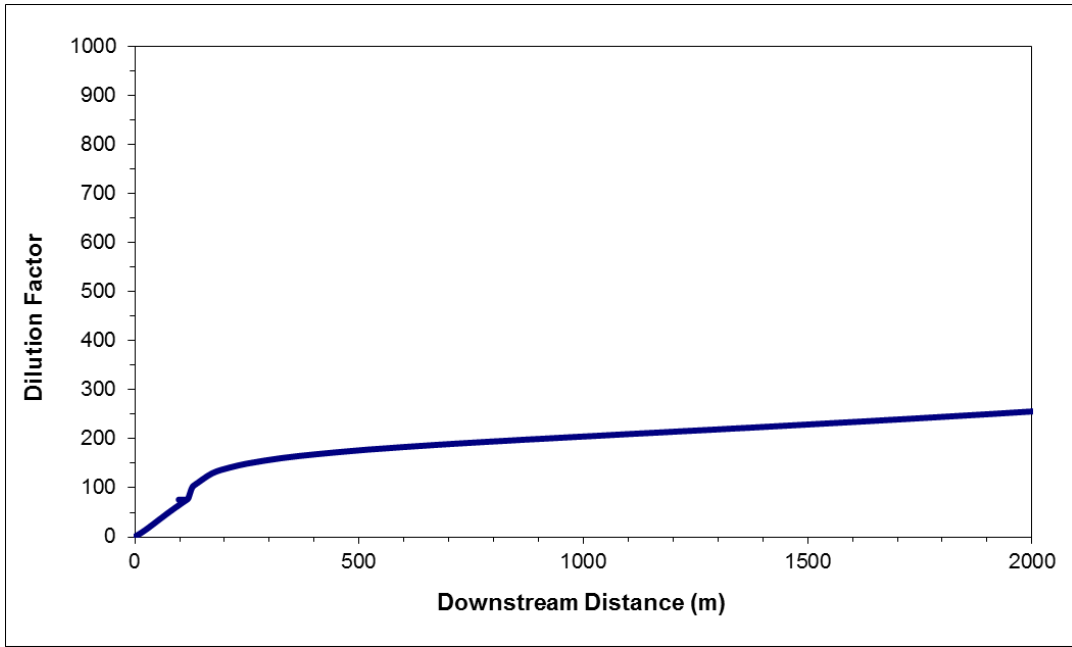


Figure 6.3 *Dilution Factor with Downstream Distance - Comingled Discharge from Jetty 2 at High Tide*

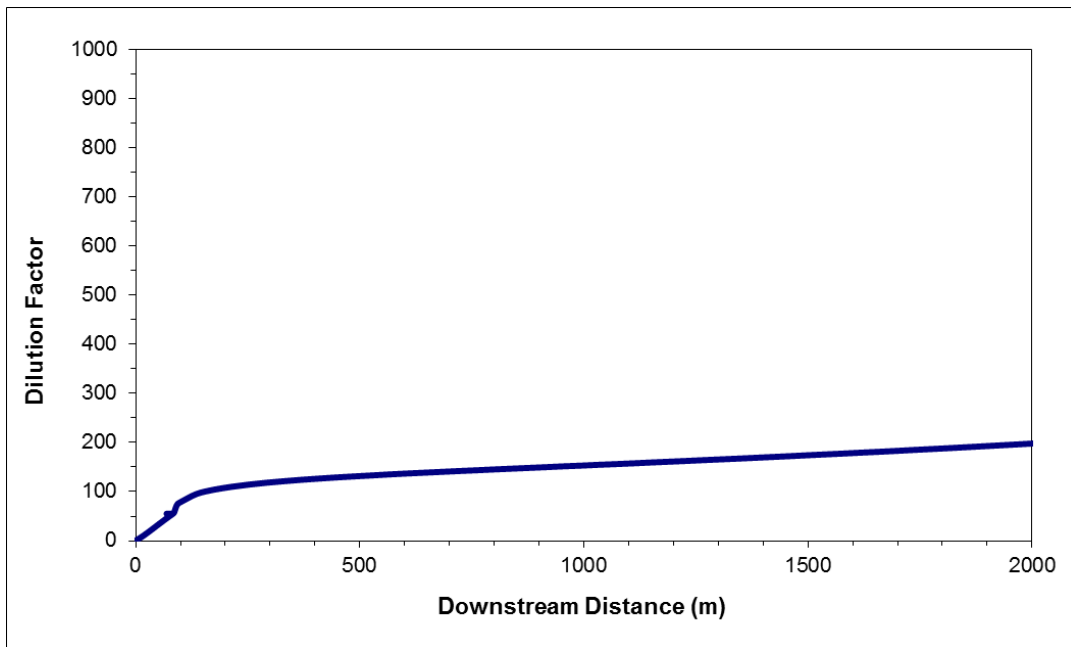


Figure 6.4 *Dilution Factor with Downstream Distance - Comingled Discharge from Jetty 2 at Low Tide*

For comingled wastewater discharge from Jetty 1, it is predicted to reach the ambient temperature and salinity standards at distances of 0.3 m and 3.4 m, respectively, at the high tide stage and to reach the ambient temperature and salinity standards at distances of 0.1 m and 1.8 m, respectively, at the low tide stage. The density of comingled wastewater discharge is higher than that of the ambient seawater. At the low tide stage with small current velocity (0.04 m/s), CORMIX treats the plume as attached to the bottom after discharge and the near-field modeling is unstable in using the assumption that the plume mixes over the full layer depth. However, at the high tide stage with larger current velocity (0.31 m/s), the plume is moving against the strong ambient currents resulting in lower dilutions in the near vicinity of the outfall. Hence, at short distances, the dilution factor is larger at the low tide stage than at the high tide stage. However, as the plume moves along the ambient currents, the dilution increases and the ambient currents dominate the plume mixing. This phenomenon results in larger dilution when the ambient currents are higher (high tide) as opposed to when ambient currents are lower (low tide).

For comingled wastewater discharge from Jetty 2, it is predicted to reach the ambient temperature and salinity standards at distances of 2.0 m and 9.9 m, respectively, at the high tide stage and to reach the ambient temperature and salinity standards at distances of 2.0 m and 9.8 m, respectively, at the low tide stage. The dilution curves for the comingled wastewater discharge from Jetty 2 is observed to be similar at the high and low tide stages.

The current speeds at Jetty 2 (both high and low tide stages) are close to that in the case of the low tide stage discharge from Jetty 1. Hence, the dilution curves in these three cases are found to be similar.

In all scenarios for comingled wastewater discharge, temperature and salinity are predicted to be in compliance with water quality standards.

A sensitivity test was planned to evaluate whether the choice of existing release depth is most optimum for plume mixing. The worst case, comingled wastewater discharge from Jetty 2 at high tide, was selected for the sensitivity test as it is the worst case because it meets both ambient standards at the farthest distance downstream. However, the CORMIX model does not allow selection of depths between -13 m and -6 m (relative to LAT), because the height of the outfall above the seabed is required to be between $1/3^{\text{rd}}$ - $2/3^{\text{rd}}$ of the local ambient water depth. This is an internal CORMIX 1 applicability criteria. Therefore, the sensitivity test was only addressed in the far-field modeling.

6.4 FAR - FIELD MODELLING

The following section presents the findings of the far-field modelling of the comingled wastewater discharge in the LNG terminal port. All maximum concentrations occur at the location and depth of discharge. It should be noted that the far-field model concentrations are average concentrations over each model grid cell. The grid cells in the port area are about 100 m in size, therefore the concentrations at the source actually represent average concentrations over the initial 50 m. For concentrations closer than 50 m from the outfalls, near-field model results should be used.

Figure 6.5 and **Figure 6.6** show the minimum value of the dilution factor over the entire simulated period for the comingled wastewater discharge at Jetty 1 under the dry and wet seasons, respectively. The lowest dilution occurs at the outfall – the discharge is diluted by a factor of 4.6 and 5.7 for dry and wet seasons, respectively. The resulting maximum constituent concentrations, including baseline concentrations, are shown in **Table 6.5** and **Table 6.6**. These maximum concentrations are given for a range of distances from the outfall: 50 m (which represents the grid cell location of the outfall), 100 m, and 500 m. These concentrations are chosen based on the highest concentration at each radius around the outfall.

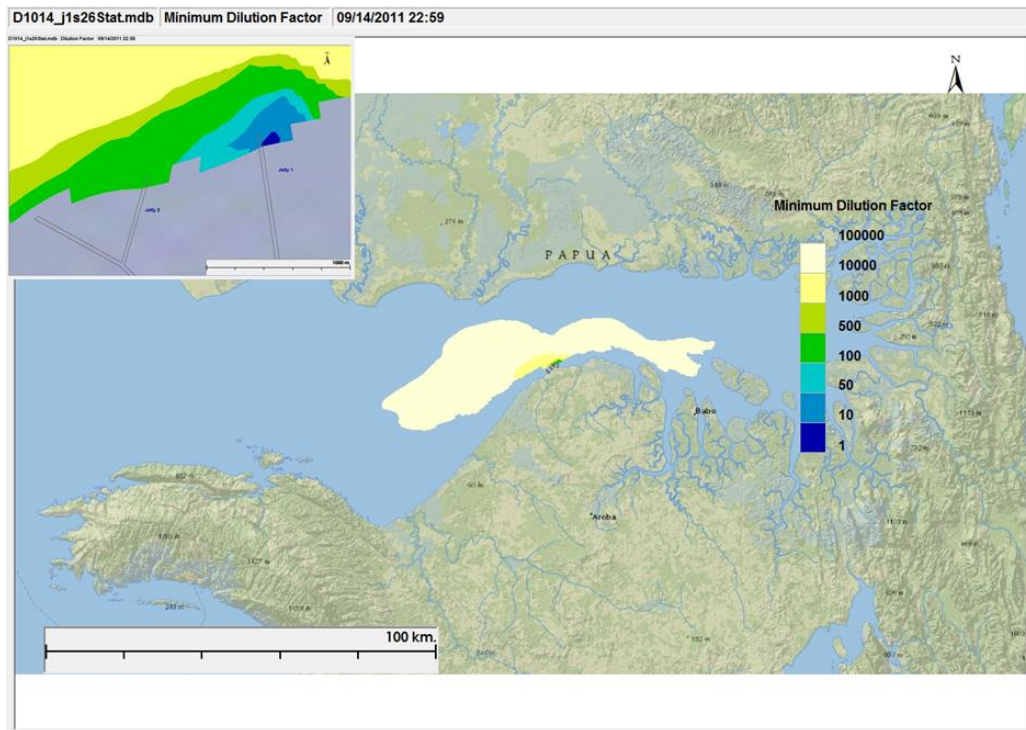


Figure 6.5 *Dry Season Contour Plot of Comingled Jetty 1 Discharge Minimum Dilution Factor*

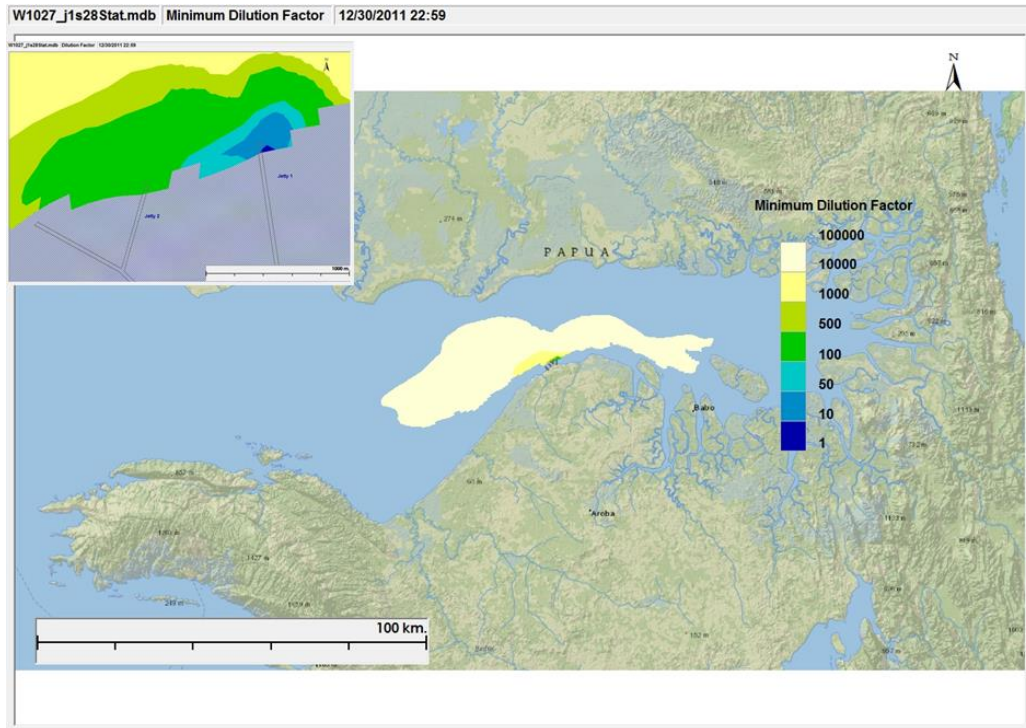


Figure 6.6 *Wet Season Contour Plot of Comingled Jetty 1 Discharge Minimum Dilution Factor*

Figure 6.7 and **Figure 6.8** show the minimum dilution factor for the comingled wastewater discharge at Jetty 2 under the dry and wet seasons, respectively. As in the Jetty 1 simulations, the lowest dilution occurs at the outfall – the discharge is diluted by a factor of 10.4 and 10.2 for dry and wet seasons, respectively. The discharge at Jetty 2 results in higher dilution and lower concentrations than at Jetty 1 mainly due to the greater dispersion that results from discharging 3 m above seabed. The resulting maximum constituent concentrations, including baseline concentrations, are shown in **Table 6.7** and **Table 6.8**.

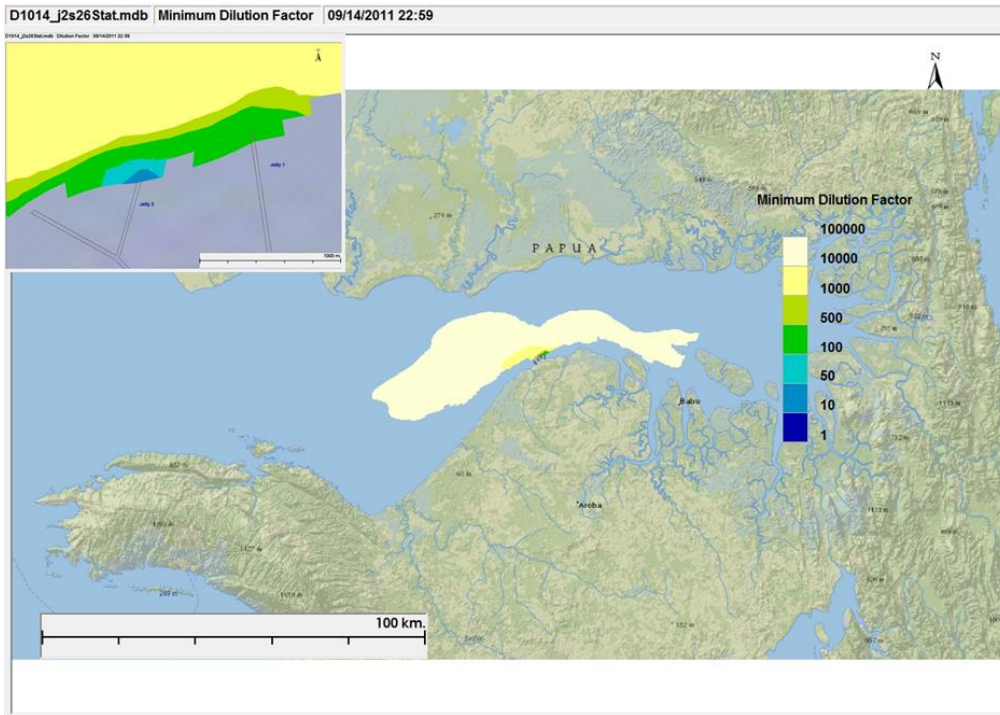


Figure 6.7 *Dry Season Contour Plot of Comingled Jetty 2 Discharge Minimum Dilution Factor*

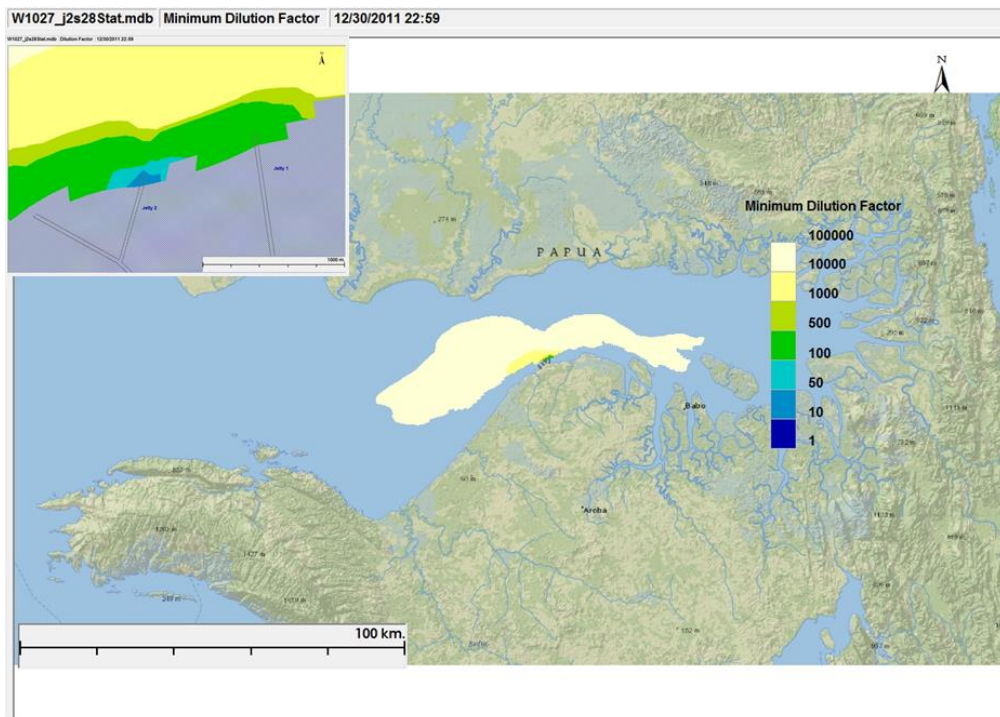


Figure 6.8 *Wet Season Contour Plot of Comingled Jetty 2 Discharge Minimum Dilution Factor*

Table 6.5 Maximum Predicted Dry Season Ambient Concentrations Resulting from Comingled Discharge for Jetty 1

Constituent	Ambient Standard	Maximum Constituent Concentration			
		Distance from Outfall			
		50 m	100 m	500 m	Baseline
Total Ammonia (mg/L as N)	0.30	0.82	0.59	0.08	<0.02
Arsenic (mg/L)	0.0120	0.0022	0.0018	0.0011	0.0010
BOD5 (mg/L)	20.0	3.8	3.3	2.2	2.1
Cadmium (mg/L)	0.0010	0.0012	0.0009	0.0003	0.0002
Chromium-VI (mg/L)	0.005	0.012	0.009	0.003	<0.002
Copper (mg/L)	0.008	0.029	0.021	0.003	0.001
Dissolved Oxygen (mg/L)	>5.00	4.34	4.70	5.46	5.55
Lead (mg/L)	0.008	0.012	0.009	0.002	<0.001
Mercury (mg/L)	0.00100	0.00007	0.00006	0.00005	<0.00005
Oil and Grease (mg/L)	1.0	1.0	1.0	1.0	<1.0
pH	6.5-8.5	8.13	8.11	8.07	8.06
Salinity (ppt)	34.0	30.8	30.1	28.7	28.5
Sulfide (mg/L)	0.010	0.002	0.002	0.002	<0.002
Temperature (°C)	32.0	30.2	29.9	29.2	29.1
Total Phenol (mg/L)	0.002	0.001	0.001	0.001	<0.001
TSS (mg/L)	80.0	60.0	50.5	30.2	27.7
Zinc (mg/L)	0.050	0.226	0.162	0.024	0.007

Constituents that have the potential to exceed ambient standards are indicated in bold.

Table 6.6 Maximum Predicted Wet Season Ambient Concentrations Resulting from Comingled Discharge for Jetty 1

Constituent	Ambient Standard	Maximum Constituent Concentration			
		Distance from Outfall			
		50 m	100 m	500 m	Baseline
Total Ammonia (mg/L as N)	0.30	0.67	0.37	0.08	<0.02
Arsenic (mg/L)	0.0120	0.0022	0.0018	0.0013	0.0013
BOD5 (mg/L)	20.0	3.4	2.8	2.1	<2.0
Cadmium (mg/L)	0.0010	0.0012	0.0008	0.0005	0.0004
Chromium-VI (mg/L)	0.005	0.010	0.007	0.003	<0.002
Copper (mg/L)	0.008	0.024	0.013	0.003	0.001
Dissolved Oxygen (mg/L)	>5.00	4.53	4.97	5.41	5.49
Lead (mg/L)	0.008	0.010	0.006	0.002	<0.001
Mercury (mg/L)	0.00100	0.00007	0.00006	0.00005	<0.00005

Constituent	Ambient Standard	Maximum Constituent Concentration			
		Distance from Outfall			
		50 m	100 m	500 m	Baseline
Oil and Grease (mg/L)	1.0	1.0	1.0	1.0	<1.0
pH	6.5-8.5	7.93	7.90	7.87	7.86
Salinity (ppt)	34.0	27.8	26.8	25.7	25.5
Sulfide (mg/L)	0.010	0.002	0.002	0.002	<0.002
Temperature (°C)	32.0	31.3	31.0	30.7	30.7
Total Phenol (mg/L)	0.002	0.001	0.001	0.001	<0.001
TSS (mg/L)	80.0	52.8	40.9	28.9	26.6
Zinc (mg/L)	0.050	0.182	0.101	0.020	0.005

Constituents that have the potential to exceed ambient standards are indicated in bold.

Table 6.7 Maximum Predicted Dry Season Ambient Concentrations Resulting from Comingled Discharge for Jetty 2

Constituent	Ambient Standard	Maximum Constituent Concentration			
		Distance from Outfall			
		50 m	100 m	500 m	Baseline
Total Ammonia (mg/L as N)	0.30	0.37	0.14	0.06	<0.02
Arsenic (mg/L)	0.0120	0.0015	0.0012	0.0010	0.0010
BOD5 (mg/L)	20.0	2.8	2.4	2.2	2.1
Cadmium (mg/L)	0.0010	0.0007	0.0004	0.0002	0.0002
Chromium-VI (mg/L)	0.005	0.007	0.004	0.003	<0.002
Copper (mg/L)	0.008	0.013	0.005	0.002	0.001
Dissolved Oxygen (mg/L)	<5.00	5.02	5.37	5.49	5.55
Lead (mg/L)	0.008	0.006	0.003	0.002	<0.001
Mercury (mg/L)	0.00100	0.00006	0.00005	0.00005	<0.00005
Oil and Grease (mg/L)	1.0	1.0	1.0	1.0	<1.0
pH	6.5-8.5	8.09	8.07	8.06	8.06
Salinity (ppt)	34.0	29.5	28.9	28.6	28.5
Sulfide (mg/L)	0.010	0.002	0.002	0.002	<0.002
Temperature (°C)	32.0	29.6	29.3	29.2	29.1
Total Phenol (mg/L)	0.002	0.001	0.001	0.001	<0.001
TSS (mg/L)	80.0	42.0	32.7	29.3	27.7
Zinc (mg/L)	0.050	0.104	0.041	0.018	0.007

Constituents that have the potential to exceed ambient standards are indicated in bold.

Table 6.8 Maximum Predicted Wet Season Ambient Concentrations Resulting from Comingled Discharge for Jetty 2

Constituent	Ambient Standard	Maximum Constituent Concentration			
		Distance from Outfall			
		50 m	100 m	500 m	Baseline
Total Ammonia (mg/L as N)	0.30	0.38	0.17	0.05	<0.02
Arsenic (mg/L)	0.0120	0.0018	0.0015	0.0013	0.0013
BOD5 (mg/L)	20.0	2.8	2.3	2.1	<2.0
Cadmium (mg/L)	0.0010	0.0009	0.0006	0.0004	0.0004
Chromium-VI (mg/L)	0.005	0.007	0.004	0.002	<0.002
Copper (mg/L)	0.008	0.014	0.006	0.002	0.001
Dissolved Oxygen (mg/L)	<5.00	4.95	5.26	5.44	5.49
Lead (mg/L)	0.008	0.006	0.003	0.001	<0.001
Mercury (mg/L)	0.00100	0.00006	0.00005	0.00005	<0.00005
Oil and Grease (mg/L)	1.0	1.0	1.0	1.0	<1.0
pH	6.5-8.5	7.90	7.88	7.87	7.86
Salinity (ppt)	34.0	26.8	26.0	25.6	25.5
Sulfide (mg/L)	0.010	0.002	0.002	0.002	<0.002
Temperature (°C)	32.0	31.0	30.8	30.7	30.7
Total Phenol (mg/L)	0.002	0.001	0.001	0.001	<0.001
TSS (mg/L)	80.0	41.3	32.8	28.0	26.6
Zinc (mg/L)	0.050	0.104	0.047	0.014	0.005

Constituents that have the potential to exceed ambient standards are indicated in bold.

Inspection of model results shows that the condition of dry or wet season has very little effect on dilution. With respect to discharge location, discharges at Jetty 2 are much more favourable, with about twice as much dilution. Concentrations decrease with distance from the outfall, as expected. The influence of the outfall drops by about an order of magnitude from 50 to 500 m.

It can be seen that a few constituents, notably heavy metals, have the potential to exceed water quality standards. However, some of these potential exceedances are a result of high detection limits of the waste stream sampling. For cadmium, chromium, and lead the waste stream is reported to have concentrations lower than the corresponding detection limits, however those detection limits are 5-10 times higher than the corresponding standard. Moreover, estimates are conservative for other reasons as indicated previously. Use of the maximum measured discharge concentration provides one such degree of conservatism. Using the median discharge concentration (**Table 6.9**) and discounting the metals that have exceedingly high detection limits shows that only ammonia and DO have the potential to exceed

standards. The DO baseline concentrations are only 0.5 mg/L above the standard, therefore only a small depression in discharge DO can result in exceedance of the standard. The assumption of 0.0 mg/L DO in the waste stream may be too conservative. Based on dilution modelling, a discharge DO value of 3.0 mg/L or higher would be sufficient to meet standards.

Table 6.9 Maximum Predicted Ambient Concentrations Resulting from Comingled Discharge using Median Discharge Concentrations

Constituent	Ambient Standard	Maximum constituent concentration			
		Jetty1		Jetty2	
		Dry	Wet	Dry	Wet
Total Ammonia (mg/L as N)	0.30	0.31	0.25	0.15	0.15
Arsenic (mg/L)	0.0120	0.0016	0.0017	0.0012	0.0015
BOD5 (mg/L)	20.0	2.1	2.0	2.1	2.0
Cadmium (mg/L)	0.0010	0.0012	0.0012	0.0007	0.0009
Chromium-VI (mg/L)	0.005	0.012	0.010	0.007	0.007
Copper (mg/L)	0.008	0.005	0.004	0.003	0.003
Dissolved Oxygen (mg/L)	>5.00	4.34	4.59	5.02	4.95
Lead (mg/L)	0.008	0.012	0.0106	0.006	0.006
Mercury (mg/L)	0.00100	0.00005	0.00005	0.00005	0.00005
Oil and Grease (mg/L)	1.0	1.0	1.0	1.0	1.0
pH	6.5-8.5	8.1	7.9	8.1	7.9
Salinity (ppt)	34.0	29.3	26.6	28.8	26.1
Sulfide (mg/L)	0.010	0.002	0.002	0.002	0.002
Temperature (°C)	32.0	29.3	30.6	29.2	30.6
Total Phenol (mg/L)	0.002	0.001	0.001	0.001	0.001
TSS (mg/L)	80.0	35.6	33.2	31.2	30.3
Zinc (mg/L)	0.050	0.017	0.013	0.011	0.010

Constituents that have the potential to exceed ambient standards are indicated in bold.

Depth Sensitivity

The discharge conditions that represent the ‘worst-case’ scenario, i.e., the conditions that result in the least dilution, is the discharge at Jetty 1 during the dry period. Sensitivity to depth is performed for this scenario by simulating the discharge to be at -6 m LAT. **Figure 6.9** shows the minimum dilution factor for the comingled wastewater discharge at Jetty 1 at -6 m LAT under the dry season. As before, the lowest dilution occurs immediately adjacent to the outfall. At this location the discharge is diluted by a factor of 21.3. This discharge represents a significant improvement in the effects of the comingled discharge. This result is due to the greater plume dispersion resulting from discharging at mid-depth above the seabed. The resulting maximum constituent

concentrations, including baseline concentrations, are shown in **Table 6.10**. As can be seen, no constituents are predicted to exceed ambient standards.

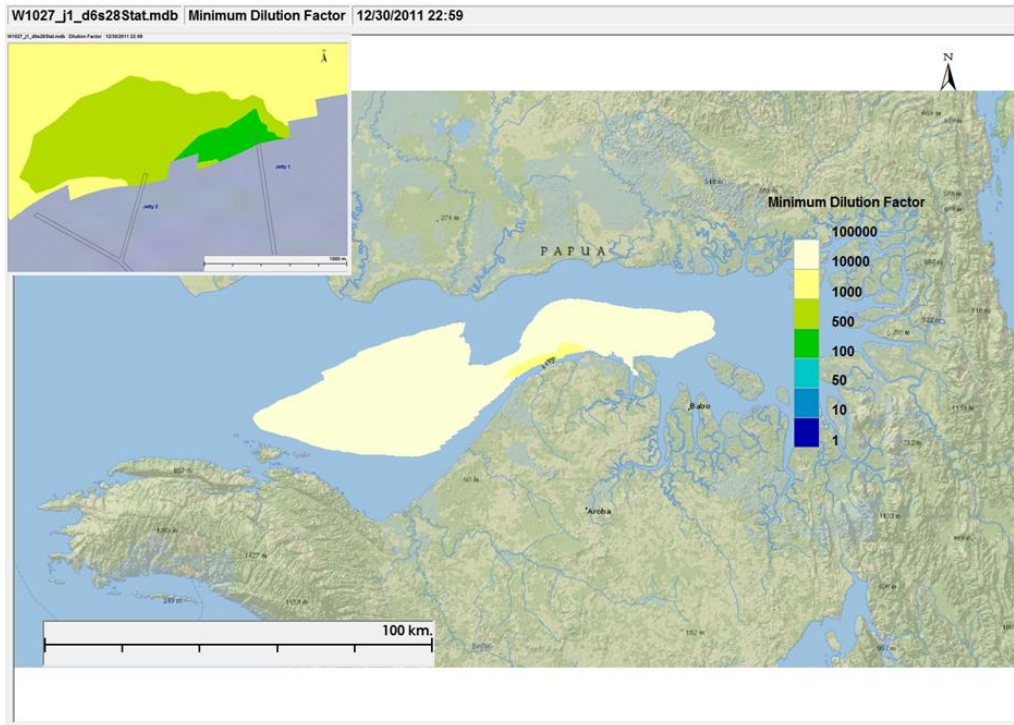


Figure 6.9 Contour Plot of Comingled Jetty 1 Discharge Minimum Dilution Factor Sensitivity (-6 m Discharge)

Table 6.10 Maximum Predicted Ambient Concentrations Resulting from Comingled Discharge Jetty 1 Depth Sensitivity

Constituent	Ambient Standard	Maximum constituent concentration	
		Discharge depth -13 m LAT	Discharge depth -6 m LAT
Total Ammonia (mg/L as N)	0.30	0.82	0.19
Arsenic (mg/L)	0.0120	0.0022	0.0012
BOD5 (mg/L)	20.0	3.8	2.5
Cadmium (mg/L)	0.0010	0.0012	0.0004
Chromium-VI (mg/L)	0.005	0.012	0.004
Copper (mg/L)	0.008	0.029	0.007
Dissolved Oxygen (mg/L)	>5.00	4.34	5.29
Lead (mg/L)	0.008	0.012	0.003
Mercury (mg/L)	0.00100	0.00007	0.00005
Oil and Grease (mg/L)	1.0	1.0	1.0
pH	6.5-8.5	8.13	8.07

Constituent	Ambient Standard	Maximum constituent concentration	
		Discharge depth -13 m LAT	Discharge depth -6 m LAT
Salinity (ppt)	34.0	30.8	28.7
Sulfide (mg/L)	0.010	0.002	0.002
Temperature (°C)	32.0	30.2	29.2
Total Phenol (mg/L)	0.002	0.001	0.001
TSS (mg/L)	80.0	60.0	29.4
Zinc (mg/L)	0.050	0.226	0.009

Constituents that have the potential to exceed ambient standards are indicated in bold.

6.5 CONCLUSION

The results of the far-field modelling indicate that the comingled wastewater discharge from the Tangguh LNG Expansion Project has the potential to exceed ambient water quality standards for some constituents. At 100 m from the outfalls, ammonia, chromium, copper, DO, lead, and zinc may exceed. However, for chromium, copper and lead, this prediction is primarily an artefact of the censored nature of the waste stream sampling data. While the estimated ammonia, DO, and zinc concentrations are very conservative due to assumptions made with respect to discharge concentration and no loss processes considered, it may be prudent to employ some simple measures that can mitigate impacts. Lower concentrations can be achieved by using the Jetty 2 outfall. Additional reductions in concentrations can also be achieved by discharging at mid-depth in the water column to allow for greater dispersion. For the same reason, it is expected (although not modelled in this study), that locating the outfall away from the jetties seaward will also increase dispersion and reduce effects.

7 *HYDROTEST WATER DISCHARGE MODELLING*

Hydrotest water discharge is a result of flushing of the pipelines with freshwater treated with biocide, oxygen scavenger, and fluorescein tracer. Flushing is achieved by filling the pipeline with treated water and then ‘pigging’ the pipeline.

7.1 *SCENARIO DESIGN*

Four offshore locations are considered for release: ROA, WDA, VRF, and UBA (see **Figure 3.1**). These locations are chosen by the Tangguh LNG based on the following rationale:

- ROA – Water in WDA-ROA pipeline discharged representing dewatering at ROA location with longest route.
- WDA – Water in ORF-ROA and ROA-WDA pipelines discharged at the same time representing higher volume.
- VRF – Water in ORF-VRF pipeline discharged representing dewatering around East Corridor.
- UBA – Water in ORF-ROA and ROA-UBA pipelines discharged representing dewatering of the longest route.

Each discharge location is considered independently. For the far-field simulations, each outfall is simulated for both representative wet and dry seasonal conditions. For near-field simulations, each outfall is simulated for two representative tidal conditions, high tide and low tide.

The chemicals added to freshwater for hydrotesting are constituents not found naturally in the environment. Therefore, it is assumed that all baseline concentrations for these additives are zero.

7.2 *DISCHARGE INFORMATION*

The ‘pig’ speed is between 0.3 and 0.5 m/s. Speed of 0.5 m/s is assumed as this would result in the highest intensity discharge rate. For a 24” diameter pipeline, the volume per kilometre is approximately 250 m³/km. The combination of speed and volume per kilometre represents a discharge flow rate of 450 m³/hr. The duration of discharge is limited to the time necessary to flush the pipeline. Each discharge location represents the hydrotesting of a different length of pipeline, therefore the discharge duration differs by location as is seen in **Table 7.1**. The discharge depth is at -3 m below LAT at all locations. The outfall pipe is 4” diameter oriented vertically downwards.

Table 7.1 *Hydrotest Water Discharge Locations*

Location	Length (km)	Volume (m ³)	Duration (hours)
ROA	14	3500	7.8
VRF	21	5250	11.7
WDA	32	8000	17.8
UBA	56	14000	31.1

As the duration of discharge is limited, the specific timing of the release for the far-field modelling is chosen from each of the wet and dry period simulations. The timing is chosen to correspond to conditions of low current speed in order to simulate ‘worst case’ conditions. The selected periods are shown in **Figure 7.1** and **Figure 7.2**.

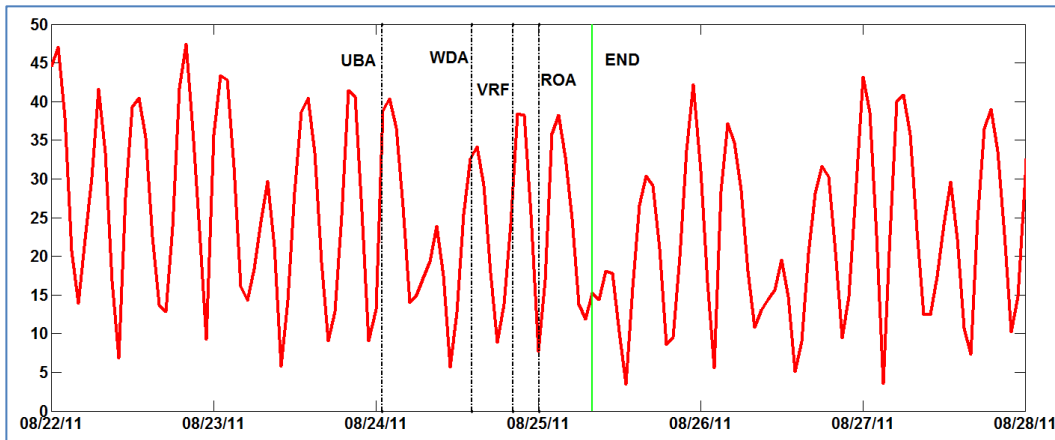


Figure 7.1 *Dry Period Surface Current Speed at Jetty 1 with Discharge Durations Shown*

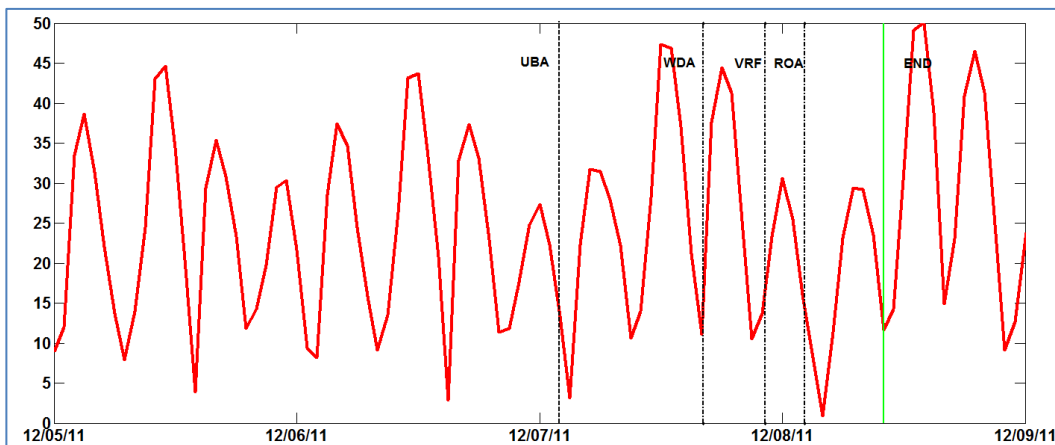


Figure 7.2 *Wet Period Surface Current Speed at Jetty 1 with Discharge Durations Shown*

The treated discharge water is assumed to have concentrations of additives as shown in **Table 7.2**.

Table 7.2 Hydrotest Water Discharge Concentrations

Constituent	Concentration (mg/L)
Oxygen scavenger	100
Biocide	550
Fluorescein Dye	30

7.3 NEAR - FIELD MODELLING

The dilution of hydrotest water from four locations (ROA, WDA, VRF and UBA) in the near-field was studied using CORMIX (described in Section 4.3). Both high and low tide stages are considered for hydrotest water discharges at each location.

At the ROA location, the current speeds extracted from the hydrodynamic model are 0.15 m/s at high tide and 0.50 m/s at low tide. At the WDA location, the current speeds are 0.16 m/s at high tide and 0.22 m/s at low tide. At the VRF location, the current speeds are 0.36 m/s at high tide and 0.14 m/s at low tide. At the UBA location, the current speeds are 0.14 m/s at high tide and 0.18 m/s at low tide. These values are used in the near-field modelling to represent the ambient currents.

The dilution curves at high and low tide stages at the four locations are presented in **Figure 7.3** to **Figure 7.10**.

At ROA location, the dilution factor at the high tide stage is larger than that at the low tide stage within approximately 500 m downstream from the discharge point. However, beyond 500 m, the dilution factor at the low tide stage is larger. At 500 m, the dilution factor at the high (low) tide stage is approximately 1400 (1300). In the near-field region, the plume behaves like a jet and travels faster with weaker dilution when the ambient current velocity is larger. Beyond the near-field region, the plume begins to disperse, and in this process, when the ambient current speed is larger, the dispersion is greater. Therefore, the dilution factor at the high tide stage (smaller current speed of 0.15 m/s) is predicted to be larger than that at the low tide stage (larger current speed of 0.50 m/s) at short distances. At long distances from the discharge point, the dilution factor becomes larger at the low tide stage due to larger currents.

At WDA location, the dilution curve is similar at the high and low tide stages, but beyond 1500 m, the dilution factor at low tide is larger. At 1500 m downstream, the dilution factor at the high (low) tide stage is approximately 2270 (2540). Such trends in the dilution factor at the high and low tide stages are also considered to be caused by the current speed difference as discussed above.

At VRF location, the dilution factor at the low tide stage is larger than that at the high tide stage within 430 m downstream. However, beyond 430 m the dilution factor at high tide is larger. At 430 m downstream, the dilution factor at high (low) tide is approximately 1320 (1150).

At UBA location, the dilution at the low tide stage is larger than that at the high tide stage. At 500 m downstream, the dilution factor at high (low) tide is approximately 420 (570).

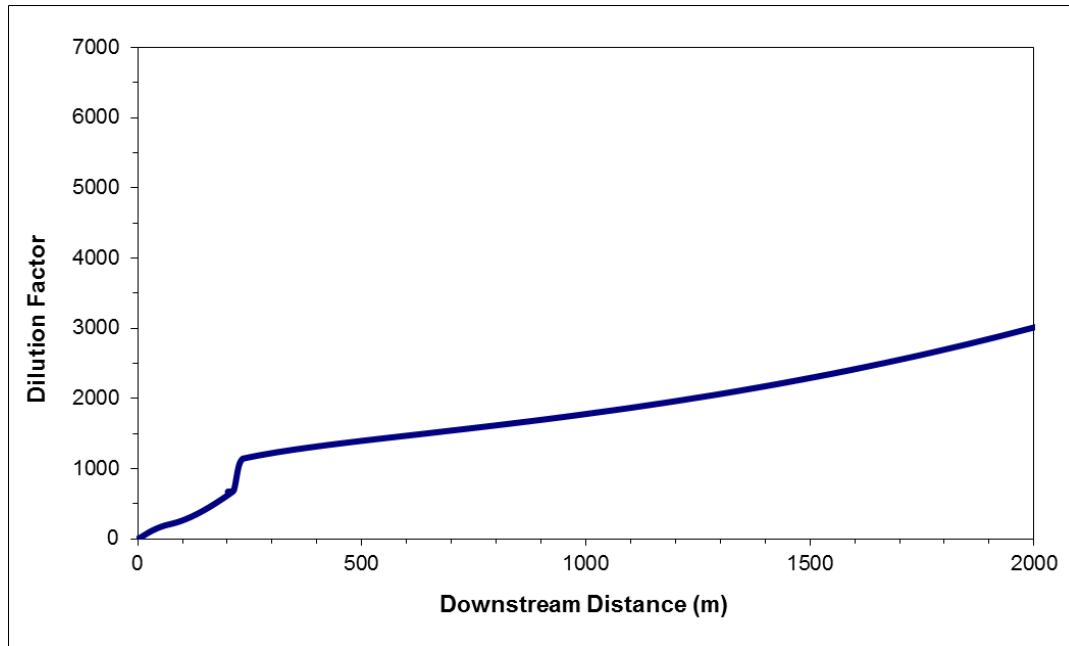


Figure 7.3 *Dilution Factor with Downstream Distance - Hydrotest Water Discharge from ROA at High Tide*

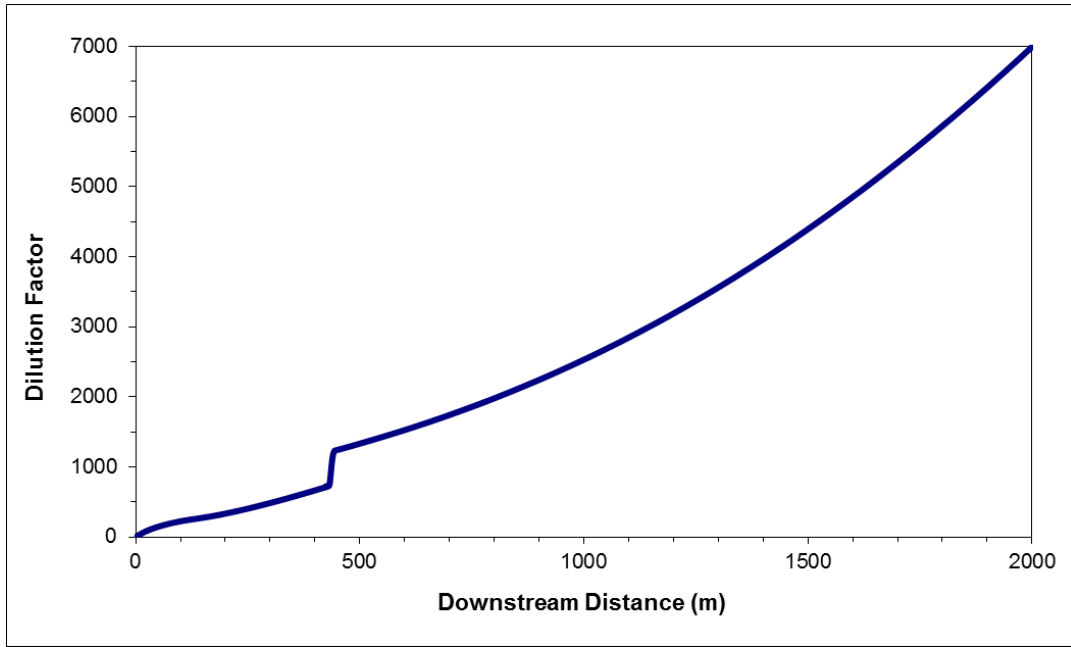


Figure 7.4 *Dilution Factor with Downstream Distance - Hydrotest Water Discharge from ROA at Low Tide*

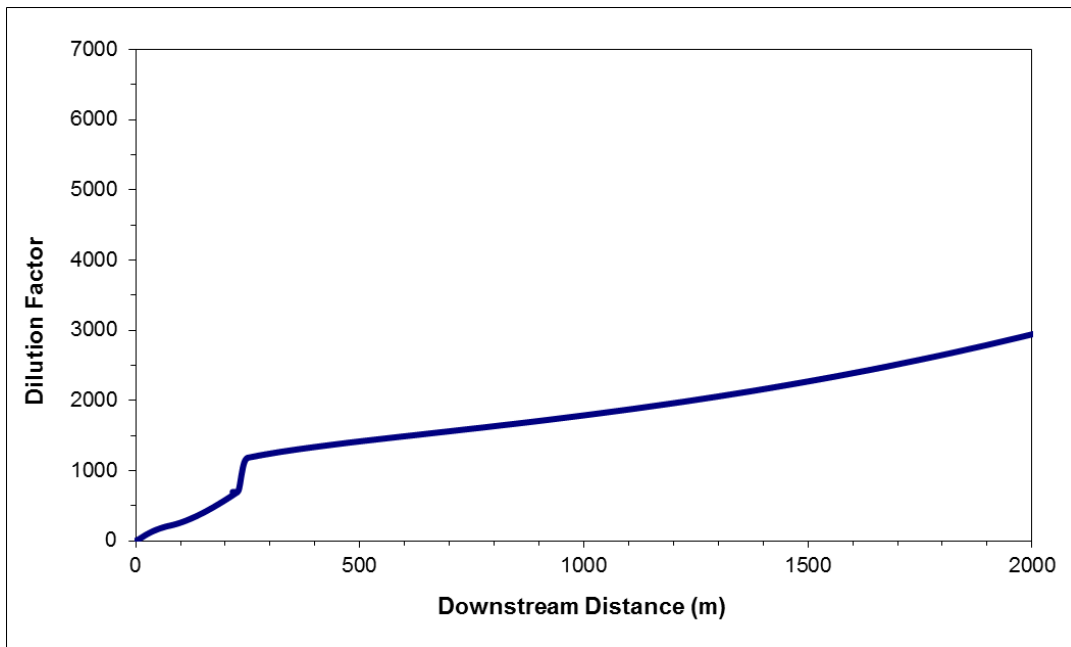


Figure 7.5 *Dilution Factor with Downstream Distance - Hydrotest Water Discharge from WDA at High Tide*

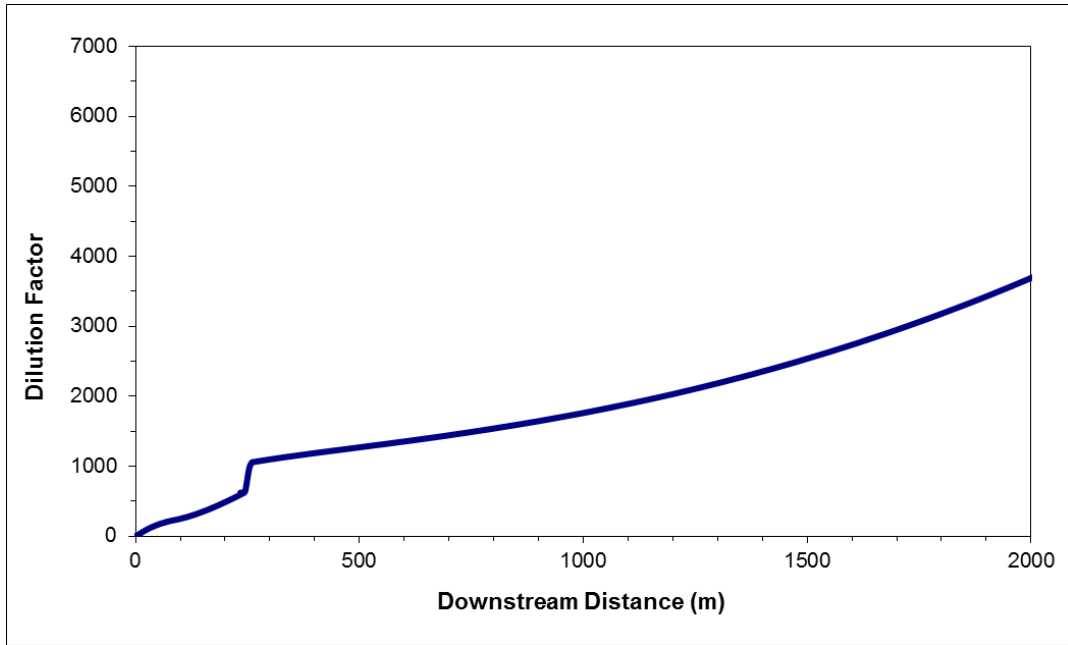


Figure 7.6 Dilution Factor with Downstream Distance - Hydrotest Water Discharge from WDA at Low Tide

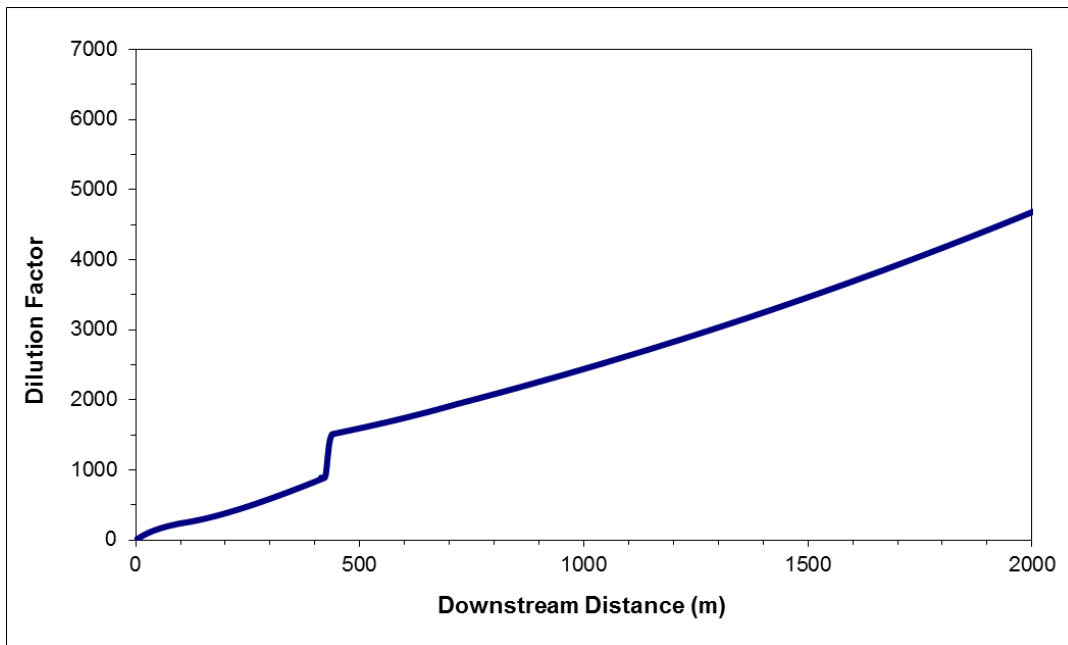


Figure 7.7 Dilution Factor with Downstream Distance - Hydrotest Water Discharge from VRF at High Tide

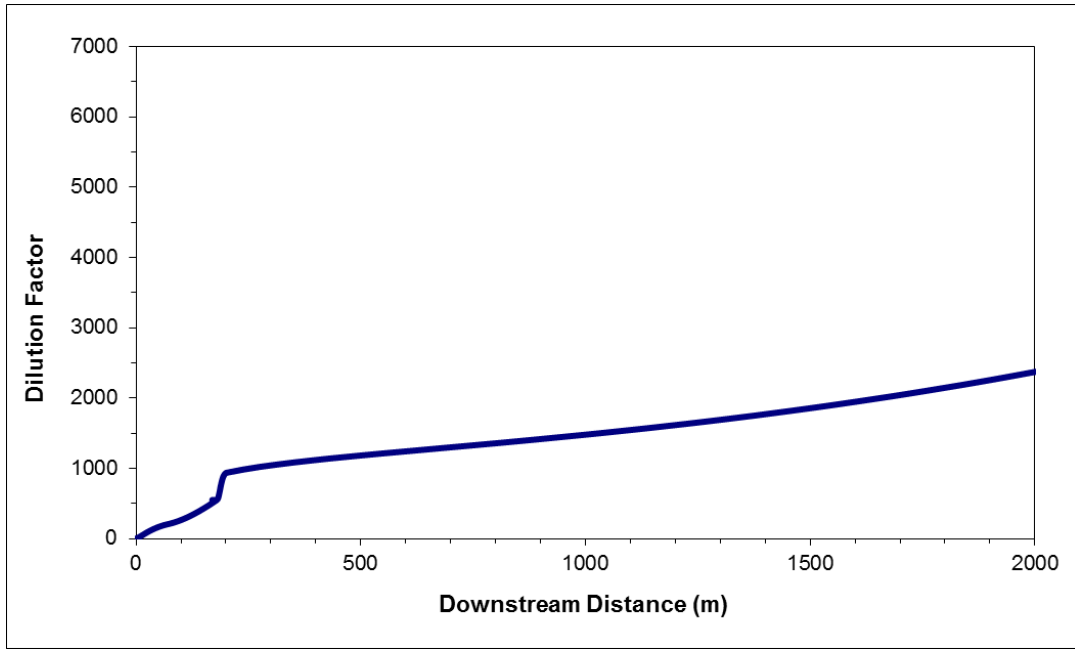


Figure 7.8 *Dilution Factor with Downstream Distance - Hydrotest Water Discharge from VRF at Low Tide*

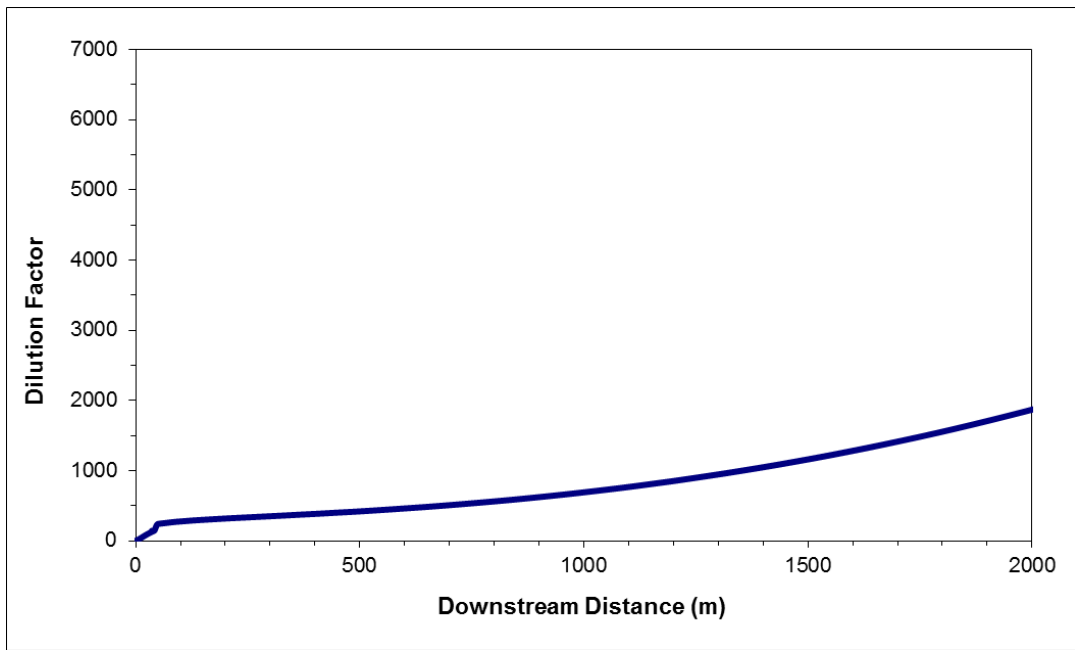


Figure 7.9 *Dilution Factor with Downstream Distance - Hydrotest Water Discharge from UBA at High Tide*

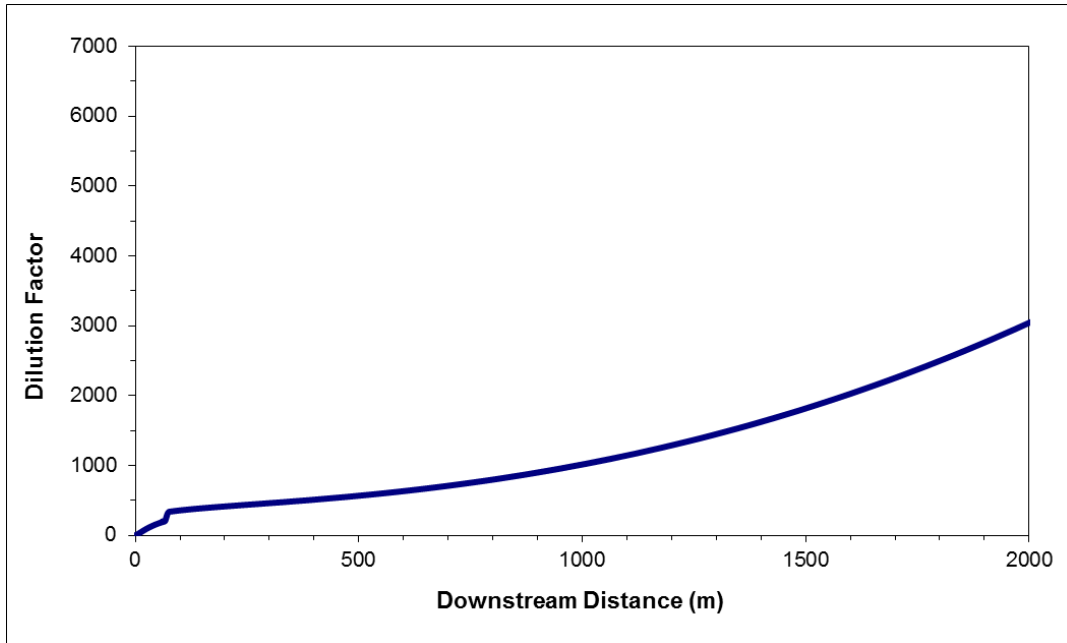


Figure 7.10 Dilution Factor with Downstream Distance - Hydrottest Water Discharge from UBA at Low Tide

7.4 FAR - FIELD MODELLING

The following section presents the findings of the far-field modelling of hydrottest discharges. As expected, discharges in the offshore areas result in considerable dilution of the discharge due to the large volume and high velocities. All maximum concentrations occur at the location and depth of discharge. It should, however, be noted that the far-field concentrations are average concentrations over each grid cell. Because grid cells offshore are 500 to 1000 m in size, the concentrations at the source represent average concentrations over 250 to 500 m. For concentrations closer than this to the outfall, near-field model results should be used.

Additionally, as the hydrottest discharges are of limited duration, the shape and direction of the resultant constituent plume depends in large part on what stage of the tidal cycle the discharge is assumed to occur. For the simulations presented, the discharge is assumed to end during ebb tide, therefore model results tend to favour seaward migration of the discharge. If discharges take place during flood tide, the constituent plume would be oriented in the reverse direction. However, it is expected that dilution would be similar due to similar current statistics. The size of the plume is small and, as such, will not result in any accumulation if oriented towards the interior sections of the Bay under flood conditions.

Figure 7.11 and **Figure 7.12** show the minimum dilution factor over the discharge duration for the hydrotest discharge at ROA under the dry and wet season. The lowest dilution (i.e., the highest concentrations) occurs at the outfall – the discharge is diluted by a factor of 2600 and 1300 for dry and wet seasons, respectively. The resulting maximum constituent concentrations are shown in **Table 7.3**.

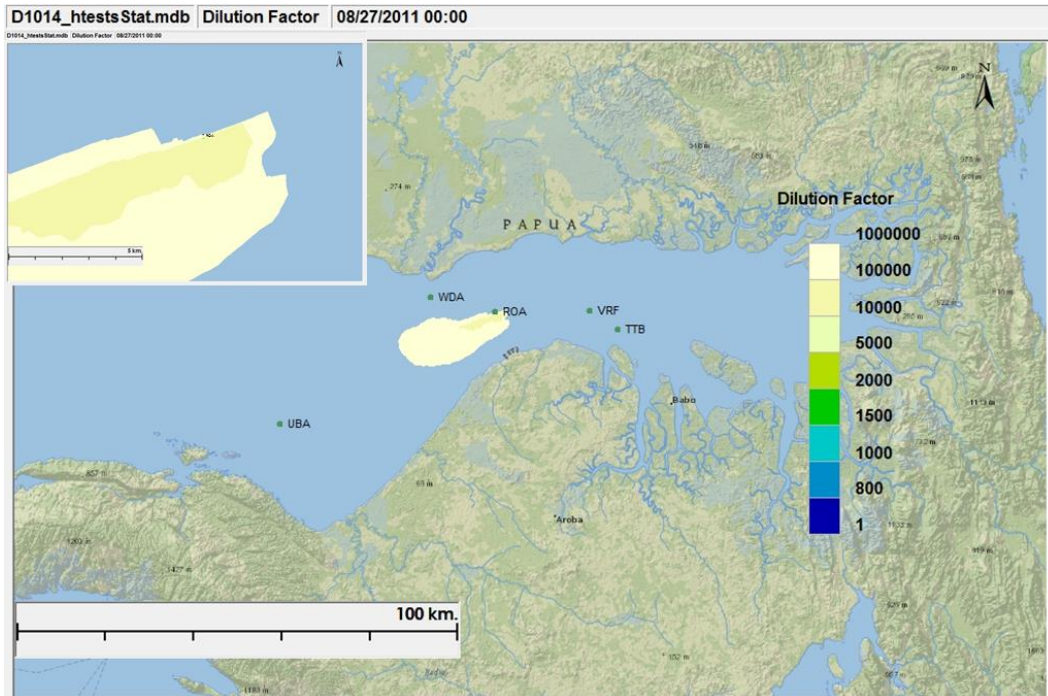


Figure 7.11 *Dry Season Contour Plot of Hydrotest ROA Discharge Minimum Dilution Factor*

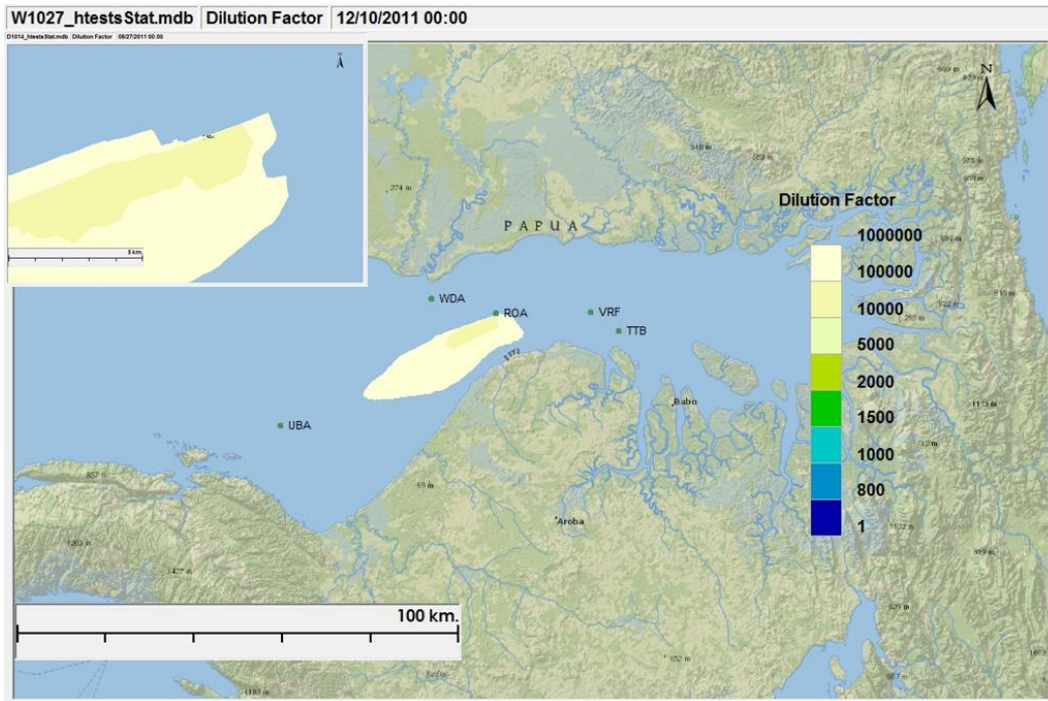


Figure 7.12 Wet Season Contour Plot of Hydrotest ROA Discharge Minimum Dilution Factor

Figure 7.13 and **Figure 7.14** show the minimum dilution factor for the hydrotest discharge at WDA. The lowest dilution values occur at the outfall and are 3300 and 2200 for dry and wet seasons, respectively. Corresponding maximum constituent concentrations are shown in **Table 7.3**.

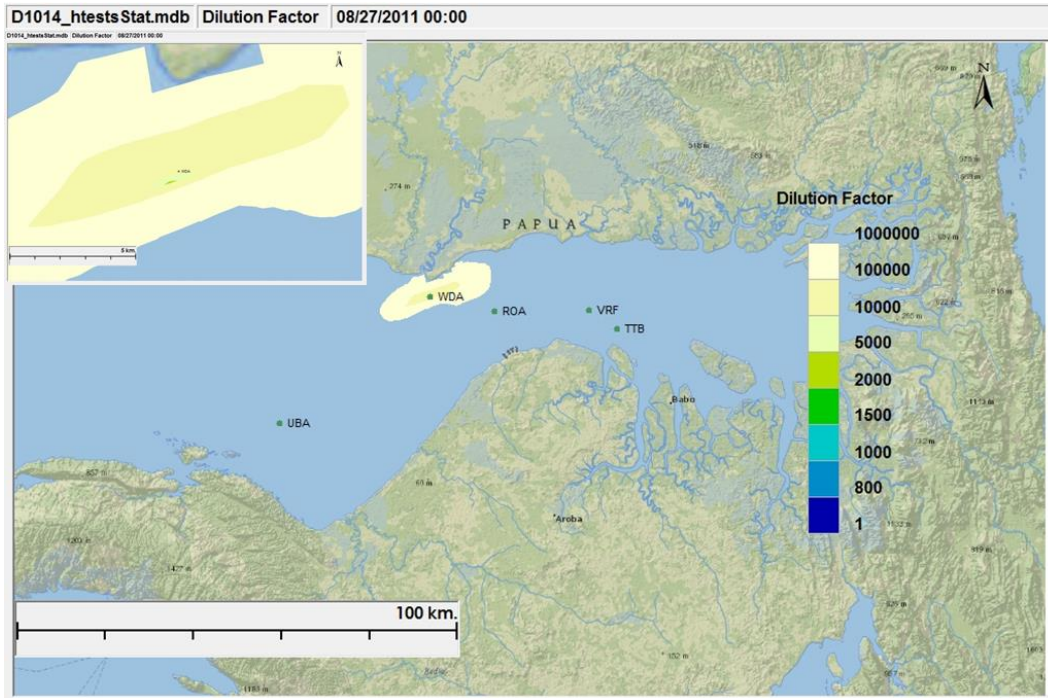


Figure 7.13 Dry Season Contour Plot of Hydrotest WDA Discharge Minimum Dilution Factor

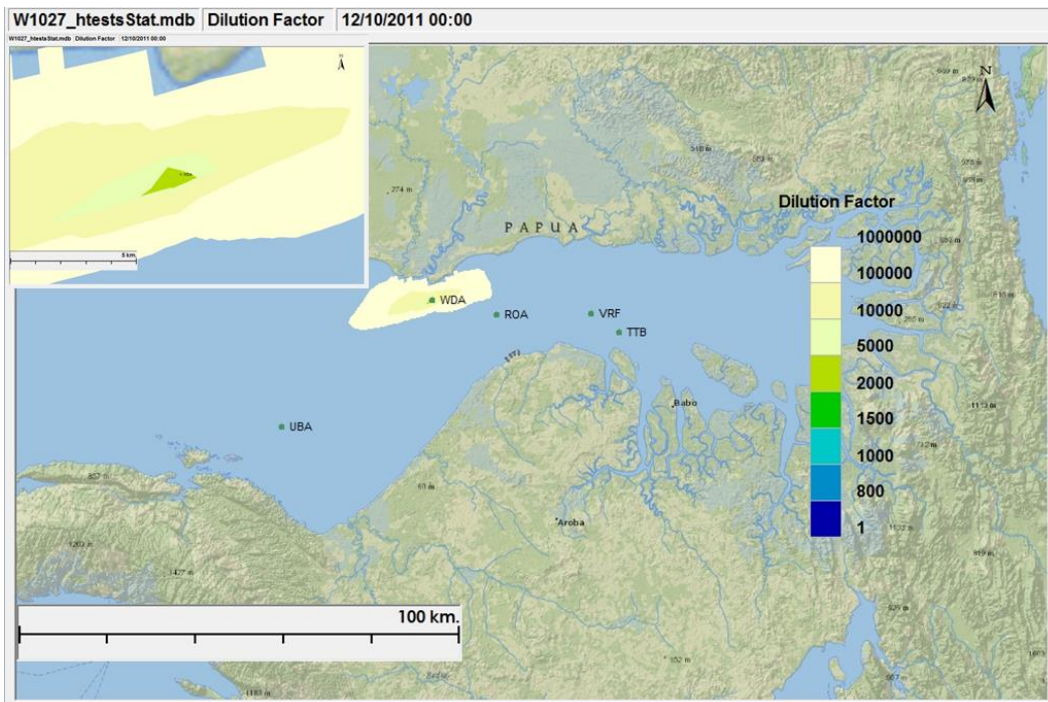


Figure 7.14 Wet Season Contour Plot of Hydrotest WDA Discharge Minimum Dilution Factor

Figure 7.15 and **Figure 7.16** show the minimum dilution factor for the hydrotest discharge at VRF. The lowest dilution results in dilution factors of 2000 and 780 for dry and wet seasons, respectively. Maximum constituent concentrations are shown in **Table 7.3**.

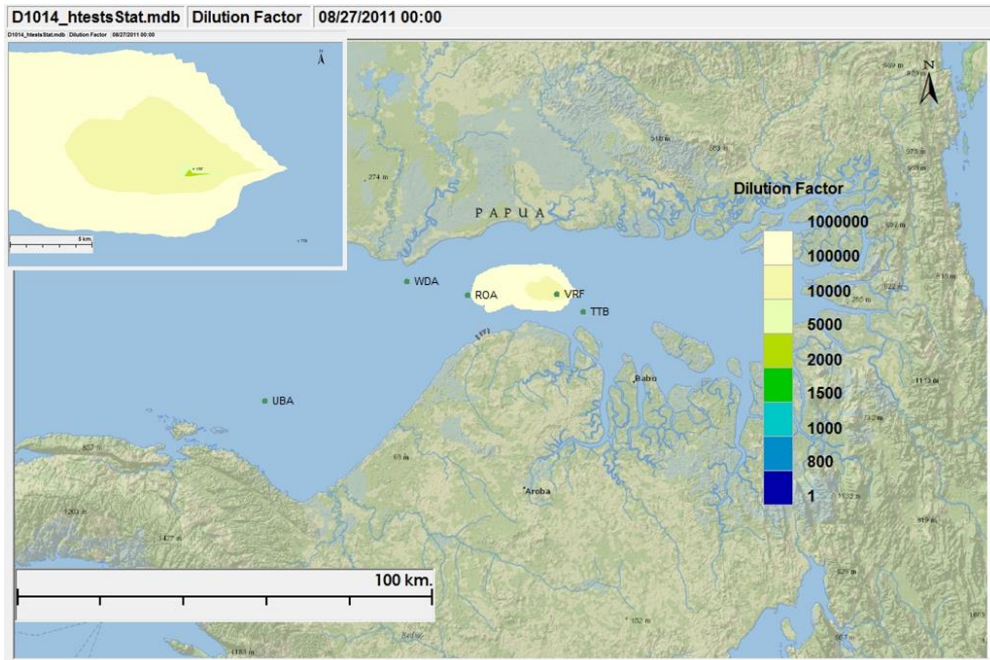


Figure 7.15 Dry Season Contour Plot of Hydrotest VRF Discharge Minimum Dilution Factor

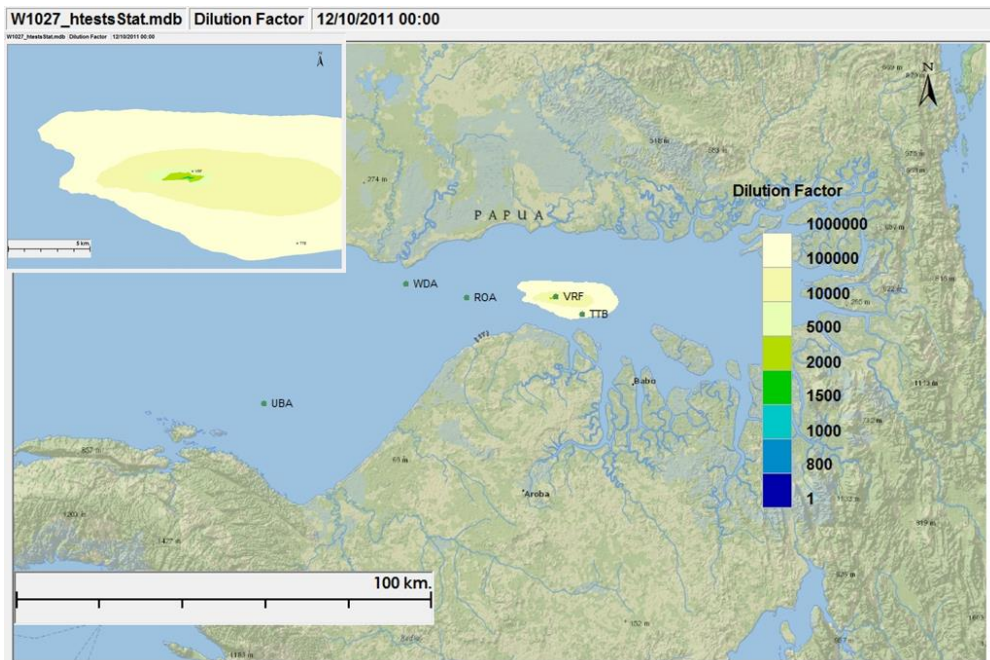


Figure 7.16 Wet Season Contour Plot of Hydrotest VRF Discharge Minimum Dilution Factor

Figure 7.17 and Figure 7.18 show the minimum dilution factor for the hydrotest discharge at UBA. The lowest dilution results in dilution factors of 4400 and 3300 for dry and wet seasons, respectively. Maximum constituent concentrations are shown in Table 7.3.

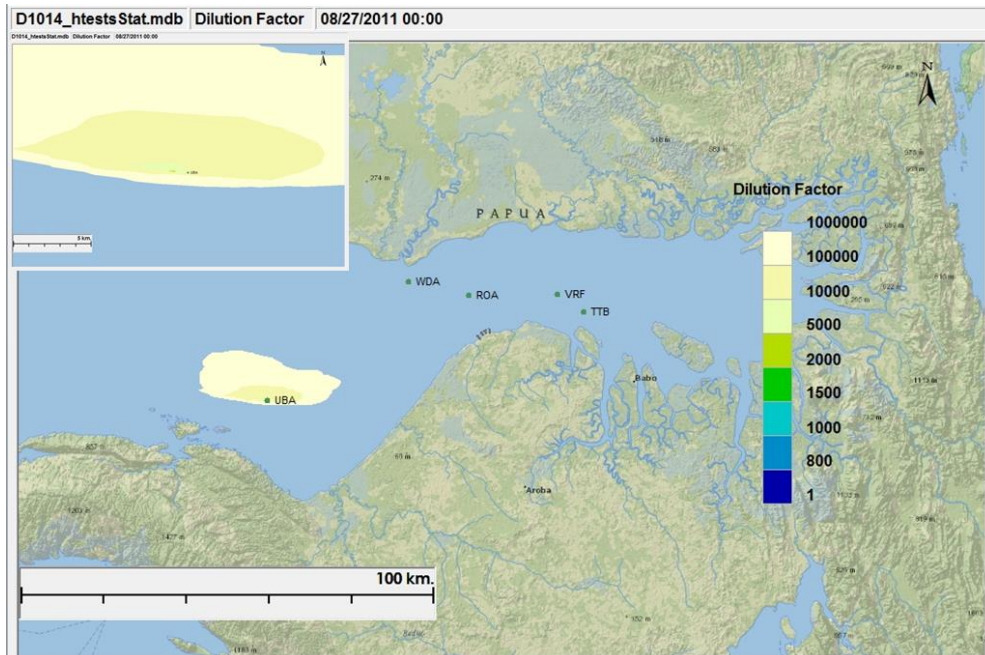


Figure 7.17 Dry Season Contour Plot of Hydrotest UBA Discharge Minimum Dilution Factor

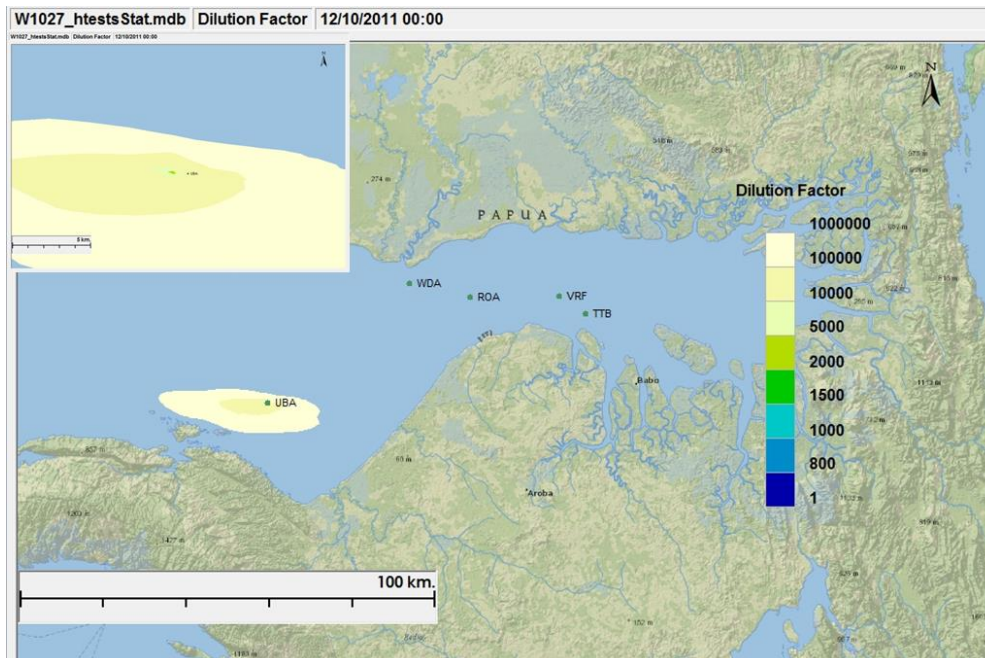


Figure 7.18 Wet Season Contour Plot of Hydrotest UBA Discharge Minimum Dilution Factor

Table 7.3 *Maximum Predicted Ambient Concentrations Resulting from Hydrotest Discharges*

Constituent	Maximum constituent concentration (mg/L)							
	ROA		WDA		VRF		UBA	
	Dry	Wet	Dry	Wet	Dry	Wet	Dry	Wet
Oxygen scavenger	0.038	0.075	0.030	0.045	0.049	0.13	0.022	0.032
Biocide	0.21	0.41	0.16	0.24	0.27	0.71	0.12	0.17
Fluorescein Dye	0.011	0.022	0.009	0.013	0.014	0.038	0.0067	0.0096

7.5 CONCLUSION

The results of the far-field modelling indicate that the discharge of hydrotest water discharge from the platforms will result in very low concentrations of the chemical additives used. While no ambient water quality standards exist for these chemicals, dilution of at least 700:1 can be achieved within the first 500 m. The location that would result in the lowest ambient concentrations is UBA, while the highest concentrations would result at VRF (likely due to the reduced depth and currents). The seasonality of discharge has some effect. Lower concentrations are achieved during the dry season likely due to increased mixing as a result of reduced stratification. The timing (i.e. tidal stage) of the discharge has a large effect on the trajectory of the plume; if potential receptors exist nearby, timing the discharge could allow avoidance of these receptors.

8 COMINGLED WASTEWATER AND HYDROTEST WATER DISCHARGE MODELLING

Hydrotest water discharges at the terminal are investigated considering the hydrotest water to be combined with the wastewater and discharged concurrently.

8.1 SCENARIO DESIGN

The same two discharge locations are considered as in Section 1: the existing outfall at the far end of Jetty 1 and the proposed outfall at the far end of Jetty 2. The full combined discharge is considered to be released from each outfall in turn. For the far-field simulations, each outfall is simulated for representative wet and dry seasonal conditions as described in Section 5.3. For the near-field simulations, each outfall is simulated for two representative tidal conditions, high tide and low tide.

8.2 RELEASE INFORMATION

The release rate, composition, and timing are identical to the information described in Section 6.2 and Section 7.2, with the two discharges released concurrently at the terminal outfalls. It is assumed that the volume of hydrotest water discharged represents the flushing of the longest length of pipeline (UBA: 14,000 m³).

8.3 NEAR - FIELD MODELLING

The dilution of hydrotest constituents is of concern, even though there are no water quality standards for these constituents. The dilution of hydrotest water discharge from Jetties 1 and 2 is predicted by CORMIX using the same ambient conditions as comingled wastewater discharge from Jetties 1 and 2. The dilution factors for the combined (comingled wastewater and hydrotest) water discharge from Jetties 1 and 2 at the high and low tide stages are presented from **Figure 8.1** to **Figure 8.4**. It should be noted that because these dilution curves are for the combined waste stream, the dilution factor for the hydrotest constituents would need to be multiplied by 5.3 ($[Q_{\text{comingled}} + Q_{\text{hydrotest}}]/Q_{\text{hydrotest}}$) to account for the initial dilution associated with combining the waste streams.

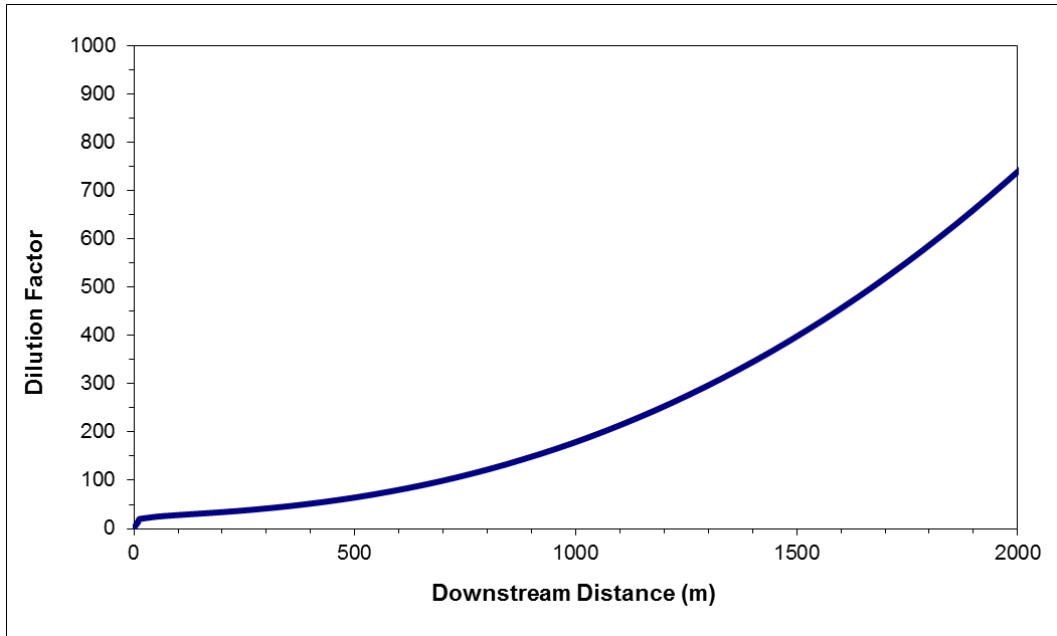


Figure 8.1 *Dilution Factor with Downstream Distance - Hydrotest Water Discharge from Jetty 1 at High Tide*

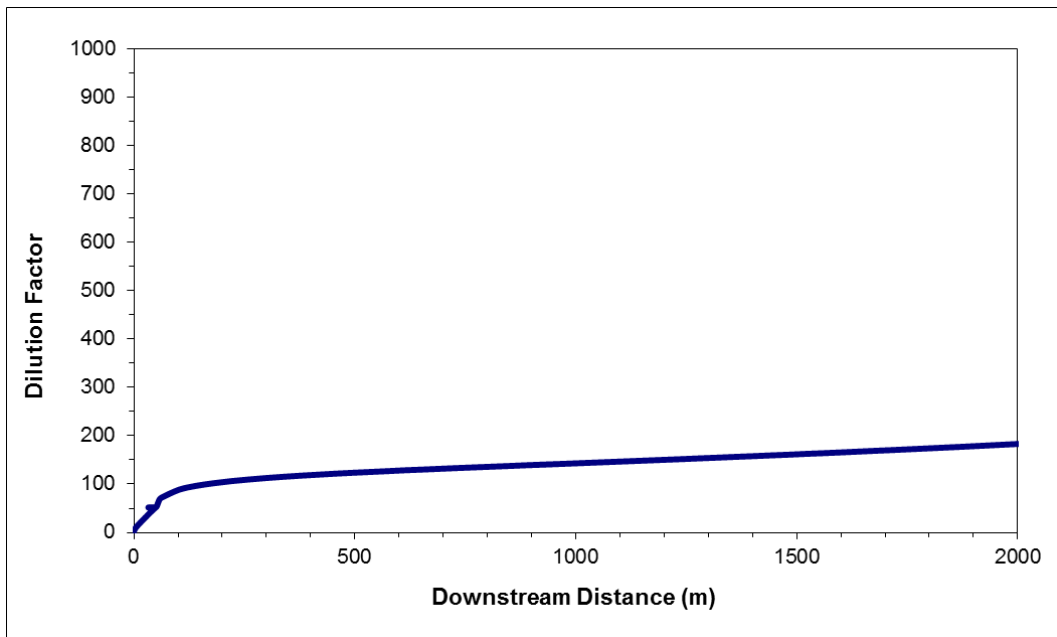


Figure 8.2 *Dilution Factor with Downstream Distance - Hydrotest Water Discharge from Jetty 1 at Low Tide*

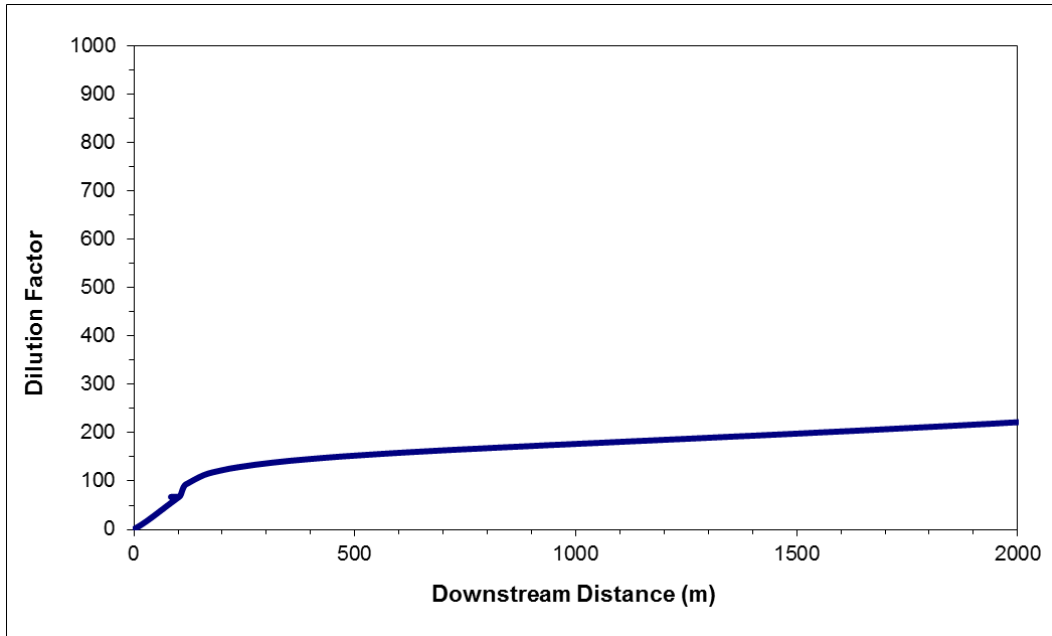


Figure 8.3 *Dilution Factor with Downstream Distance -Hydrotest Water Discharge from Jetty 2 at High Tide*

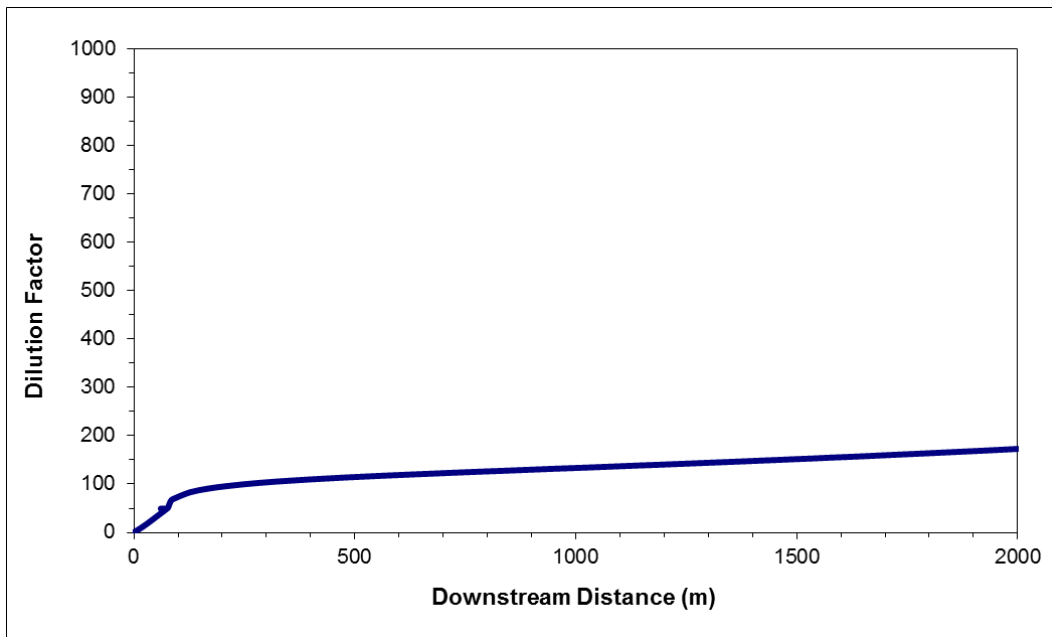


Figure 8.4 *Dilution Factor with Downstream Distance -Hydrotest Water Discharge from Jetty 2 at Low Tide*

For the hydrotest water discharge from Jetty 1, the current velocity at the high tide stage (0.31 m/s) is larger than that at low tide stage (0.04 m/s), and hence a higher dilution factor is expected for the high tide stage. At the high tide stage, the dilution factor is predicted to be 28 (65) at 100 m (500 m) downstream. At the low tide stage, the dilution factor is predicted to be 88 (123) at 100 m (500 m).

For the hydrotest water discharge from Jetty 2, the current velocities at the high tide and low tide stages are quite similar, 0.042 m/s and 0.048 m/s, respectively. Hence, the dilution process at the high and low tide stages are observed to be similar. At the high tide stage, the dilution factor is predicted to be 66 (153) at 100 m (500 m) downstream from the discharge point. At the low tide stage, the dilution factor is predicted to be 75 (115) at 100 m (500 m) downstream from the discharge point. Under the high tide condition for Jetty 2, CORMIX works under the assumption of vertically fully mixed plume. The assumption is a result of low ambient velocities. However, the assumption is not accurate and is attributable to CORMIX's calculation limitations. Under these circumstances, results from the FF model should be considered.

Generally, the dilution of hydrotest water discharge from Jetties 1 and 2 is not observed to be as fast as the dilution of discharge from the ROA, WDA, VRF and UBA locations.

8.4 FAR - FIELD MODELLING

As expected, discharges in the nearshore areas by the terminal result in much less dilution of the discharge than offshore. All maximum concentrations occur at the location and depth of discharge. The grid cells in the port area are about 100 m in size, therefore the concentrations at the source represent average concentrations over the initial 50 m. For concentrations closer than this to the outfalls, near-field model results should be used.

Figure 8.5 and **Figure 8.6** show the minimum dilution factor for the hydrotest portion of the combined waste stream at Jetty 1 under the dry and wet seasons, respectively. The lowest dilution occurs at the outfall – the discharge is diluted by a factor of 21 and 27 for dry and wet seasons, respectively. The resulting maximum constituent concentrations are shown in **Table 8.1**.

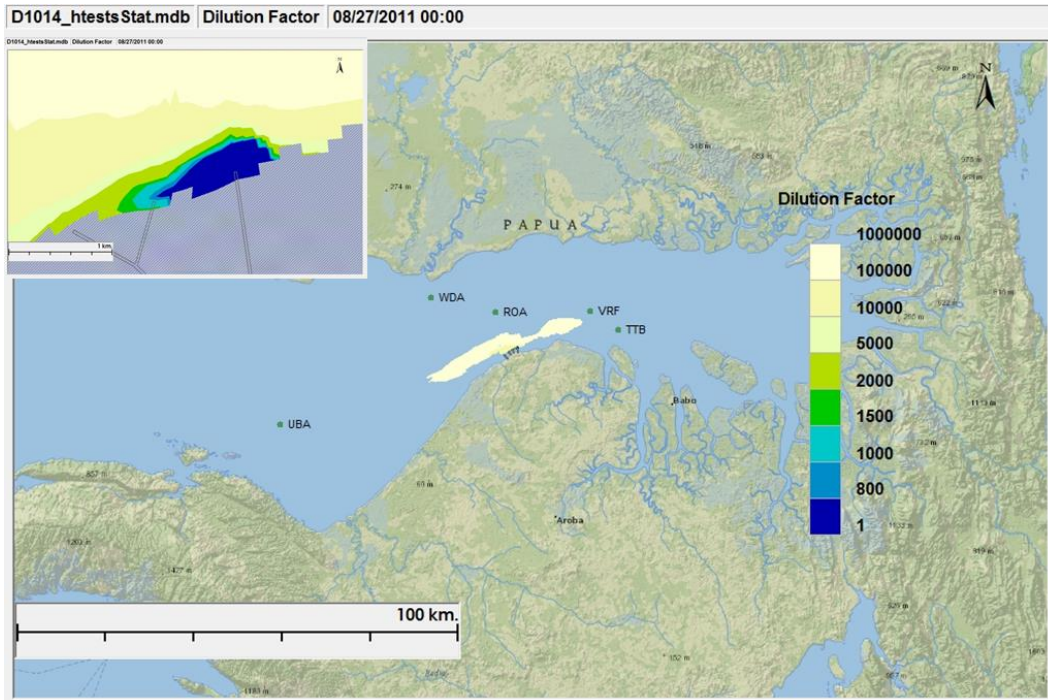


Figure 8.5 *Dry Season Contour Plot of Combined Hydrotest and Comingled Jetty 1 Discharge Minimum Dilution Factor*

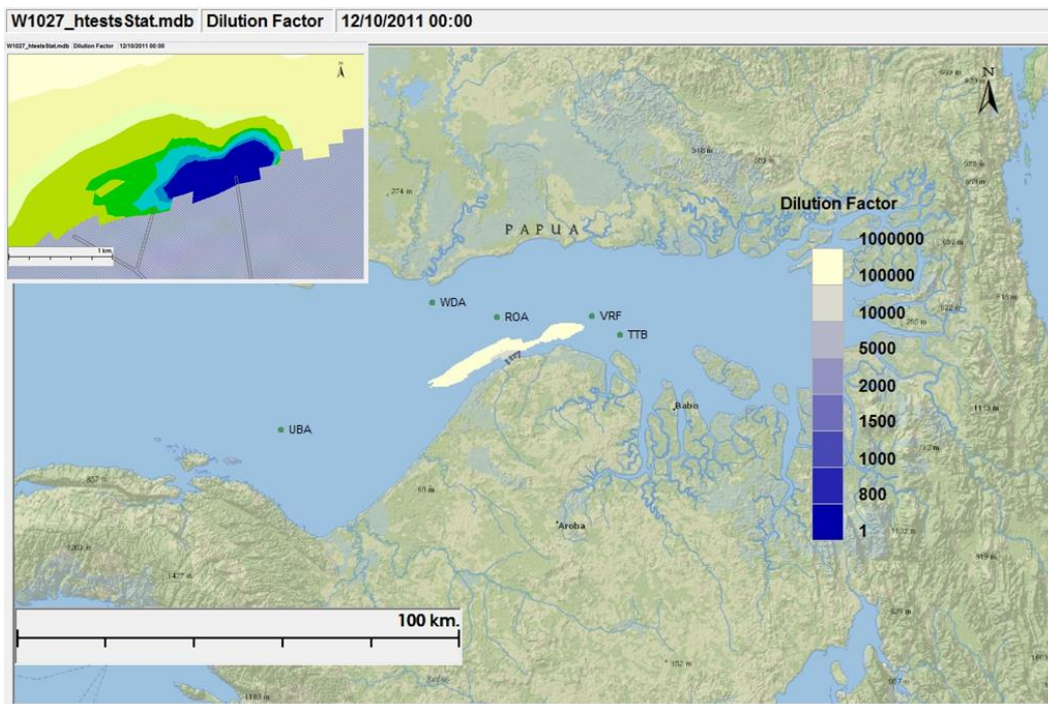


Figure 8.6 *Wet Season Contour Plot of Combined Hydrotest and Comingled Jetty 1 Discharge Minimum Dilution Factor*

Figure 8.7 and **Figure 8.8** show the minimum dilution factor for the hydrotest portion of the combined waste stream at Jetty 2 under the dry and wet seasons, respectively. The lowest dilution occurs at the outfall – the discharge is diluted by a factor of 49 and 44 for dry and wet seasons, respectively. The discharge at Jetty 2 results in higher dilution than at Jetty 1 due to the greater dispersion that results from discharging 3 m above seabed. The resulting maximum constituent concentrations are shown in **Table 8.1**.

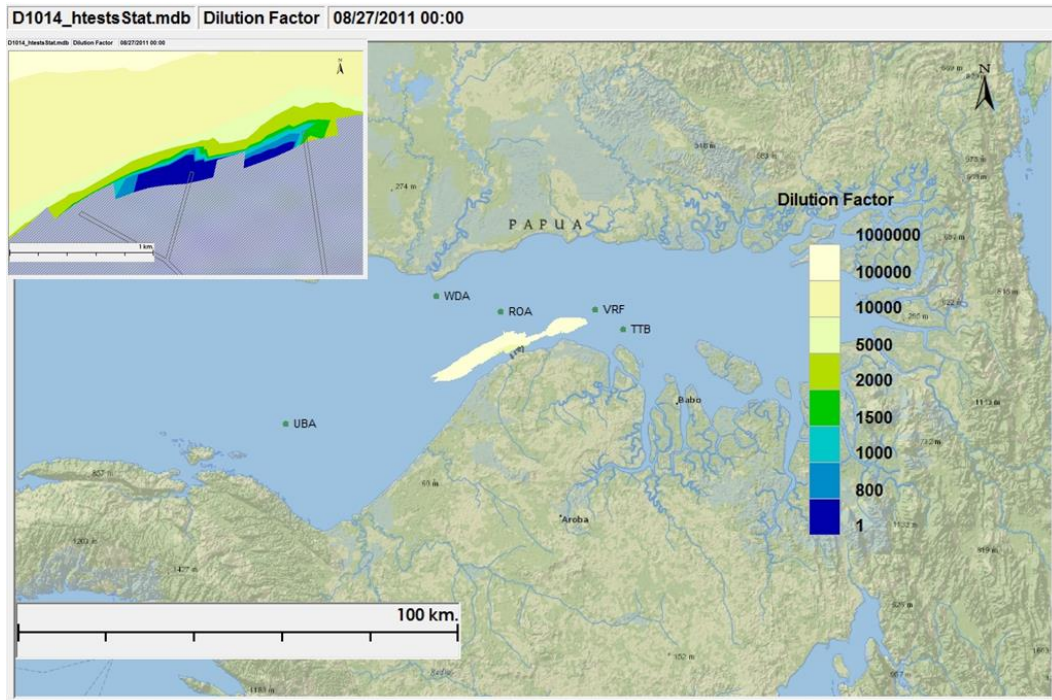


Figure 8.7 *Dry Season Contour Plot of Combined Hydrotest and Comingled Jetty 2 Discharge Minimum Dilution Factor*

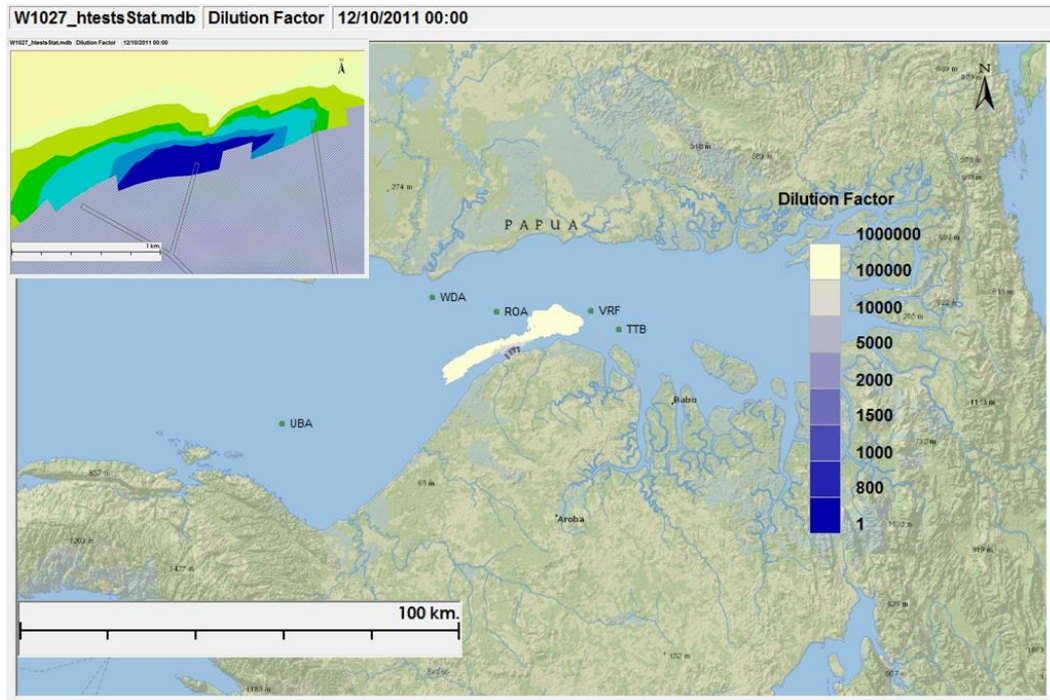


Figure 8.8 Wet Season Contour Plot of Combined Hydrotest and Comingled Jetty 2 Discharge Minimum Dilution Factor

Table 8.1 Maximum Predicted Ambient Concentrations Resulting from Combined Hydrotest and Comingled Discharges at 50m and 100m

Constituent	Maximum constituent concentration (mg/L)							
	Jetty1				Jetty2			
	Dry		Wet		Dry		Wet	
	50m	100m	50m	100m	50m	50m	50m	100m
Oxygen Scavenger	4.8	3.1	3.7	2.2	2.0	0.6	2.3	0.7
Biocide	26.	17.	20.	12.	11.	3.6	13.	3.9
Fluorescein Dye	1.4	0.9	1.1	0.7	0.6	0.2	0.7	0.2

8.5 CONCLUSION

The results of the far-field modelling indicate that the discharge of hydrotest water from the jetty outfalls in the Terminal port will result in much higher concentrations of the chemical additives than discharge at the offshore platforms. This is primarily due to the decreased dispersion associated with the shallower depth and proximity to the shore. Dilution factors at the jetties are about 20 to 50 in the first 50 m. Dilution is over an order of magnitude higher at the platforms than the jetties. As also seen in Section 6.4, Jetty 2 does result in about twice as much dilution as Jetty 1.

During a dredging operation, material is released due to sediment disturbance during dredging and from leaks and overflows from the dredge equipment. It is important to estimate the fate of these dredge materials, which may result in an increase in regional TSS, and in the buildup of sediment near the dredge site.

Model scenarios considered in this study consist of releases of dredged materials during dredging at the base of the BOF (**Figure 3.2**) under metocean conditions representing the same wet and dry seasons used to examine other impacts in this study. The BOF site is used for this modelling because it has the largest amount of dredging needed and therefore represents a worst case.

The physical, chemical and biological impacts of dredge material discharged into surface waters are assessed using three-dimensional fate and transport modelling. The modelling uses data obtained from planned dredge operations and the currents developed as part of this study. Inputs to dredge transport and fate modelling consist of the following:

- metocean conditions (current speed and direction) calculated by the hydrodynamic model;
- depths, the shape of the seafloor, and the distances to and configuration of nearby shorelines; and,
- volumes, properties, and spill durations for released substances and dredge materials.

Model output is used to estimate the sedimentation rate, total suspended solids added to the water column, and thickness of the footprint of settled materials deposited on the seafloor. Scenarios and their results are summarized in the following sections.

9.1

ASSESSMENT CRITERIA

The potential for dredged material to impact aquatic organisms has been assessed through a comparison with sediment deposition volumes and concentrations of TSS above ambient. Acceptable levels of each of these criteria have been based on international literature and previously applied standards as discussed below.

The World Bank's guidance document specifically for offshore oil and gas development offers no guidance value for TSS related to the discharge of cuttings (IFC, 2007a). Though not directly relevant for an offshore discharge of cuttings, the World Bank values provided for wastewater and ambient water quality lists 50 mg/L TSS as a limiting value for treated sanitary sewage discharge (IFC, 2007b). The Indonesian regulations allow for a maximum of 80 mg/L TSS as a protective threshold for mangrove-lined water bodies.

Thickness thresholds vary by species and sediment impermeability. Ellis and Heim (1985) (MarLIN, 2011) suggest a threshold thickness value of 5 cm above the substratum during a month to limit impacts on benthic communities.

Based on the above, the following set of threshold criteria has been taken for the current assessment:

- Criterion 1 - The maximum allowable total suspended solids in the water column in areas supporting mangroves should be no greater than 80 mg/L.
- Criterion 2 - The maximum allowable thickness deposited should not exceed 5 cm in a month period.

No sedimentation rate criteria are used due to the absence of any corals.

9.2 SCENARIO DESIGN

The potential dispersion and deposition of released dredge materials has been quantified using computer modelling techniques. Modelling allows the prediction of the water level, ocean current speeds and directions for periods of interest. Released material will pass vertically through the water column, because dredge materials are denser than the receiving water. Dredge materials dispersion is fundamentally a three-dimensional phenomenon.

Estimates of dredge material volumes are provided by the Tangguh LNG. Specific gravity and particle size distributions are assumed based on previous offshore dredging experience. Discharges are simulated for two different seasons: dry (August) and wet (December). A summary of the scenarios is shown in **Table 9.1**. Dredging is modelled for a constant 8 hour release for the full simulation period of each season. All drilling fluids and cuttings are released at mid-depth (2.5 meters below LAT).

Table 9.1 Scenario List

Site	Season	Scenario
BOF	Wet	1W
	Dry	1D

9.3 DREDGING AND SEDIMENT DATA

Dredge material dispersion modelling is performed to determine the amount of suspended sediment concentrations added to the water column above background and the bottom accumulation of the discharged material (the “footprint”) for assessment of potential adverse impacts to benthic organisms. The dredge material modelling uses the near-field model DREDGE and the far-field sediment fate and transport module, GEMSS-GIFT (Generalized Integrated Fate and Transport).

For the far-field modelling, a two-dimensional (2-D) grid has been constructed covering an area 2 km by 2 km, with 17 m by 17 m grid cells at each location. Subgrids are used to represent complex shoreline and structures. An example grid is shown **Figure 9.1**. This grid is used for computations of sedimentation rate and depositional thickness. A three-dimensional (3-D) adaptive grid was constructed for TSS concentrations, covering areas where suspended sediments travel. This approach provides adaptive resolution with high resolution when the TSS plume is located near the release site and larger coverage when the TSS plume has spread. An example of this adaptive gridding is shown in **Figure 9.2**. Different grids for suspended sediments and settled sediments are used due to their typical travel distances. The total water column depth at the dredge site is 5 m.

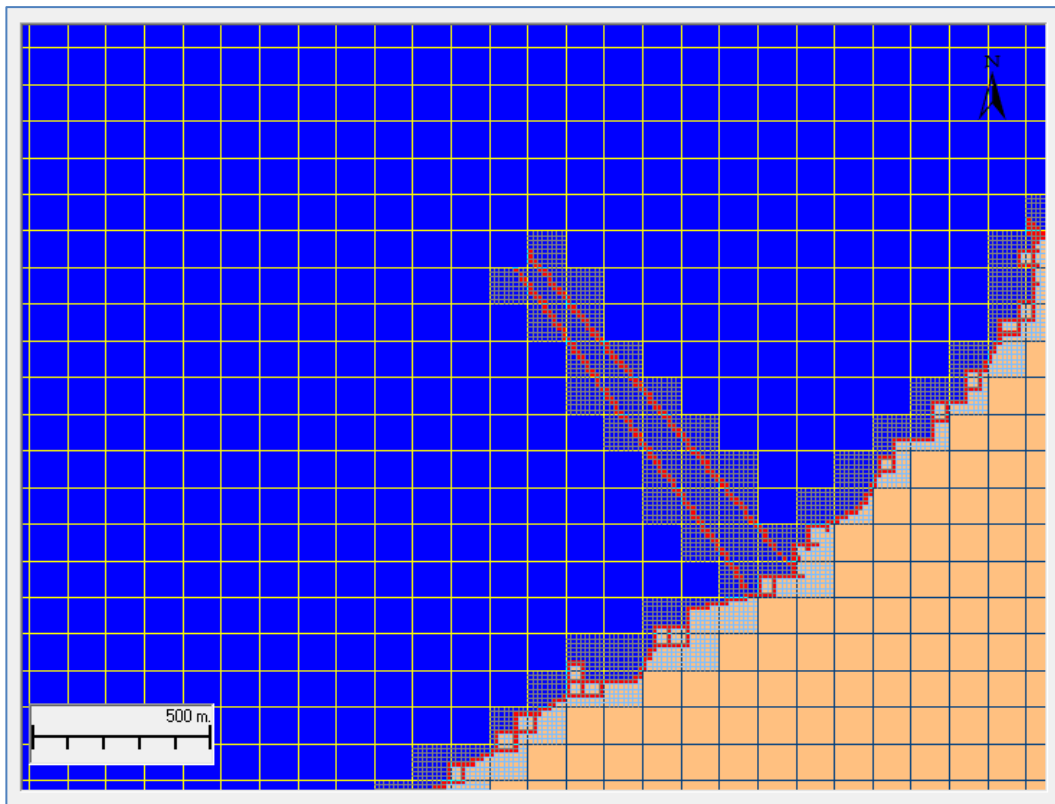


Figure 9.1 Dredge Grid with Subgrids to Represent Complex Shorelines and Structures. Structure Shown in this Grid is the Bulk Offloading Facility

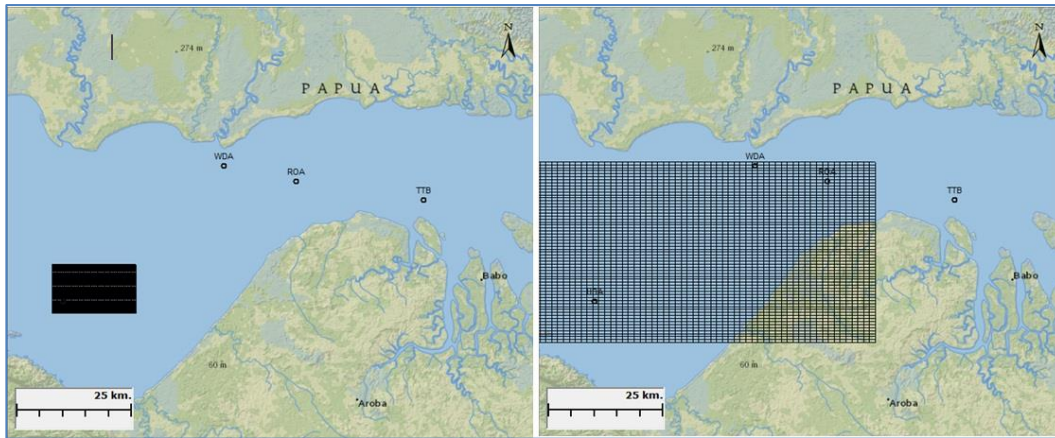


Figure 9.2 Sample Screenshots of the Adaptive TSS Grid for Two Different Times

The planned dredging is assumed to occur eight hours a day with a total dredge material volume of 2000 m³. Based on the dredge duration of eight hours per day, the dredging rate is 250 m³/hr. A conservative assumption of 1% loss is used to estimate the release of material during dredging operation. These estimated release amounts along with the release durations are provided in **Table 9.2**.

Table 9.2 Discharge Characteristics

Scenario	Release Amount (m ³ /hr)	Release Duration (hrs/day)
1W	2.5	8
1D	2.5	8

Particle size distributions for dredge materials are provided in **Table 9.3** based on data provided by the Tangguh LNG. Dredge material density, due to lack of site specific data, is assumed, and is based on previous work experience as provided in **Table 9.4**.

Table 9.3 Dredge Material Particle Size Distribution

Sizes (μm)	Volume Fraction %
4	23
30	44
125	30
2000	3

Table 9.4 Dredge Material Density

Material	Density (kg/m ³)
Dredge material	2650

9.4 NEAR - FIELD MODELLING

To assess the potential dispersion and deposition of dredged marine sediments, the United States Army Corps of Engineers’ (USACE) DREDGE (Hayes and Je, 2008) model is used. This model is a steady-state calculation, developed to estimate impacts from proposed dredging operations. DREDGE computes the rate at which sediments become suspended as the result of hydraulic and mechanical dredging operations, and then computes the resulting suspended sediment plume dimensions and configuration using site-specific information.

According to the proposed dredging program available at the time of this modelling study, an open clamshell, mechanical dredge with a volume of 16-18 m³ is assumed for this study. Using Nakai's Turbidity Generation Unit (TGU) (Palermo et al., 2008) method, a source rate of 1.84 kg/s (1% of source) is calculated. This source rate represents the portion of the sediments resuspended into the water column as a result of turbulence generated by the machinery or leakage of materials during removal. A cycle time of 55 seconds is assumed in the setup. This time is estimated based on the time an open clamshell dredge will take to complete one full cycle at the two different depths. **Table 9.5** details the set of input parameters that are used in the DREDGE simulations.

Table 9.5 Input Parameters

Parameter	Units	Value
Bucket Type	NA	Open Clamshell
Bucket Size	m ³	18
Cycle Time	s	55
Settling Velocity	m/s	0.00002
Water Depth	m	5.15
In-situ Dry Density	kg/m ³	1300
Fraction of Particles Smaller Than 74 µm	NA	67%
Fraction of Particles Smaller Than Particles With Settling Velocity	NA	70%
Lateral Diffusion Coefficient	cm ² /s	10 ⁷
Vertical Diffusion Coefficient	cm ² /s	1.0
Specific Gravity		2.65
Mean Particle Size	µm	35
Source Strength	kg/s	1.84 (1% of source)

The TSS introduced during dredging depends on a number of factors ranging from the type of dredging conducted, dredge cycle duration, depth at the site being dredged and ambient water velocities. Ambient velocities are available from the hydrodynamic modelling results completed for the project, as shown in **Table 9.6**.

Table 9.6 *Velocity Averages for Four Tide Simulations*

Tide Stage	Average Velocity (m/s)
High	0.40
High Slack	0.18
Low	0.10
Low Slack	0.05

Input data listed in **Table 9.5** and **Table 9.6** are provided to DREDGE for the simulation. DREDGE returns the spatially varying water column distribution of TSS. The results are in the form of TSS concentration contours and TSS concentrations values in a spatial matrix. The TSS concentrations are highest along the centerline, the line passing through the dredge location. **Figure 9.3** shows TSS concentrations at different distances along the centerline for all simulations. **Figure 9.4** through **Figure 9.7** show the TSS contours obtained from DREDGE. The maximum TSS concentration of 1.0 mg/L is predicted during high slack tide close to the dredging site, whilst the minimum TSS concentration of 0.6 mg/L is obtained during the low slack water stage. It should be noted that these TSS concentrations are the incremental TSS values above the background TSS, and only represent the TSS released due to one dredge cycle.

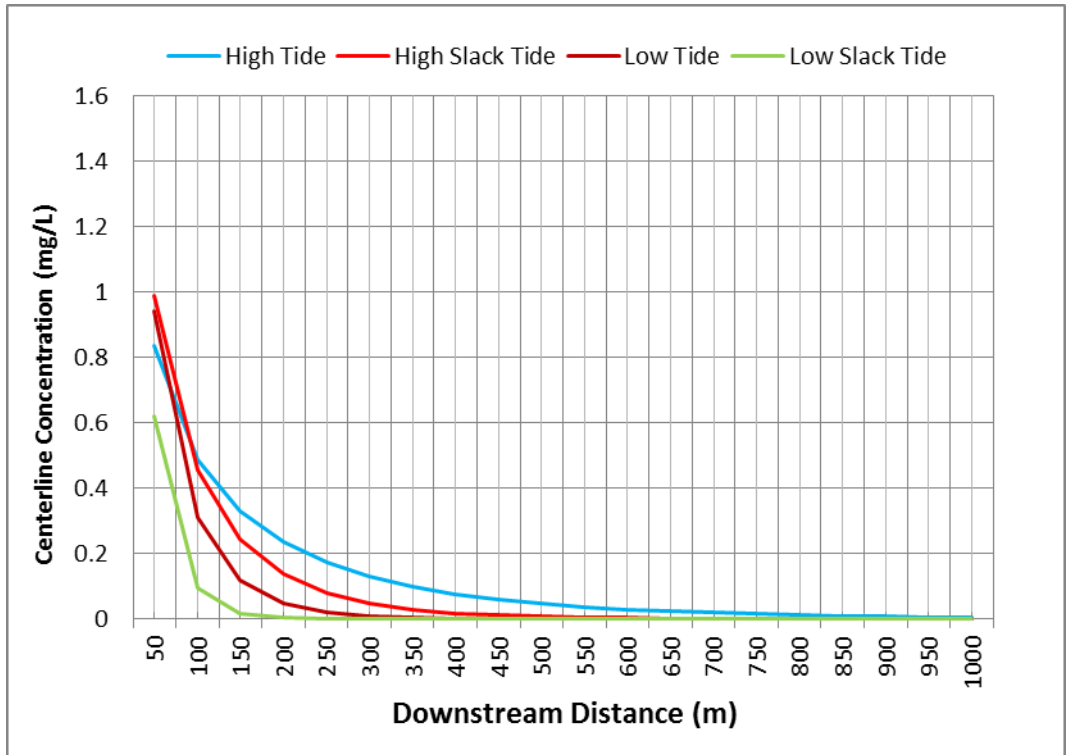


Figure 9.3 Centerline TSS Concentration Versus Downstream Distance in Each Simulation

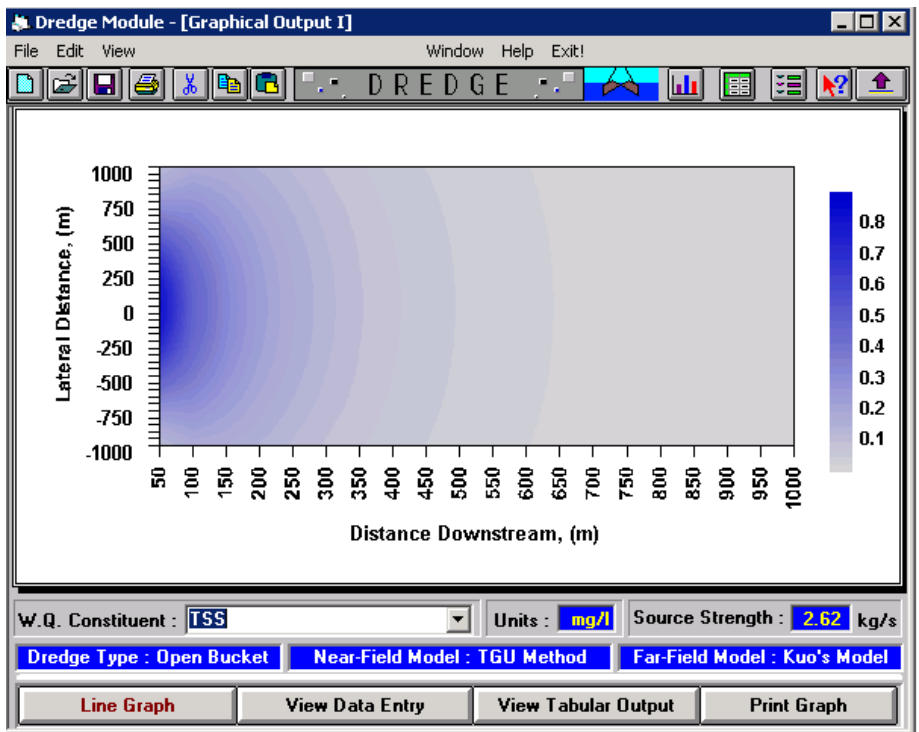


Figure 9.4 TSS Concentration (mg/L) Contours for High Tide

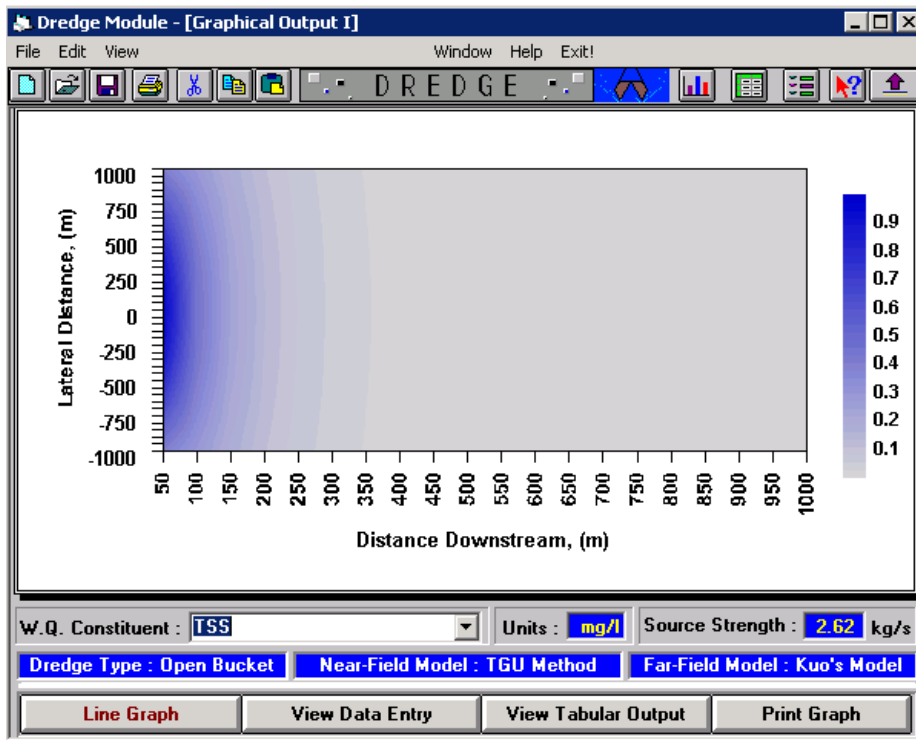


Figure 9.5 TSS Concentration (mg/L) Contours for High Slack Tide

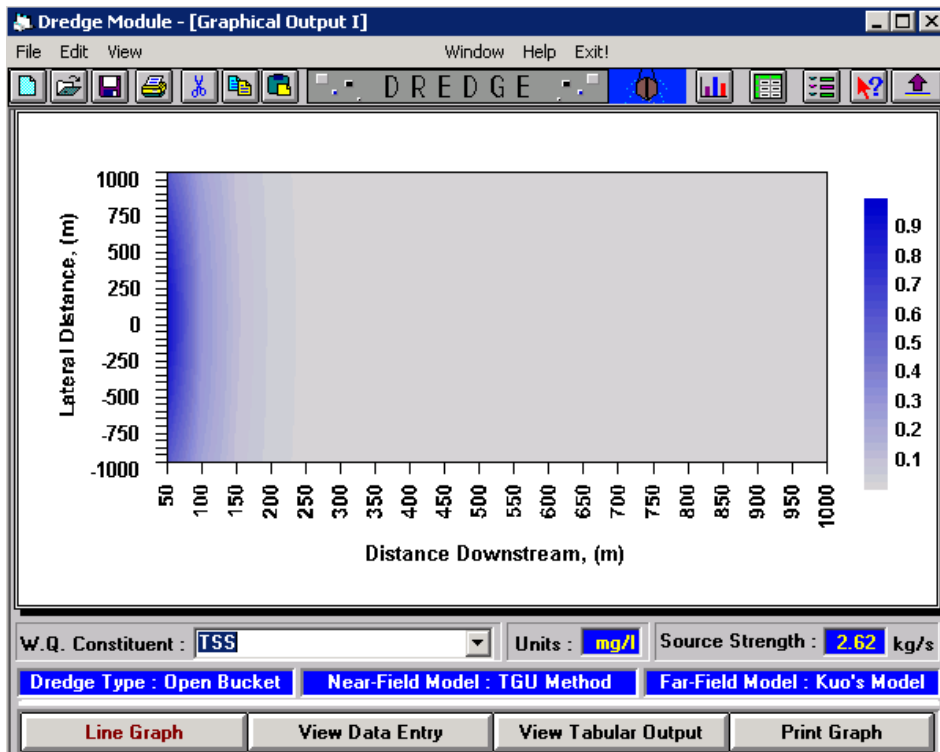


Figure 9.6 TSS Concentration (mg/L) Contours for Low Tide

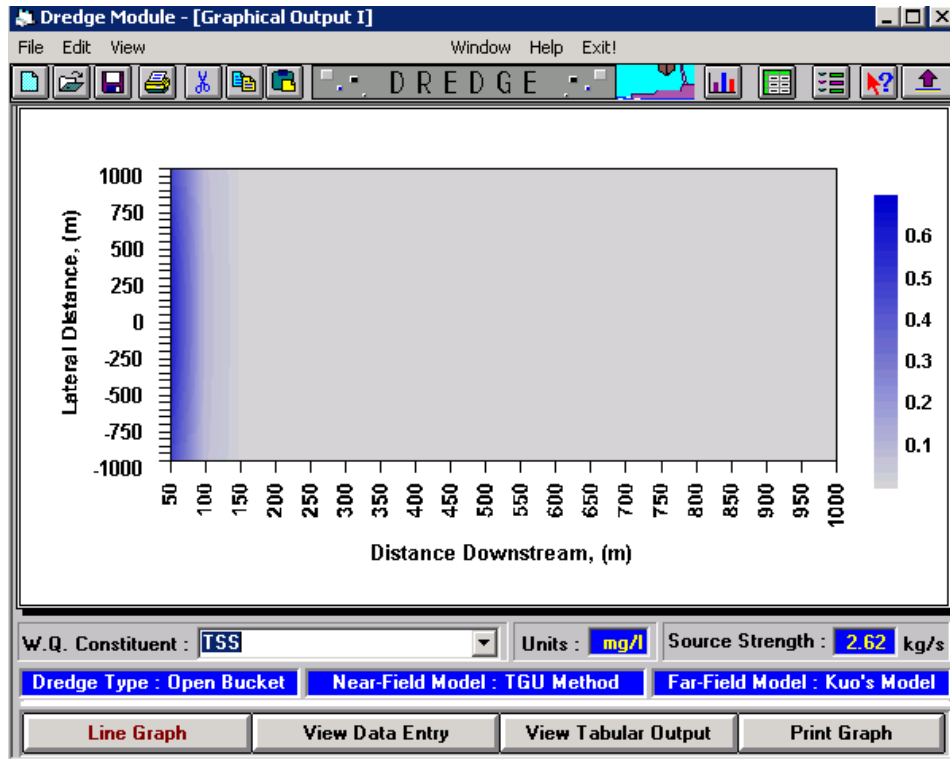


Figure 9.7 TSS Concentration (mg/L) Contours for Low Slack Tide

9.5 FAR - FIELD MODELLING

This section provides results obtained from the far-field model during dredging operations at the BOF site. In both scenarios (1W and 1D), a total of 20 m³ of dredge material is released daily over an eight hour period. The dredge release occurs every day for the entire simulation period. The actual dredging operation will occur over several months. However, a period of 30 days is sufficient in predicting the potential fate and transport of suspended solids and sedimentation resulting due to the dredging operation.

In Scenario 1D, the maximum incremental instantaneous TSS value is 4.8 mg/L. A snapshot of the TSS plume during the drilling operation at a time and vertical location when the maximum TSS occurred is shown in **Figure 9.8**. The plume is limited to the region around the bulk offloading facility. The TSS values drop quickly below 5 mg/L at distances greater than 200 m from the dredging location. The maximum instantaneous sedimentation rate was 2623 mg/cm²-d and the maximum sediment thickness was 136.2 mm, both of which occur at the dredge site and are instantaneous. High sedimentation rates are predicted due to the shallow water depths (~5 m) in the dredging area. Released sediments settle quickly in the vicinity of BOF without experiencing considerable spreading. **Figure 9.9** and **Figure 9.10** show the snapshot of

sedimentation rate and sediment thickness at times when maximums occurred. Note that both sedimentation rate and sediment thickness are transient in nature due to continuous deposition and erosion occurring under the varying hydrodynamic conditions. Additionally, the release of sediment during the dredging will be spread out covering the entire dredge location. However, in the modelling study the entire dredge-related release occurs at one location making the analysis highly conservative. Both sedimentation rate and sediment thickness drop to less than 100 mg/cm²-d and 1 mm, respectively, within 500 m from the dredge location. These results clearly show that the resulting TSS and sedimentation due to the drilling are a localized phenomenon.

In Scenario 1W, the incremental TSS, sedimentation rates and sediment thickness are comparable to its dry season counterpart. The maximum incremental TSS is predicted to be 11.8 mg/L, and maximum sedimentation rate and sediment thickness are predicted to be 15100 mg/cm²-d and 58.7 mm, respectively. **Figure 9.11**, **Figure 9.12** and **Figure 9.13** show the maximum incremental instantaneous TSS plume, sedimentation rate and sediment thickness resulting from the dredging at BOF under wet seasons conditions.

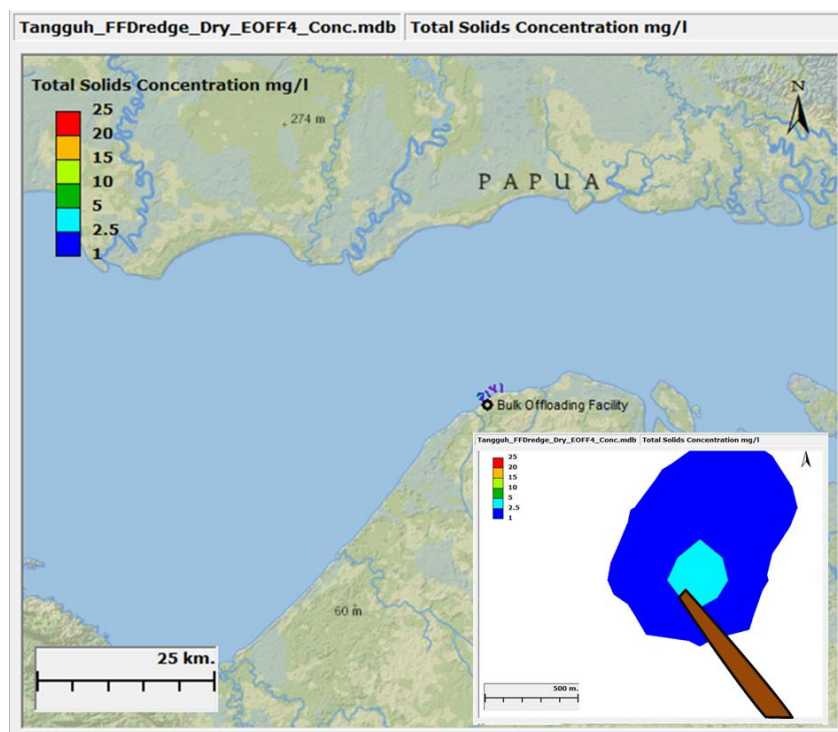


Figure 9.8 *Maximum Incremental TSS Concentrations during Dredging at BOF under Dry Season Conditions*

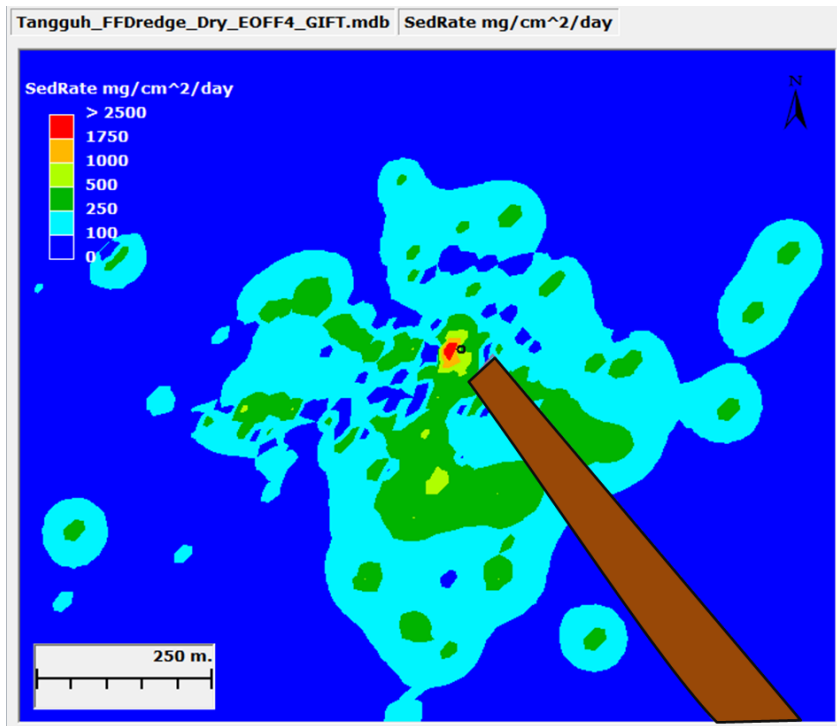


Figure 9.9 Maximum Sedimentation Rate during Dredging at BOF under Dry Season Conditions

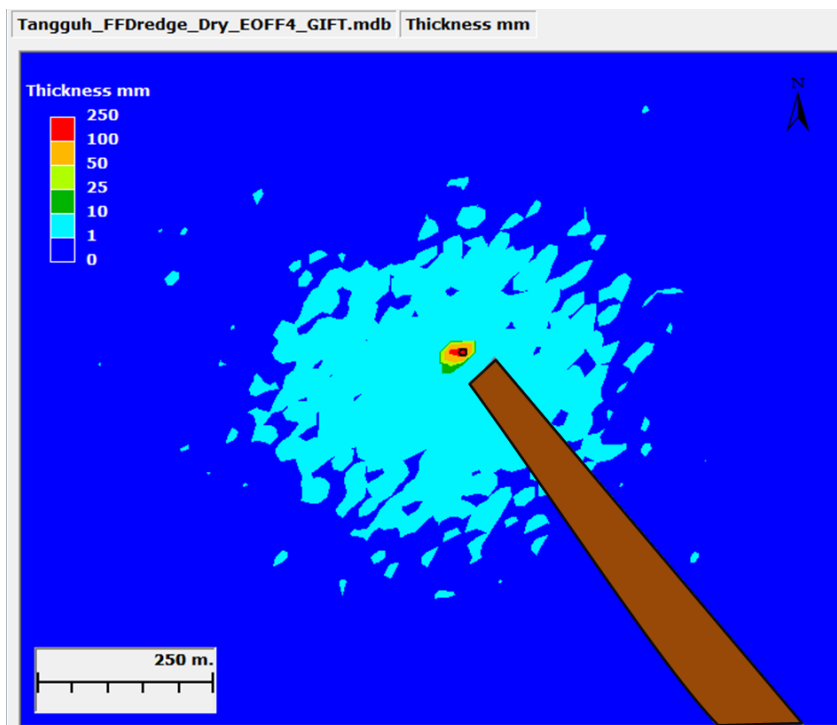


Figure 9.10 Maximum Sediment Thickness during Dredging at BOF under Dry Season Conditions

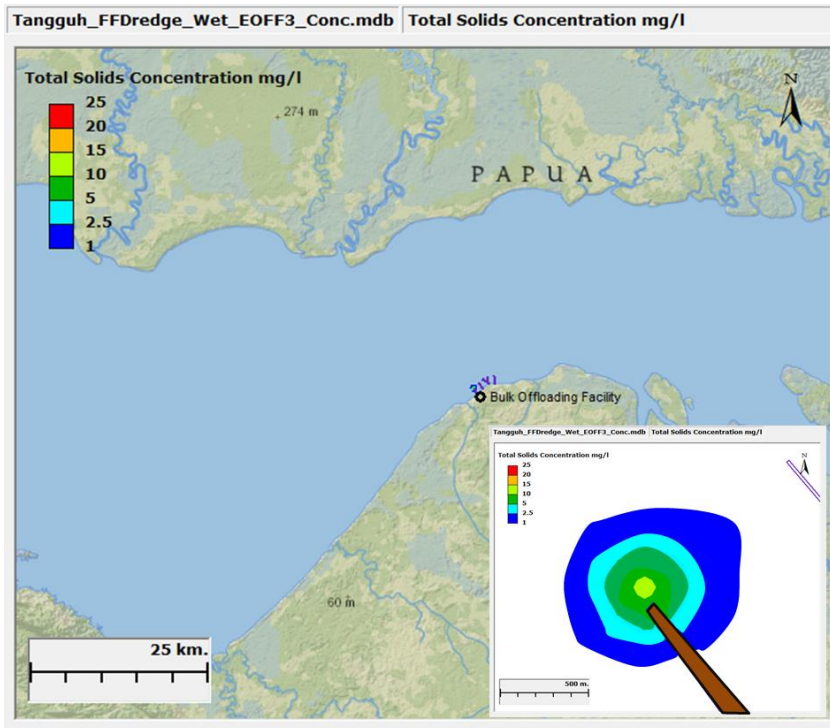


Figure 9.11 Maximum Incremental TSS Concentration during Dredging at BOF Under Wet Season Conditions

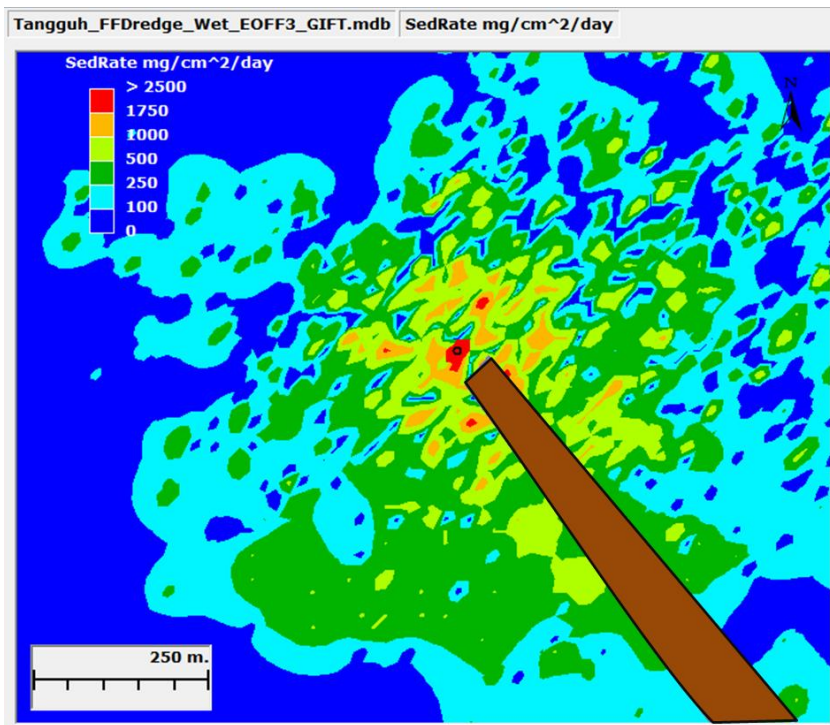


Figure 9.12 Maximum Sedimentation Rate during Dredging at BOF under Wet Season Conditions

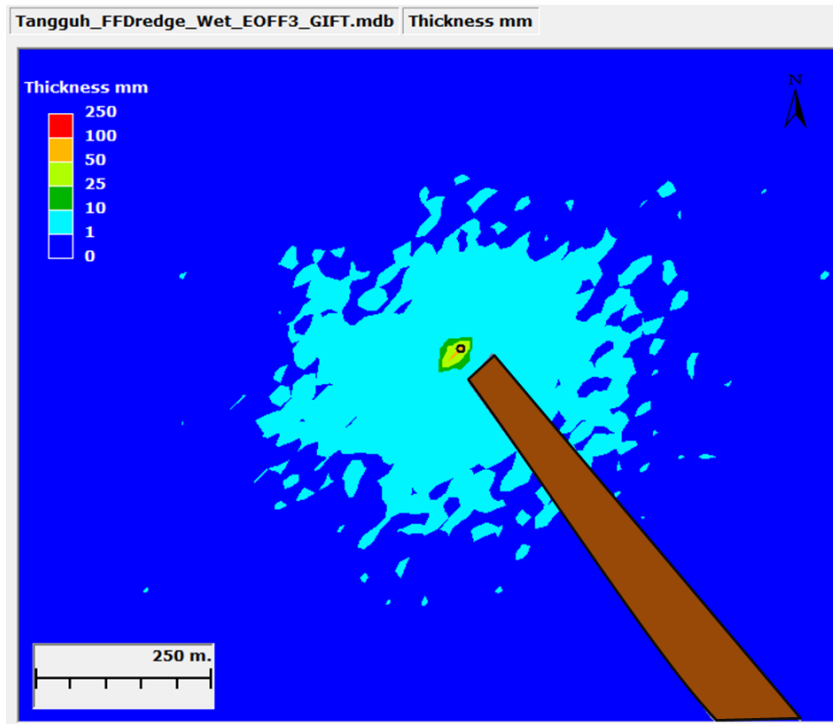


Figure 9.13 Maximum Sediment Thickness during Dredging at BOF under Wet Season Conditions

9.6 CONCLUSION

The results of the modelling and the plots presented indicate that the deposition of dredge operation-related sediments only occurs in the vicinity of the dredge location, mostly within 500 m. The results shown are maximums predicted during the dredging operation. These maximums only occur for a short period of time as the ambient conditions are transient and the plume quickly spreads or settles to the bottom. The TSS plume, similar to sedimentation plume, is limited in extent due to shallow depths that facilitate quick settling of sediments. The maximum incremental TSS is predicted to be only 11.8 mg/L. The maximum baseline TSS during dry period is 27 mg/L which when added to the incremental maximum TSS due to dredging results in a TSS value of 38.8 mg/L, well below the ambient seawater quality standard for mangrove-lined water bodies of 80 mg/L. These predicted results show that the proposed dredging operations are unlikely to result in exceedance of applicable environmental standards or create any significant impacts. **Table 9.7** shows the summary of resulting TSS, sedimentation rate and sediment thickness.

Table 9.7 Summary of Predicted Results for Dredging Operation Scenarios

Scenario	Maximum Increase in TSS (mg/L)	Maximum Increase in Sedimentation Rate (mg/cm²-day)	Maximum Increase in Depositional Thickness (mm)	Area of Depositional Thickness > 5 cm (m²)
1D	4.8	2623	136.2	590
1W	11.8	15111	58.7	80

10 DREDGE DISPOSAL MODELLING

The dredged material from the BOF site is planned to be disposed at two locations within Bintuni Bay. The disposal of dredged material poses potential risks to the marine and benthic communities due to the increase in TSS and deposition of disposed materials. The scenarios considered for the assessment of potential impacts from dredge disposal use the east disposal site (**Figure 3.1**) under both wet and dry seasons as in the previous scenarios. The east disposal site is selected due to its proximity to sensitive receptors and therefore represents a conservative case relative to impacts.

Similar to the dredging assessment, the physical, chemical and biological impacts of dredge material disposed into surface waters at the proposed disposal site are assessed using three-dimensional fate and transport modelling. Both near-field and far-field assessments are done. While GEMSS-GIFT is used for the far-field modelling, a different model, STFATE, is used for the near-field modelling.

10.1 SCENARIO DESIGN

The estimates of dredge material volumes are provided by the Tangguh LNG. Specific gravity and particle size distributions are assumed based on previous dredging experience. Discharges are simulated for two different seasons: dry (August) and wet (December). A summary of the scenarios can be seen in **Table 10.1**. Dredge disposal is modelled for two ten minute releases four hours apart for each of the two seasons. Planned dredging suggests eight hours per day of continuous dredging of 2000 m³ of material. Disposal barges with a capacity of 1000 m³ will be used to dispose these dredged materials twice a day. It is anticipated that all dredge material can be disposed within 10 minutes. All dredged material is released 3 meters below LAT.

Table 10.1 Scenario of Dredge Material Disposal

Site	Season	Scenario
East disposal site	Wet	2W
	Dry	2D

10.2 DISPOSAL AND SEDIMENT DATA

The disposed sediments are the same as the ones dredged at BOF. Therefore, the properties needed for the disposal modelling are the same as the ones used for the dredge modelling discussed in Section 1.

A two-dimensional (2-D) grid was constructed covering an area 15 km by 15 km, with 50 m by 50 m grid cells at each location. The grid is shown in **Figure 10.1**. This grid is used for computations of sedimentation rate and depositional thickness. A three-

dimensional (3-D) adaptive grid has been constructed for TSS concentrations as shown in Section 1.

The estimated release amounts and durations are provided in **Table 10.2**.

Table 10.2 Discharge Characteristics

Scenario	Release Amount (m ³ /release)	# of Releases per day	Time between releases (hrs)	Release Duration
2W	1000	2	4	10 min
2D	1000	2	4	10 min

Particle size distributions for dredge materials are provided in **Table 9.3** based on data provided by the Tangguh LNG. Dredge material density is assumed based on previous work experience are provided in **Table 9.4**.

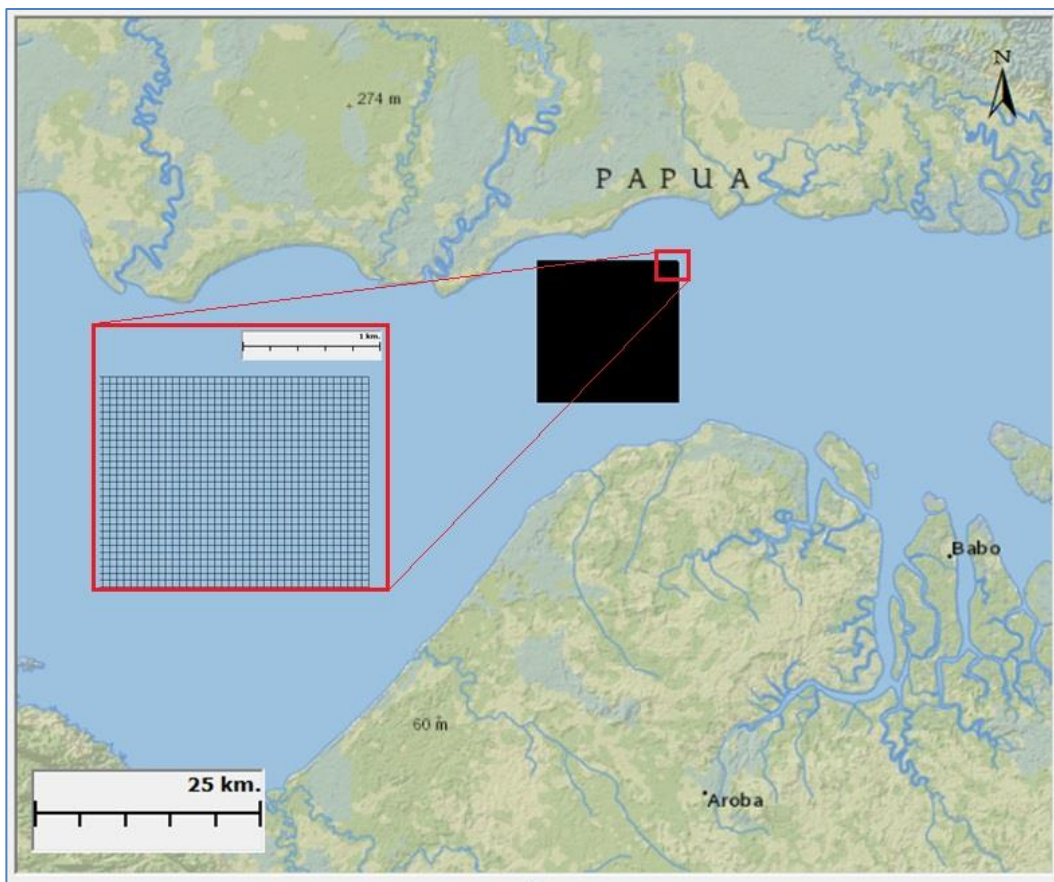


Figure 10.1 Dredge Grid with Used to Model the Fate and Transport of Dredge Disposal

10.3

NEAR - FIELD MODELLING

STFATE simulations are run for a single release of 1,000 m³ of dredge material from a split-hull barge at the center of the East Disposal Site. The hopper barge proposed for use has dimensions of 30 m × 10 m and the draft of the vessel is 3 m light and 1 m laden. The barge is assumed to be moving at a speed of 1 knot (0.5 m/s) during disposal. It takes 10 minutes to empty the disposal vessel.

The model grid used for the STFATE runs is 2286 m x 2286 m. This extent is needed to display the entire bottom dump within the grid. An average depth of 5.15 m is used for the grid. The roughness height at the seabed bottom is assumed to be 0.0015 m.

Current velocity profiles are set up for four different tide stages: high tide, high slack tide, low tide and low slack tide. Tidal velocities at a depth of 2 m are set according to the hydrodynamic modelling results (**Table 10.3**). Logarithmic current profiles are used to account for the vertical variation in current from the water surface to bottom.

Table 10.3 *Current Components at a Depth of 10 ft at the East Disposal Site*

Tide Stage	u-velocity (z-direction) (m/s)	v-velocity (x-direction) (m/s)
High	0.70	0.02
High Slack	0.16	-0.30
Low	-0.60	-0.11
Low Slack	-0.16	-0.08

To set up a realistic model case, it is assumed the dredged material in the barge has three layers, due to settling in the barge during transport to the dump site. The bottom layer has a higher volumetric concentration of sand, and the top layer has a lower concentration of sand and slightly higher concentrations of silts and clays. The average bulk density for all layers is about 1300 kg/m³.

The STFATE model is used to simulate the concentration of suspended sand, silt and clay every hour over a four hour period. The STFATE model output consists of particle concentrations in the water column at specified depths and time intervals over the simulation period. The model predicts that the larger sand particles and clumps deposit on the bottom in less than 1 hour. The output presented here is for silt and clay concentrations at hours 1 and 4 for the seabed.

Table 10.4 summarizes the dimensions and position of the silt and clay clouds on the bottom. **Figure 10.2** to **Figure 10.5** present the sea floor accumulation of the settled material. The maximum sediment deposition thickness on the bottom is approximately 30 mm over the four tide stages. The average radial extent of the deposited material is approximately 200–400 m from the dump release center.

Figure 10.6 to **Figure 10.9** are contour plots of the maximum silt and clay concentration at hours 1 and 4 after the release, for each tide stage, and show the results of the STFATE simulation of a single release on the bottom. The dredged material release location is noted by the small blue triangle. The enclosed contour lines show the horizontal extent of the silt and clay particle clouds out to various concentration levels. Please note concentration values are incremental TSS values above the background TSS, and only represent the TSS released due to a single disposal release. The results show high initial incremental TSS concentrations with a rapid decrease in silt and clay incremental concentrations to values less than 20 and 1.0 mg/L within, respectively, 1 and 4 hours after the release. The radial extent of the predicted silt and clay clouds at hour 1 when particle concentrations fall to 20 mg/L is in the order of 150 m. At hour 4 the sediment (silt/clay) clouds with incremental concentration above 1 mg/L enlarge to 400 m in radius.

The centroid of the silt and clay cloud travels approximately 60 m under low slack tide and up to 300 m under high tide within 4 hours of the initial release. The maximum silt/clay concentration at cloud centroids reaches 120 mg/L after the initial release to the disposal site. The model predicted incremental concentrations of silt and clay clouds at the water surface are smaller than those at the bottom. However, the spatial spreading at the surface is similar to that at the bottom.

The maximum allowable TSS increase of 53 mg/L (80 mg/L standard – 27 mg/L background) at the bed layer of the water column is exceeded, but confined within the 100 m radius of the sediment clouds within the first hour of the initial release. TSS increases above 53 mg/L after the first hour are not predicted, and they drop below 1 mg/L within 4 hours of the release during one disposal cycle.

Table 10.4 *Dimensions and Position of the Silt and Clay Clouds on the Bottom*

Tide Stage	Type	Maximum Concentration at Cloud Centroid at Hour 4 (mg/L)	Travel Distance of Cloud Centroid Within 4 Hours (m)	Radial Extent of Clouds Falling to 20 mg/L (m)	Maximum Overall Deposited Sediment Thickness (mm)
High	Silt	80	300	120	30
	Clay	120	375	180	-
High Slack	Silt	90	180	135	30
	Clay	100	150	120	-
Low	Silt	90	150	135	30
	Clay	100	60	180	-
Low Slack	Silt	90	150	135	30
	Clay	100	100	180	-

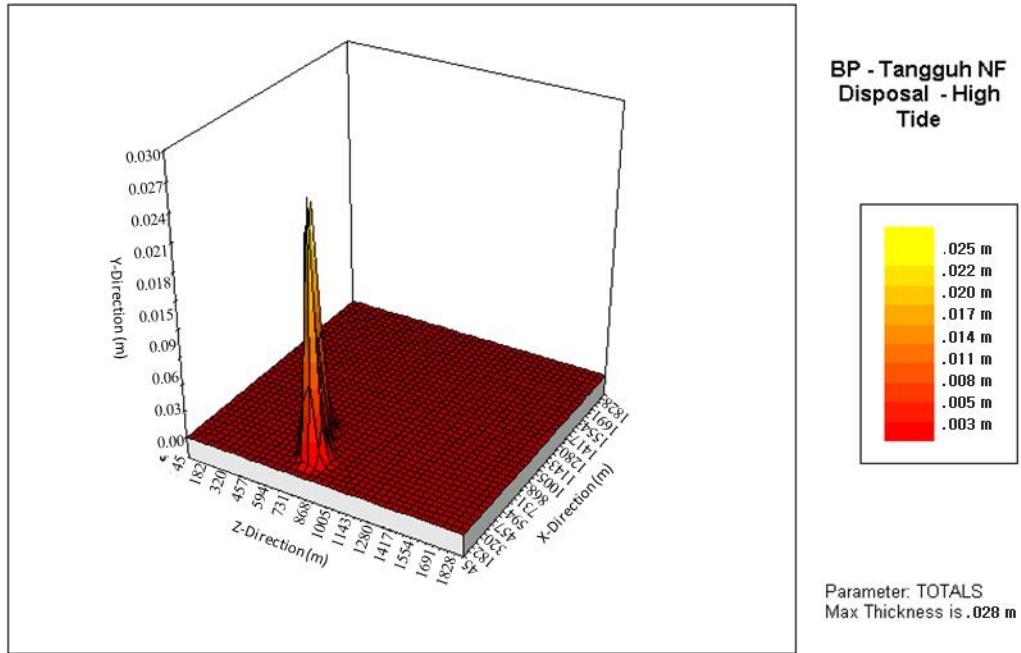


Figure 10.2 Maximum Seabed Deposition Thickness at the High Tide

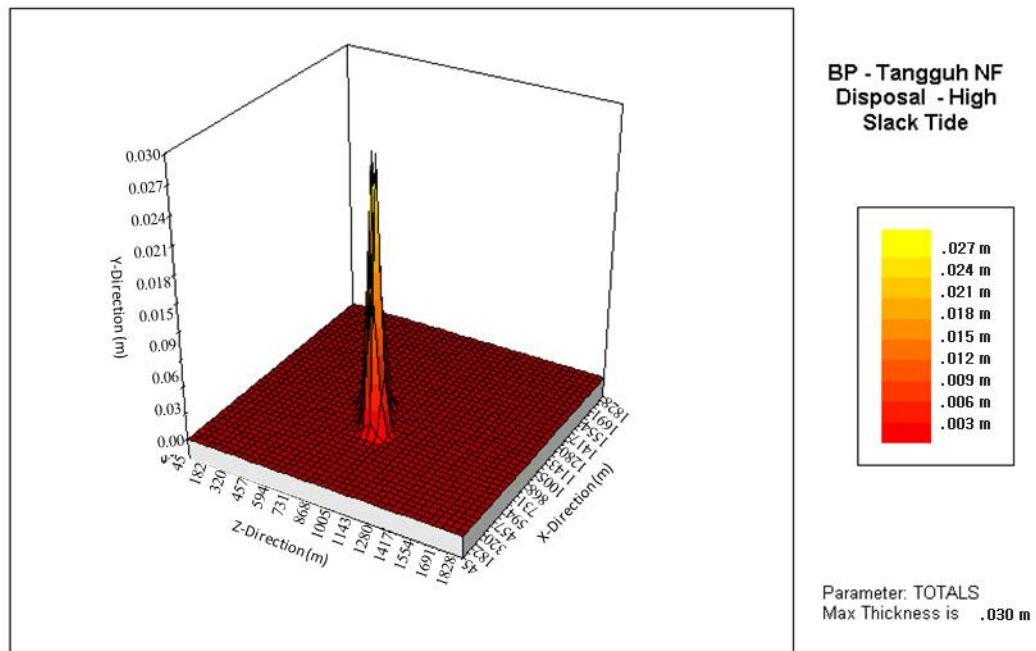


Figure 10.3 Maximum Seabed Deposition Thickness at the High Slack Tide

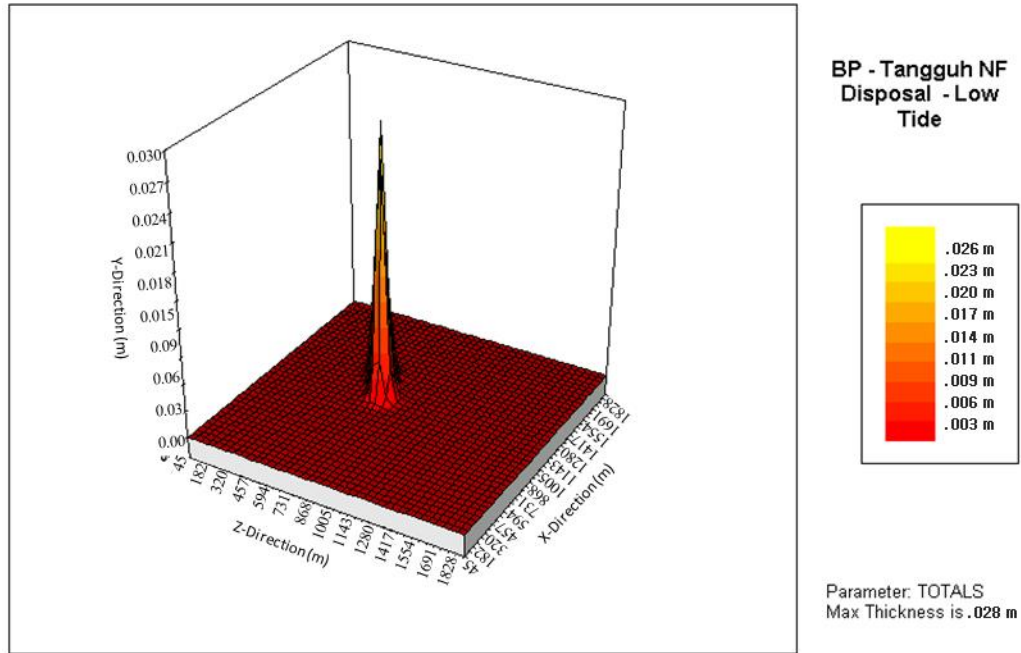


Figure 10.4 Maximum Seabed Deposition Thickness at the Low Tide

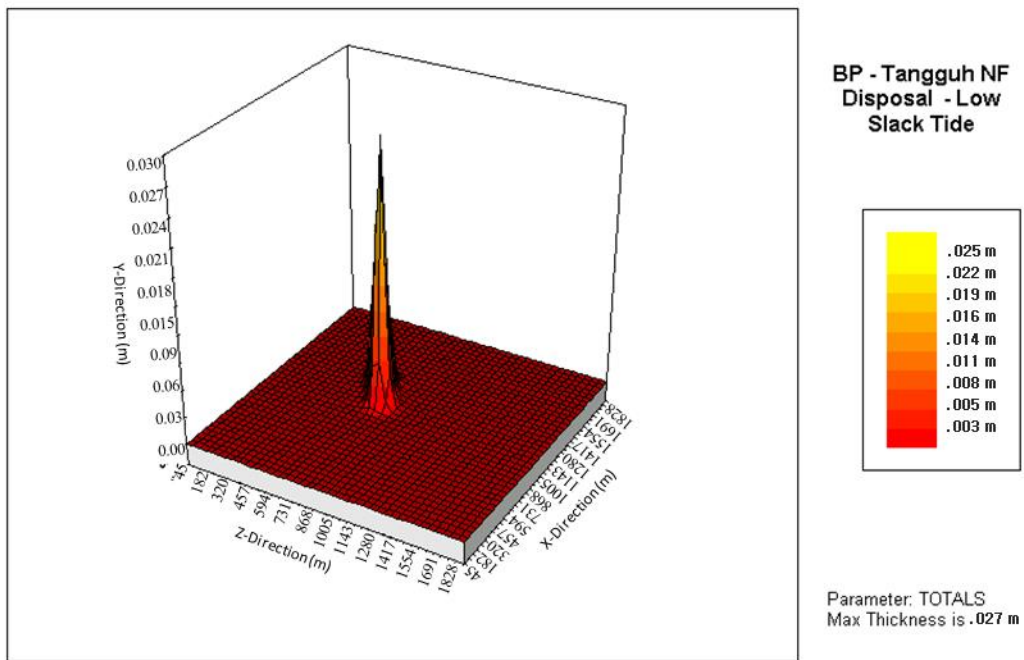
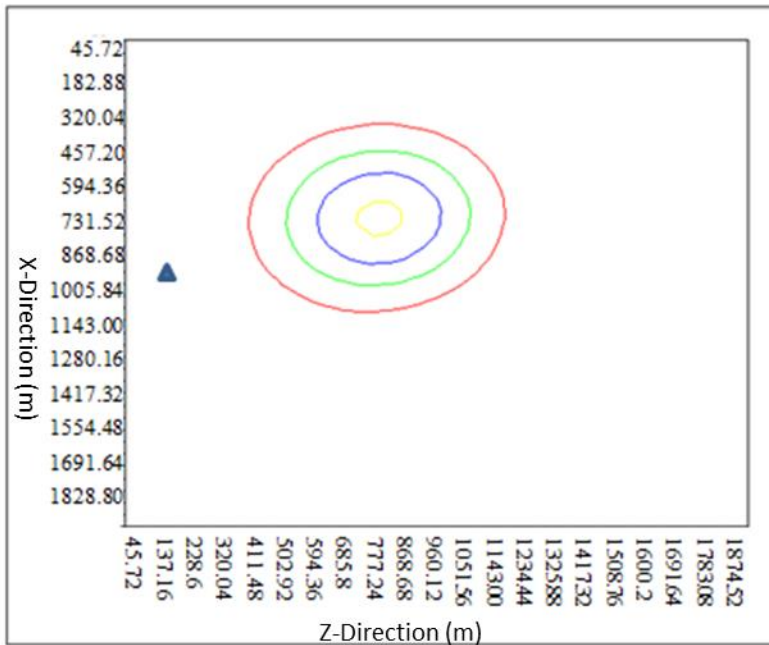
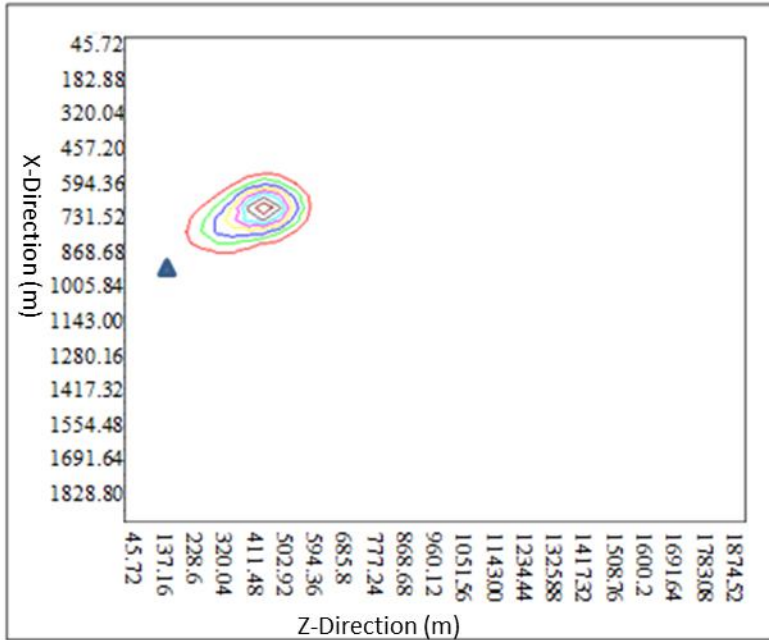


Figure 10.5 Maximum Seabed Deposition Thickness at the Low Slack Tide



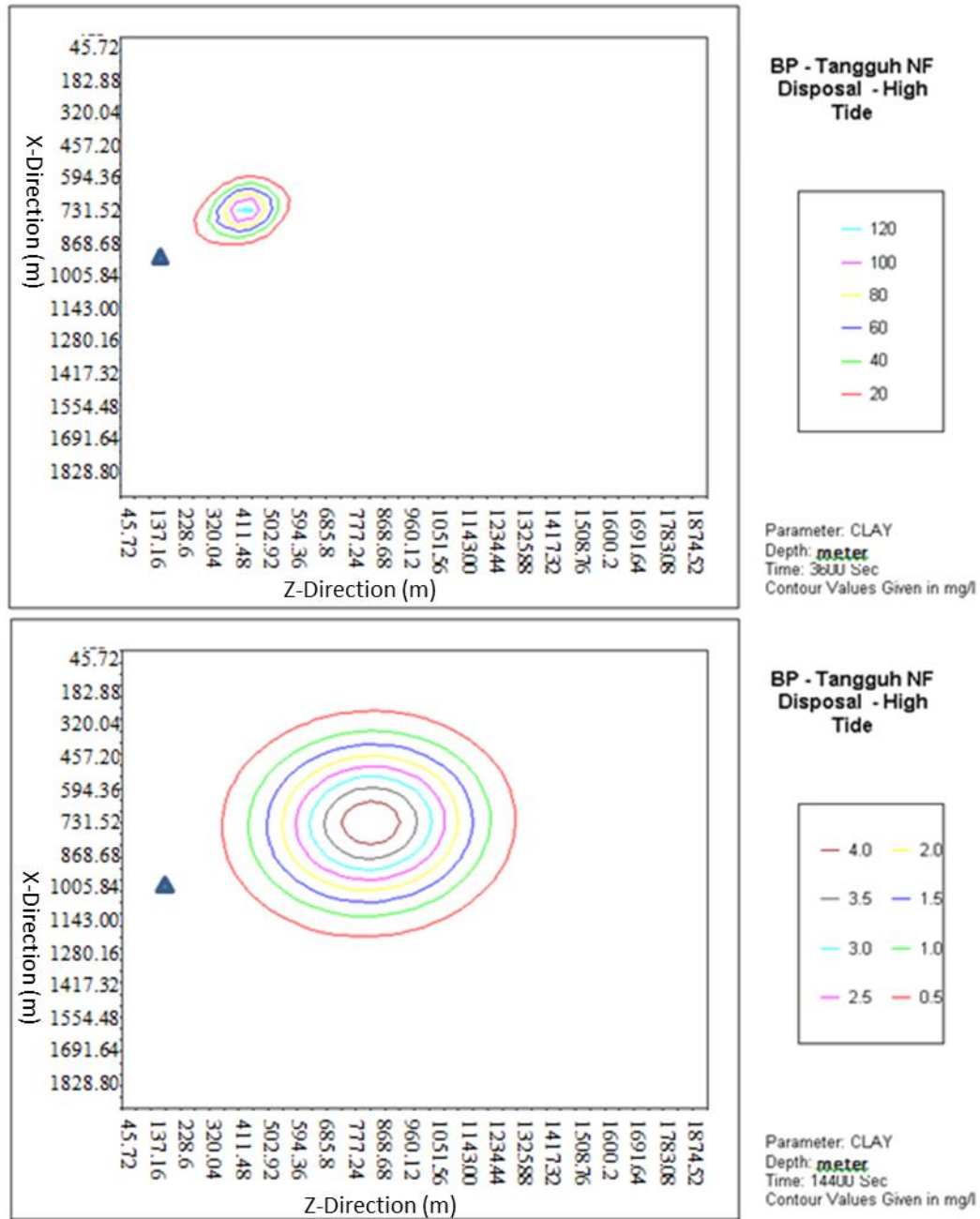
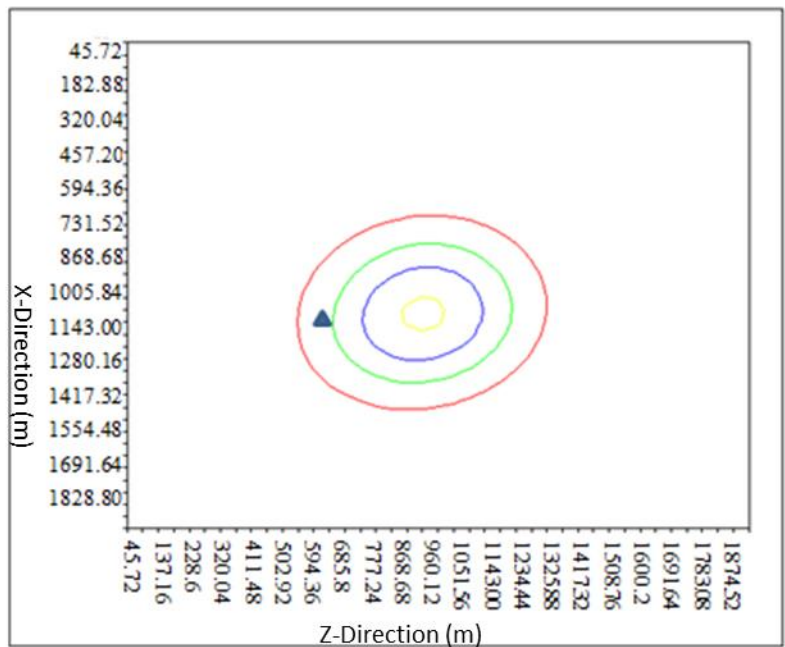
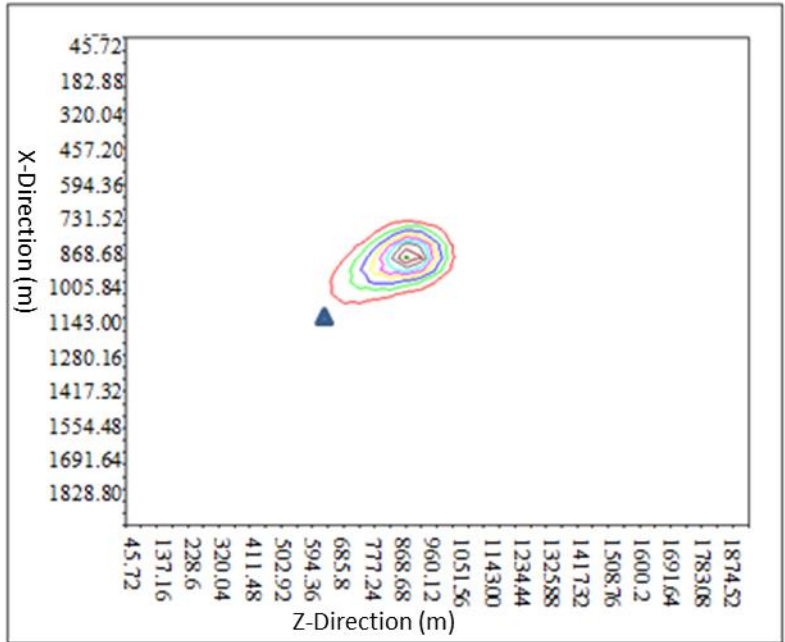


Figure 10.6 Plan View of the Maximum Silt and Clay Particle Concentrations (mg/L) at the Sea Bottom at Hours 1 and 4 Resulting from a Single Release - High Tide Stage



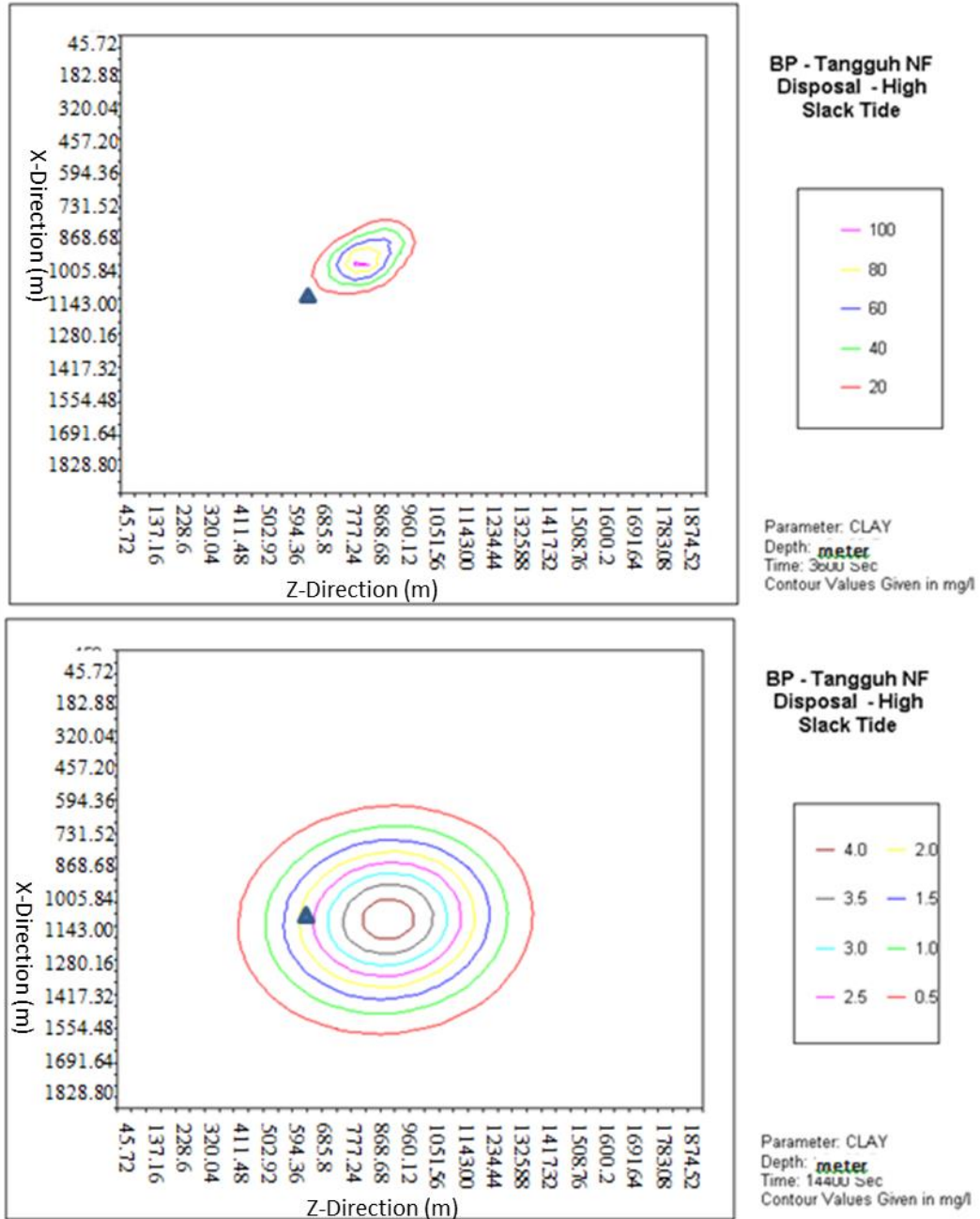
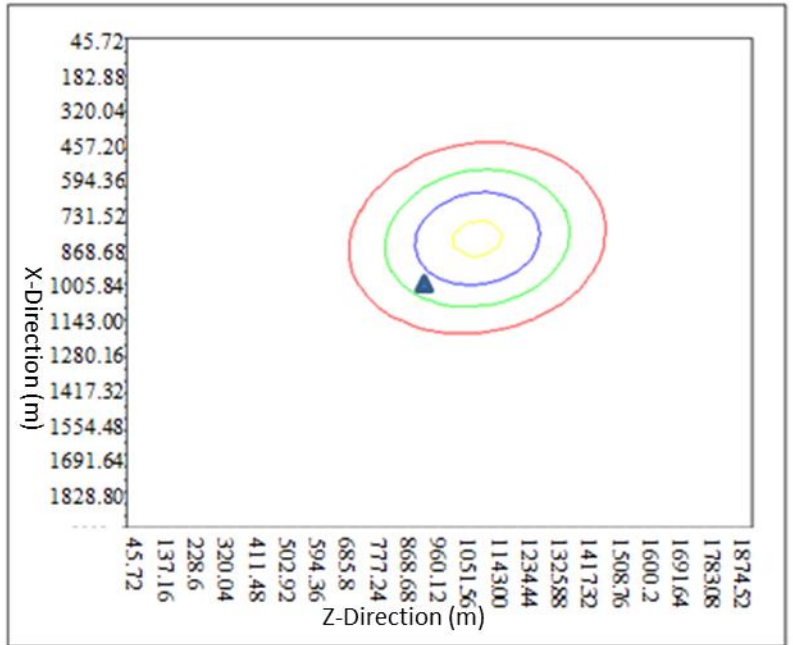
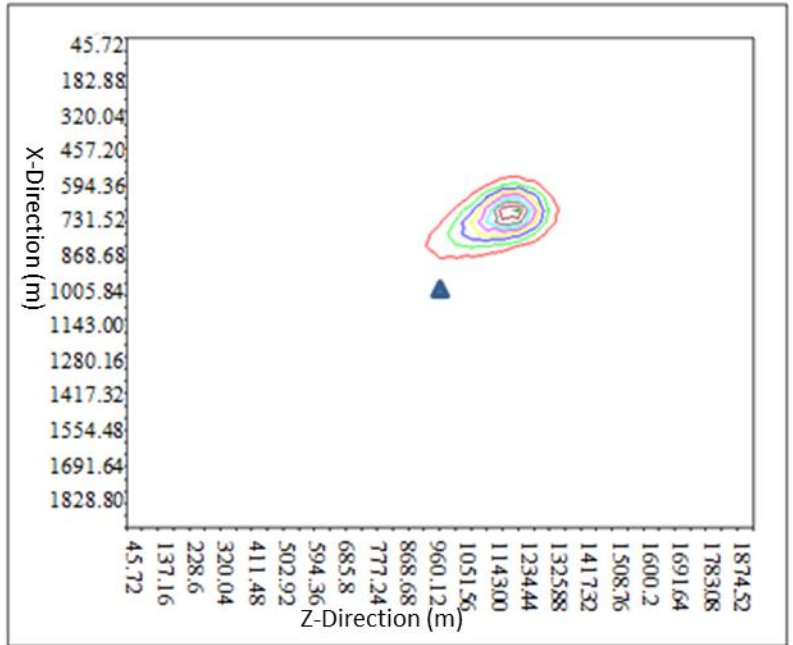


Figure 10.7 Plan View of the Maximum Silt and Clay Particle Concentrations (mg/L) at the Sea Bottom at Hours 1 and 4 Resulting from a Single Release - High Slack Tide Stage



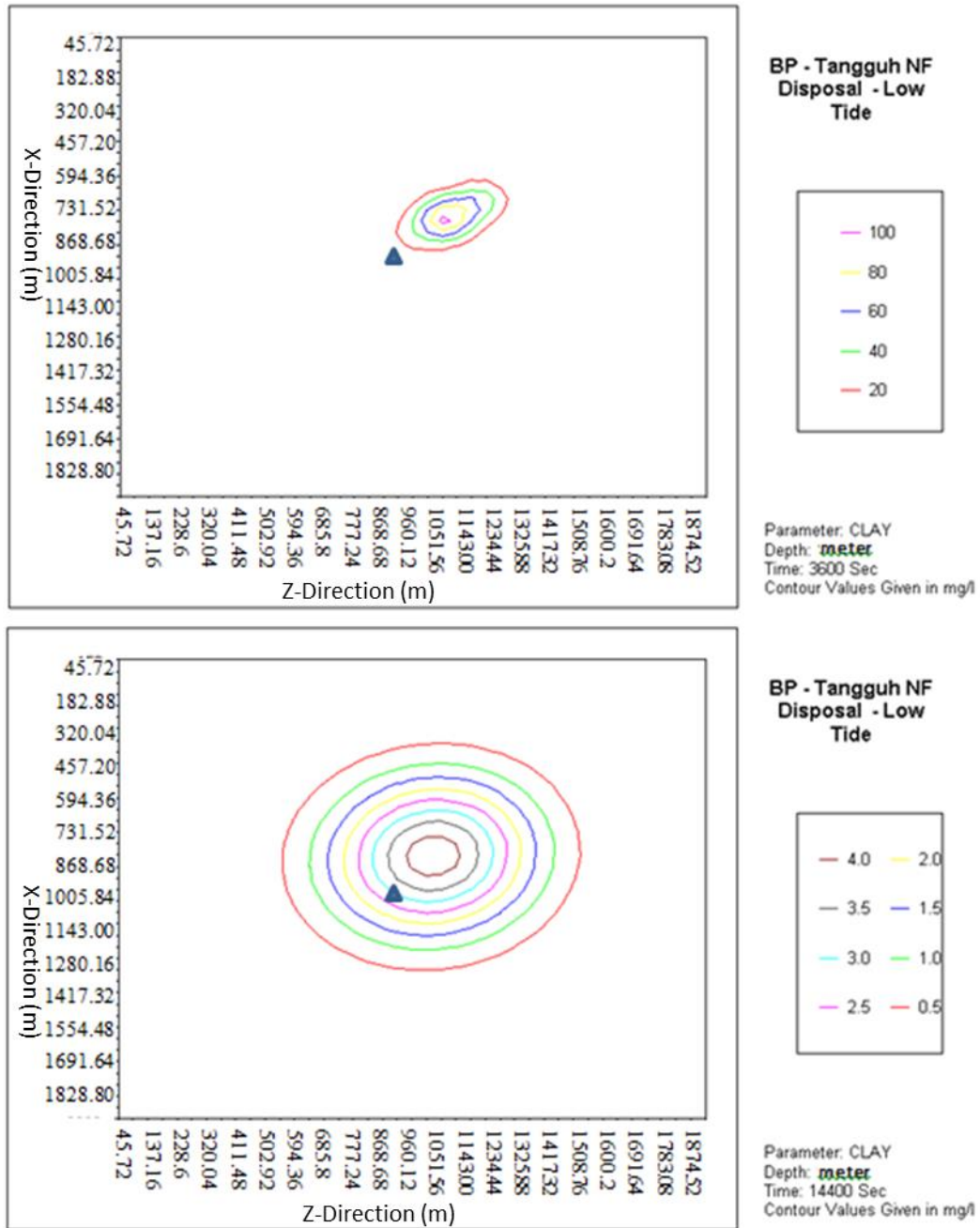
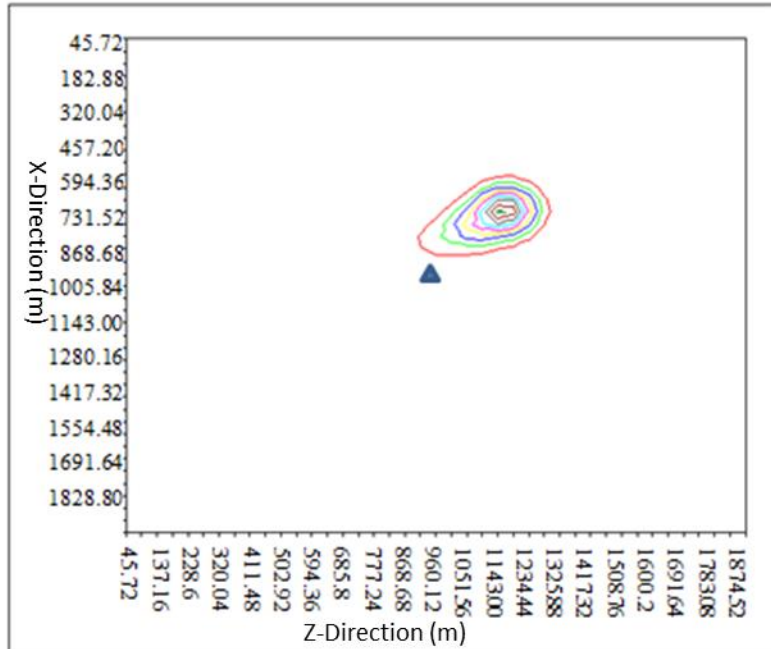


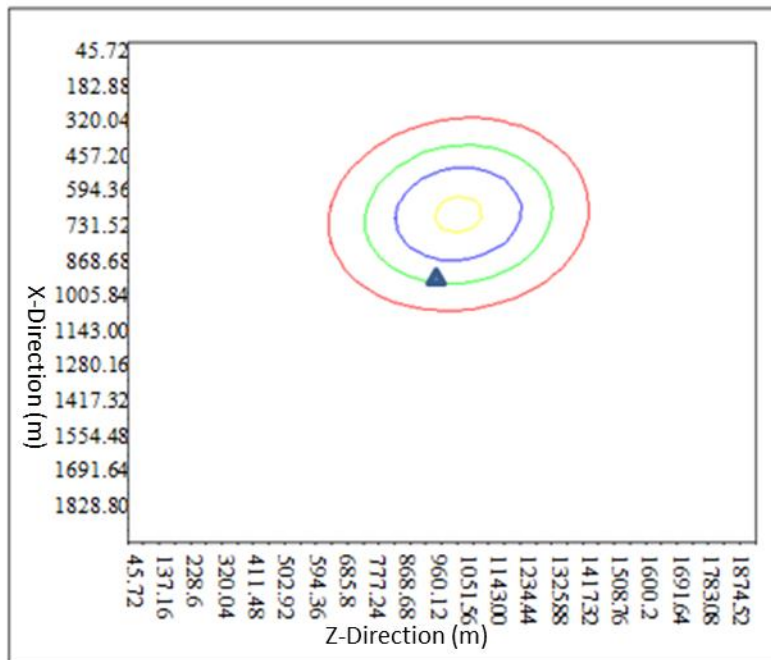
Figure 10.8 Plan View of the Maximum Silt and Clay Particle Concentrations (mg/L) at the Sea Bottom at Hours 1 and 4 Resulting from a Single Release - Low Tide Stage



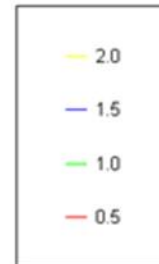
BP - Tangguh NF Disposal - Low Slack Tide



Parameter: SILT
 Depth: 1 meter
 Time: 3600 Sec
 Contour Values Given in mg/l



BP - Tangguh NF Disposal - Low Slack Tide



Parameter: SILT
 Depth: 1 meter
 Time: 14400 Sec
 Contour Values Given in mg/l

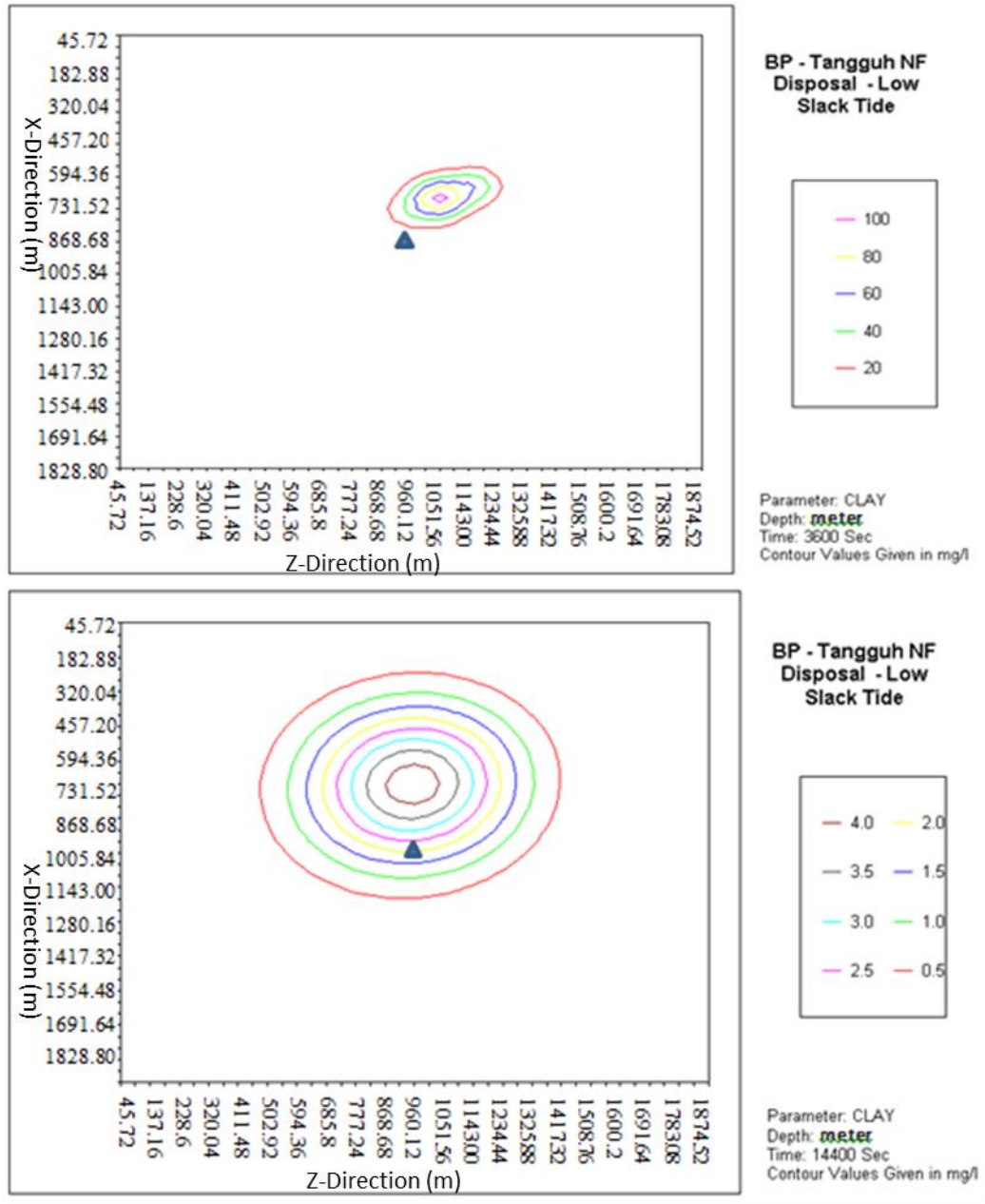


Figure 10.9 Plan View of the Maximum Silt and Clay Particle Concentrations (mg/L) at the Sea Bottom at Hours 1 and 4 Resulting from a Single Release - Low Slack Tide Stage

10.4 FAR - FIELD MODELLING

This section provides results obtained from the far-field model during dredge disposal at the east disposal site. In both scenarios (2W and 2D), a total of 2000 m³ of dredge material is released daily spread over two releases of 10 minutes each. The dredge disposal is repeated every day for entire simulation period. The actual dredging operation will occur over several months. However, the daily release is the same and a period of 30 days is sufficient in predicting the potential fate and transport of suspended solids and sedimentation resulting from the dredge disposal.

In Scenario 2D, the maximum incremental instantaneous TSS value is 3.9 mg/L. A snapshot of the TSS plume during disposal at a time and vertical location when the maximum TSS occurred is shown in **Figure 10.10**. The plume is limited to the region around the east disposal site. The TSS values drop quickly below 2.5 mg/L at distances greater than 1.0 km from the disposal location with the entire extent of the TSS plume (>1.0 mg/L) shown within 10.0 km. The maximum instantaneous sedimentation rate is 218 mg/cm²-d and the maximum sediment thickness is 36.2 mm, both of which occur at the disposal site. The disposal of dredged sediments repeatedly occurs at the same location in the model. This may not be the case in practice as the barge will likely dispose sediments at different locations within the vicinity of the disposal site during each trip, making the model results conservative. **Figure 10.11** and **Figure 10.12** show the snapshot of sedimentation rate and sediment thickness at times when maximums occurred. Both sedimentation rate and sediment thickness drop to less than 50 mg/cm²-d and 2.5 mm, respectively, within 500 m from the disposal location. These results clearly show that the increases in the resulting TSS and sedimentation due to the dredge disposal are a localized phenomenon.

In Scenario 2W, the incremental TSS, sedimentation rates and sediment thickness are comparable to its dry season counterpart. The maximum incremental TSS is predicted to be 5.5 mg/L, and maximum sedimentation rate and sediment thickness are predicted to be 277 mg/cm²-d and 28.2 mm, respectively. **Figure 10.13**, **Figure 10.14** and **Figure 10.15** show the maximum instantaneous incremental TSS plume, sedimentation rate and sediment thickness resulting from the dredge disposal at the east disposal site under wet season conditions.

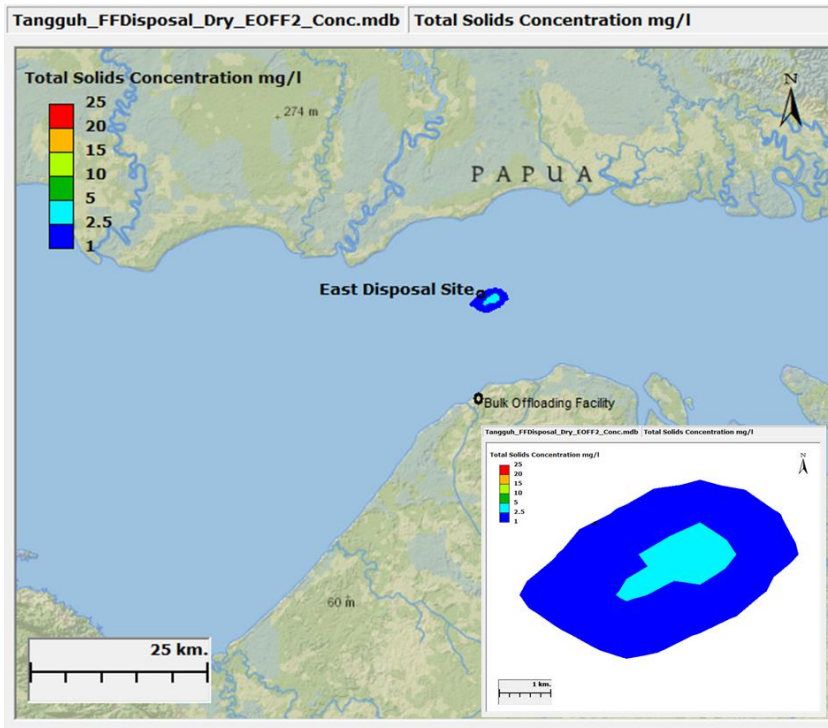


Figure 10.10 Maximum Incremental TSS during Dredge Disposal at the East Disposal Site under Dry Season Conditions

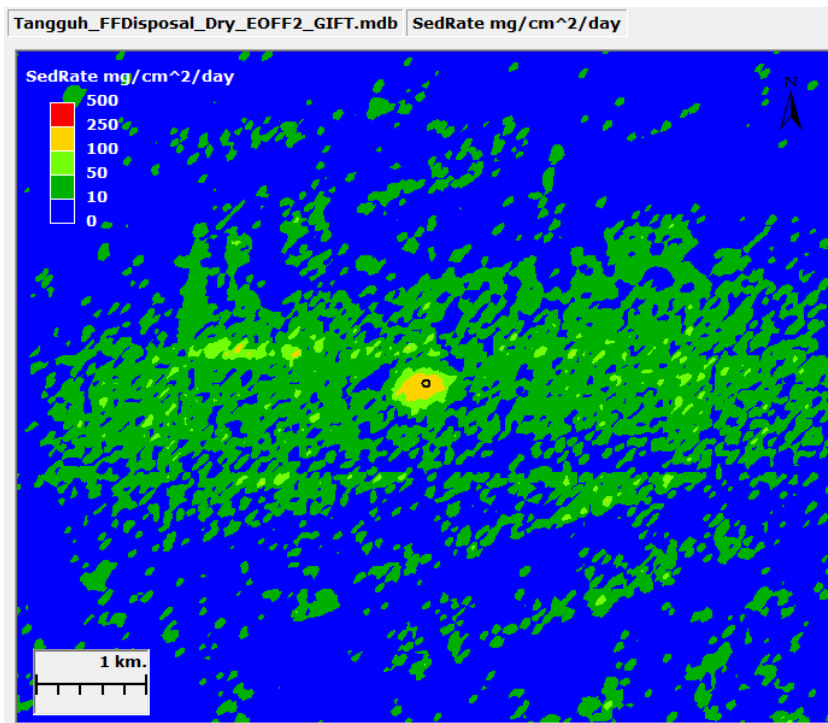


Figure 10.11 Maximum Sedimentation Rate during Dredge Disposal at the East Disposal Site under Dry Season Conditions

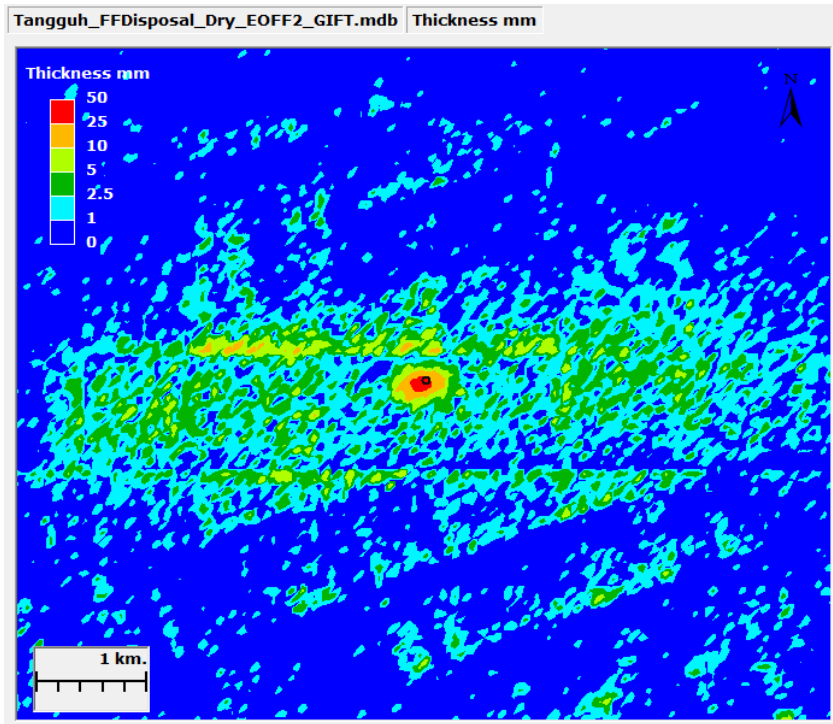


Figure 10.12 Maximum Sediment Thickness during Dredge Disposal at the East Disposal Site under Dry Season Conditions

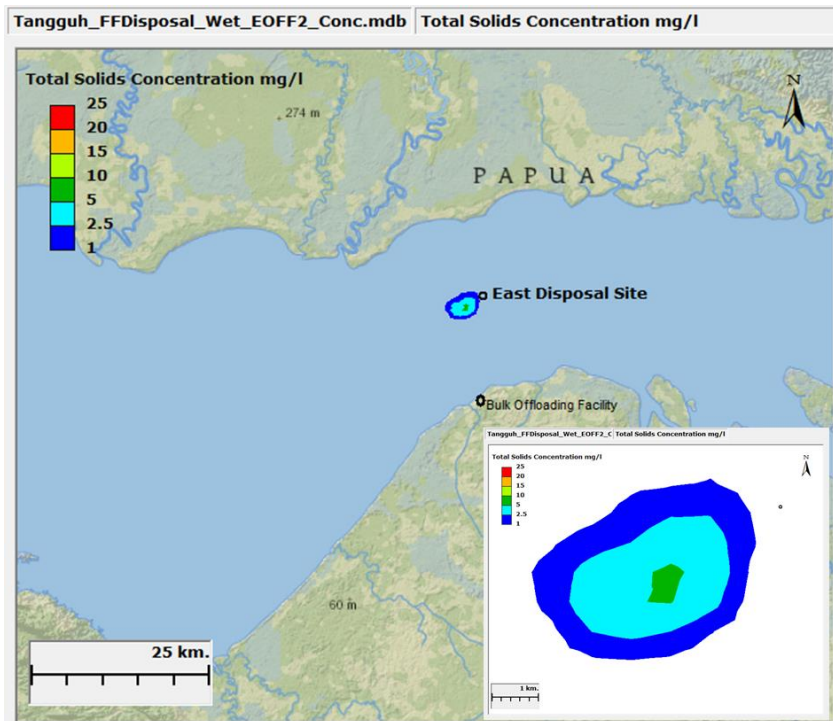


Figure 10.13 Maximum Incremental TSS during Dredge Disposal at the East Disposal Site under Wet Season Conditions

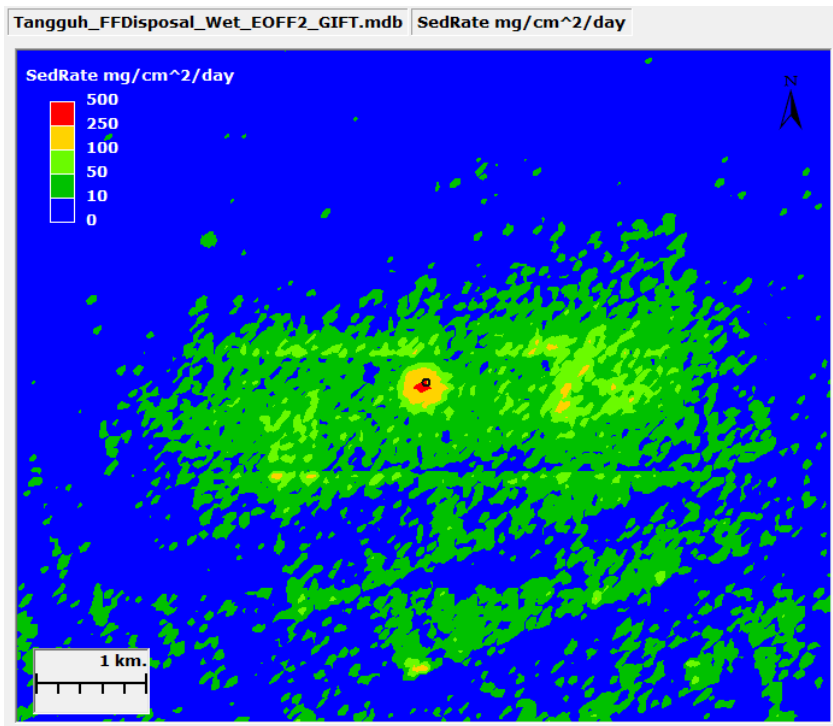


Figure 10.14 Maximum Sedimentation Rate during Dredge Disposal at the East Disposal Site under Wet Season Conditions

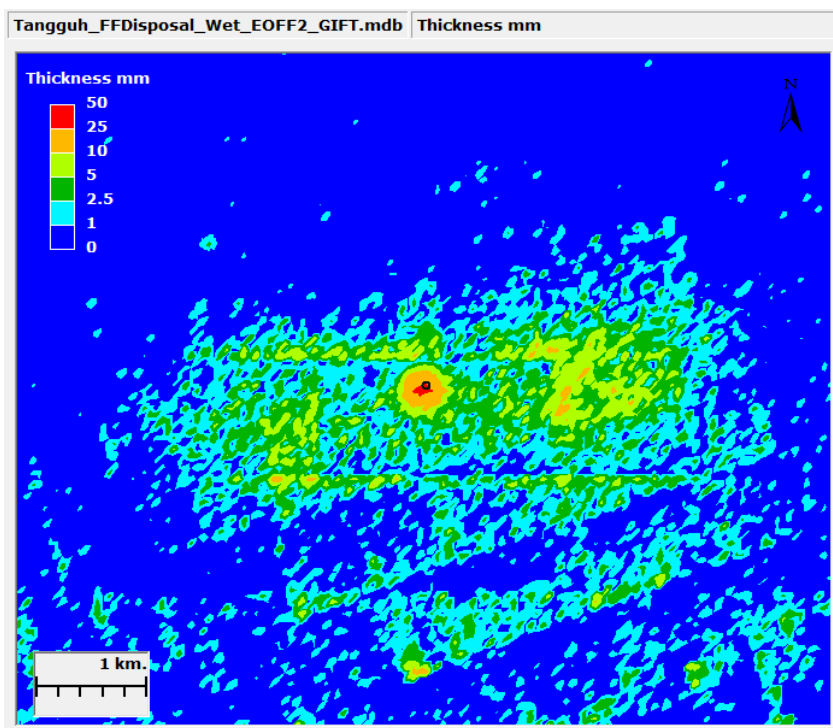


Figure 10.15 Maximum Sediment Thickness during Dredge Disposal at the East Disposal Site under Wet Season Conditions

10.5 CONCLUSION

The results of the modelling and the plots presented indicate that the disposal of dredge material results in only a localized increase in TSS over seawater quality and sediment deposition, mostly within 10 km with TSS > 2.5 mg/L within 1.0 km. The results shown are maximums predicted during the disposal operation. These maximums only occur for a short period of time as the ambient conditions are transient and the plume quickly spreads or settles to the bottom. The extent of the TSS plume and sedimentation plume are predicted to be similar. The maximum incremental TSS over ambient seawater quality is predicted to be only 5.5 mg/L. The maximum baseline TSS during dry period is 27 mg/L which when added to the incremental maximum TSS due to disposal results in a total TSS value of 32.5 mg/L, well below the ambient seawater quality standard for mangrove-lined water bodies of 80 mg/L. These predicted results show that the proposed disposal of dredged materials unlikely to result in exceedance of applicable environmental standards or create significant impacts. **Table 10.5** shows the summary of resulting TSS above ambient seawater quality, sedimentation rate, sediment thickness, and area of depositional thickness above 5 cm.

Table 10.5 Summary of Predicted Results for Dredging Operation Scenarios

Scenario	Maximum TSS Above Ambient Seawater Quality (mg/L)	Maximum Sedimentation Rate (mg/cm ² -day)	Maximum Depositional Thickness (mm)	Area of Depositional Thickness > 5 cm (m ²)
2D	3.9	218	36.2	0
2W	5.5	277	28.2	0

The Tangguh LNG expansion project also involves drilling of additional production wells. These wells are located at various fields throughout the Bintuni Bay. During drilling, cuttings and muds are released. These cuttings and muds may impact the aquatic and benthic communities due to increased TSS in the water column and increased sedimentation to the seabed. It is therefore important to estimate the change in ambient TSS and sedimentation attributable to these drilling operations.

A selection of four wells was made based on their relative and unique locations in relation to the various sensitive receptors. Model scenarios consisted of releases of estimated drill cuttings and muds for these four wells (**Figure 3.1**) under site specific metocean conditions for a wet and dry season.

The physical, chemical and biological impacts of drill cuttings (the latter includes residual drilling mud) discharged on surface waters at the proposed wells were assessed using three-dimensional fate and transport modelling. The modelling used data obtained from proposed drilling design and hydrodynamic modelling done as part of this study. Inputs to the model consist of the following:

- metocean conditions (current speed and direction) predicted by the hydrodynamic model which are used by the drilling model to transport drill cuttings and drill muds;
- depths, the shape of the seafloor, and the distances to and configuration of nearby shorelines; and,
- volumes, properties, and spill durations for released substances and drill cuttings.

The model was used to estimate the sedimentation rate, total suspended solids added to the water column, and thickness of the footprint of settled materials deposited on the seafloor. These scenarios and their results are summarized in this section.

11.1

SCENARIO DESIGN

The potential dispersion and deposition of released drill cuttings has been quantified using hydrodynamic computer modelling techniques. Modelling allows the prediction and description of the water level, ocean current velocity and direction in the sea. Released material will pass vertically through the water column because drill cuttings are denser than the receiving water. The drill cuttings dispersion is fundamentally a three-dimensional phenomenon.

Estimates of drill cuttings (including residual drilling mud) volumes were provided by the Tangguh LNG. Specific gravity and particle size distributions were assumed based on previous offshore drilling experience. Discharges were simulated for two different seasons: dry (August) and wet (December). A summary of the scenarios can be seen in **Table 11.1**. Both water based muds (WBM) and synthetic oil based muds (SBM) are planned to be used by the Tangguh LNG. All drilling fluids and cuttings will be released from the drilling rig 5 meters below LAT.

Table 11.1 Scenario List

Site	Season	Scenario Name	Waterbody depth at site (m)
ROA	Wet	3W	36
	Dry	3D	
TTB	Wet	4W	28
	Dry	4D	
WDA	Wet	5W	62
	Dry	5D	
UBA	Wet	6W	22
	Dry	6D	

11.2 DRILLING MUD AND DRILL CUTTINGS DATA

The 3-dimensional model, GIFT, used for dredging-related impacts was also used for drill cuttings and mud release. A two-dimensional (2-D) grid was constructed covering an area 1 km by 1 km, with 20 m by 20 m grid cells at each location. An example grid is shown below in **Figure 11.1** at site. This grid was used for computations of sedimentation rate and depositional thickness.

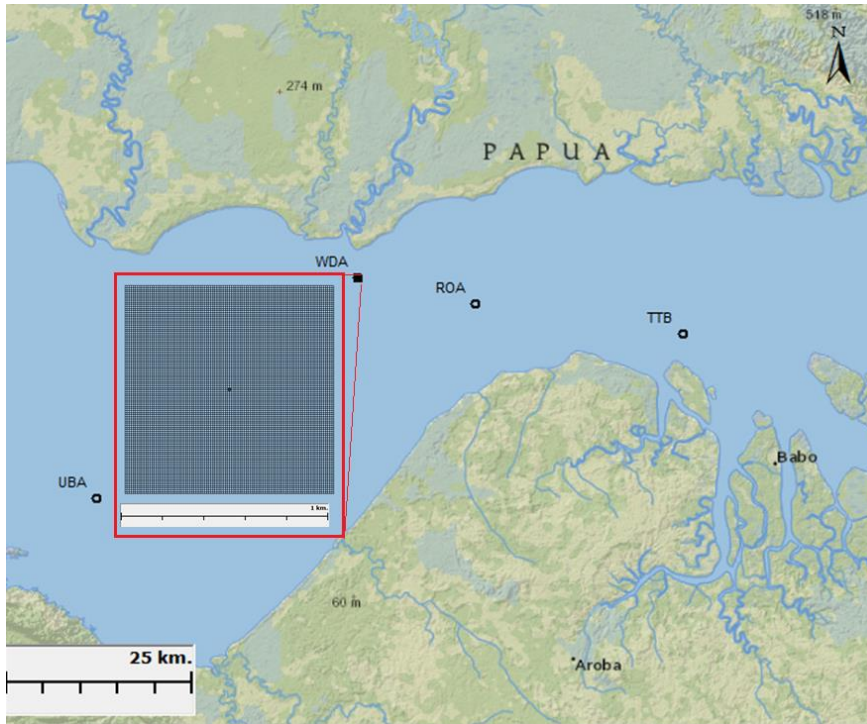


Figure 11.1 *Sedimentation and Depositional Thickness Grid*

Estimated types and release amounts of the materials discharged, well physical characteristics, and release durations are provided in **Table 11.2**.

Table 11.2 *Discharge Characteristics*

Days	Mud	Cuttings
1	1500	624.5
2	1500	624.5
3	1500	624.5
4	1500	624.5
5-7	0	0
8	1500	624.5
9	1500	624.5
10	1500	624.5
11-13	0	0
14	1500	624.5
15	1500	624.5
16-18	0	0
19	1500	624.5
20-22	0	0
Total (bbl)	15000	6245

Particle size distributions for drill cuttings and muds are provided in **Table 11.3** based on values provided in previous similar drilling projects. Drill cuttings and mud density used in the study are provided in **Table 11.4**.

Table 11.3 *Drill Cuttings and Muds Particle Size Distribution*

Drill Cuttings		WBM		SBM	
Particle Size (µm)	Volume Fraction %	Particle Size (µm)	Volume Fraction %	Particle Size (µm)	Volume Fraction %
52	2	1	2.2	52	2
170	9	1.5	3	170	9
450	15	3	8.6	450	15
910	18	5	20.2	910	18
2600	16	7.5	9.1	2600	16
4400	15	15	20.8	4400	15
15000	25	30	19.5	15000	25
		35	2		
		75	11.4		
		150	3.3		

Table 11.4 *Drill Cuttings and Muds Densities*

Material	Density (kg/m ³)
Cuttings	2650
WBM	1510
SBM	2059

11.3 FAR - FIELD MODELLING

This section provides results obtained from the far-field model during drilling operations at ROA, TTB, WDA and UBA. In all of the eight scenarios, a total of 991 m³ of drill cuttings and 356 m³ of drill muds were released at ROA. The entire drilling operation over which this release occurred lasted a total of 26.5 days. The model was run for an additional 4 days after drilling ceases to capture the fate of these drill cuttings and mud towards the end of the release.

11.3.1 *Drilling at ROA*

In Scenario 3W, the maximum instantaneous incremental TSS value was 3.0 mg/L. A snapshot of the TSS plume during the drilling operation at a time and vertical location when the maximum TSS occurred is shown in **Figure 11.5**. The centre plume is elongated and oriented towards east. The TSS values drop quickly below 0.5 mg/L at distances greater than 250 m from the drilling location. The maximum instantaneous sedimentation rate was 594 mg/cm²-d and the maximum sediment thickness was 10.1 mm, both of which occurred at the drill site. **Figure 11.6** and **Figure 11.7** show the snapshot of sedimentation rate and sediment thickness at times when maximums occurred. Note that both sedimentation rate and sediment thickness are transient in nature due to continuous deposition and erosion occurring under the varying hydrodynamic conditions. Both sedimentation rate and sediment thickness drop to less than 100 mg/cm²-d and 3.0 mm, respectively, within 250 m from the drilling location. These results clearly show that the resulting incremental TSS and sedimentation due to the drilling are a localized phenomenon.

In Scenario 3D, the incremental TSS, sedimentation rates and sediment thickness are comparable to its wet season counterpart. The maximum incremental TSS was predicted to be 3.0 mg/L, and maximum sedimentation rate and sediment thickness were predicted to be 608 mg/cm²-d and 11.4 mm, respectively. Error! Reference source not found., Error! Reference source not found. and Error! Reference source not found. show the maximum instantaneous incremental TSS plume, sedimentation rate and sediment thickness resulting from the drilling at ROA under wet seasons conditions.

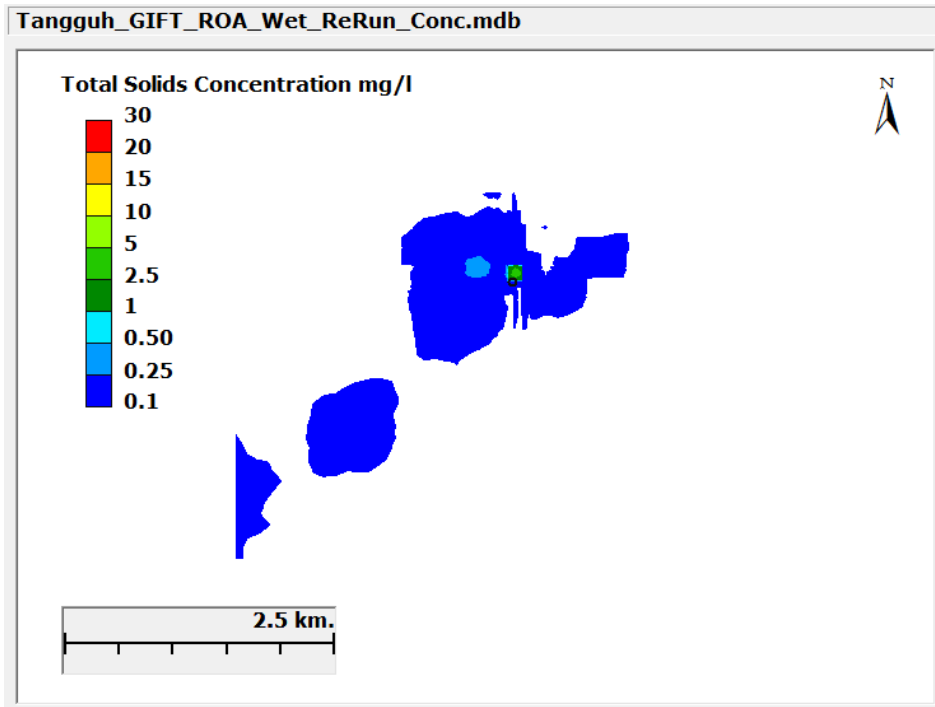


Figure 11.2 Maximum Incremental TSS Concentrations during Drilling at ROA under Wet Season Conditions

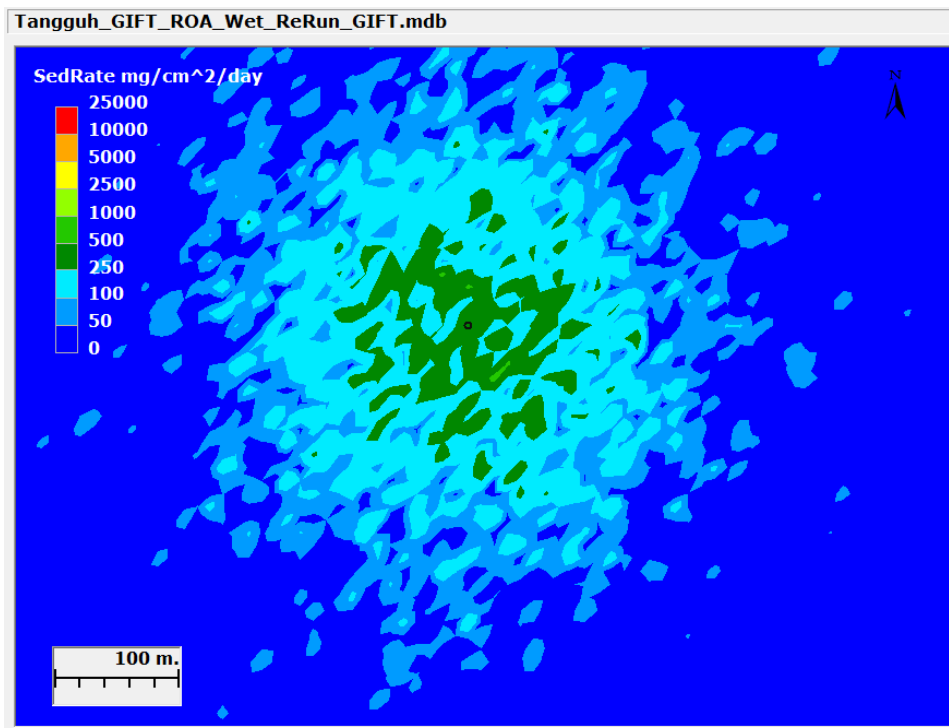


Figure 11.3 Maximum Sedimentation Rate during Drilling at ROA under Wet Season Conditions

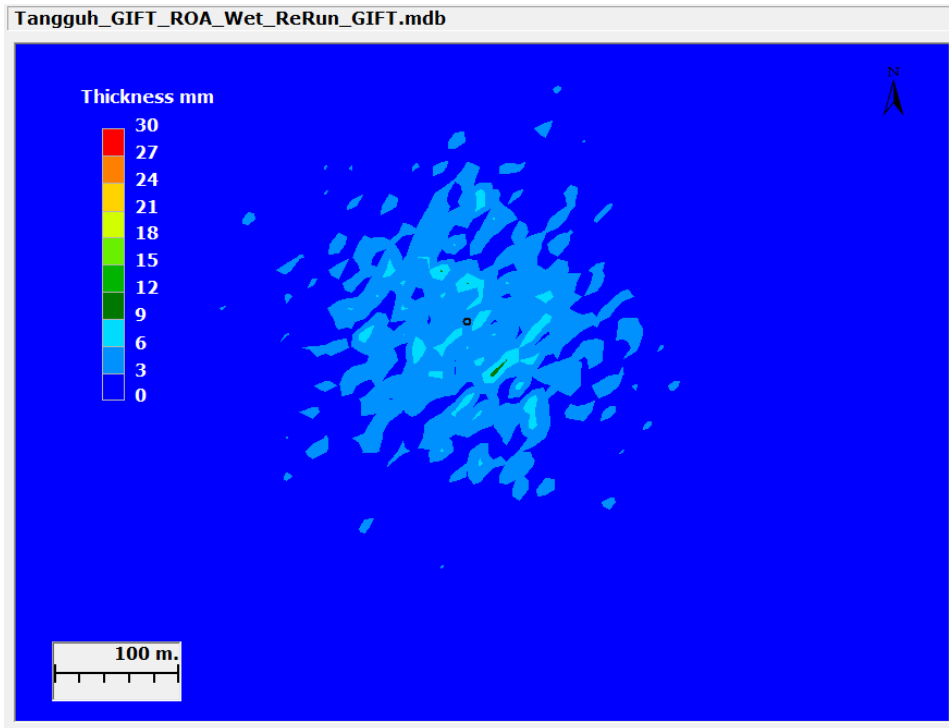


Figure 11.4 Maximum Sediment Thickness during Drilling at ROA under Wet Season Conditions

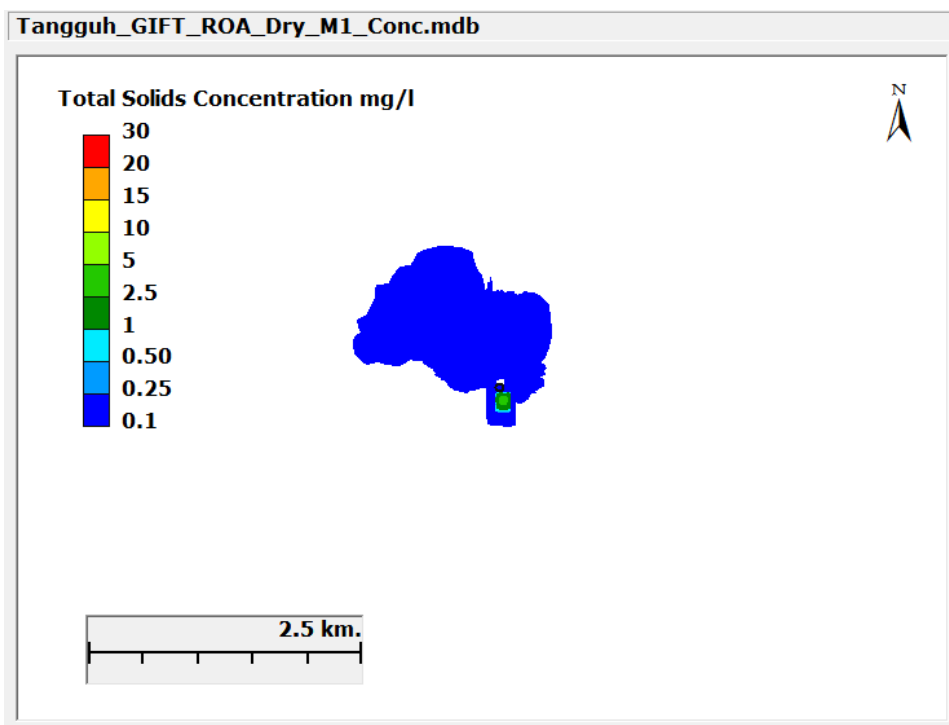


Figure 11.5 Maximum Incremental TSS Concentrations during Drilling at ROA under Dry Season Conditions

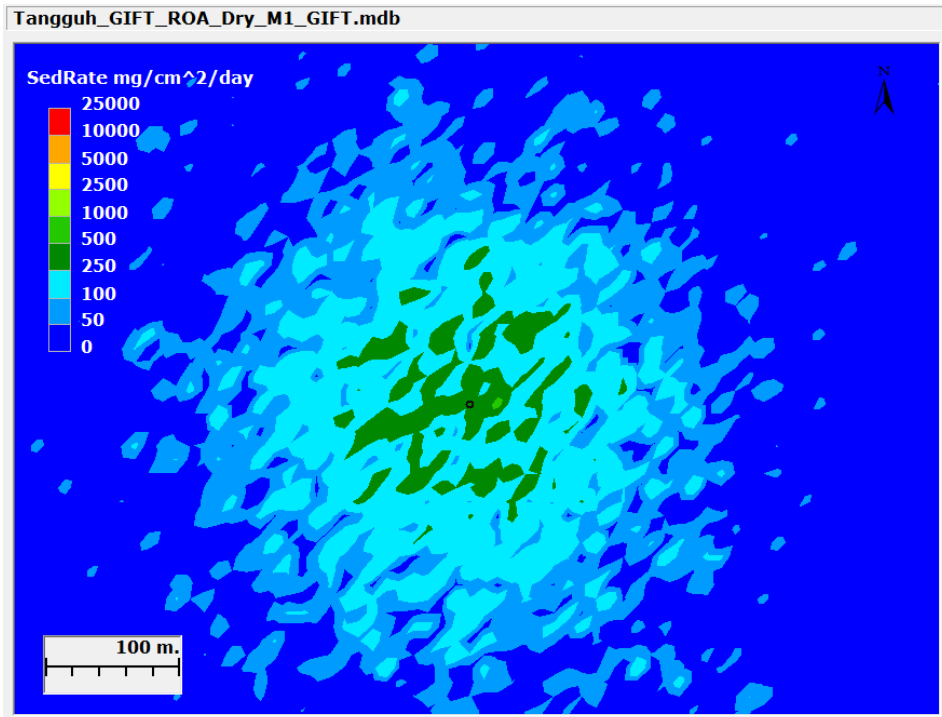


Figure 11.6 Maximum Sedimentation Rate during Drilling at ROA under Dry Season Conditions

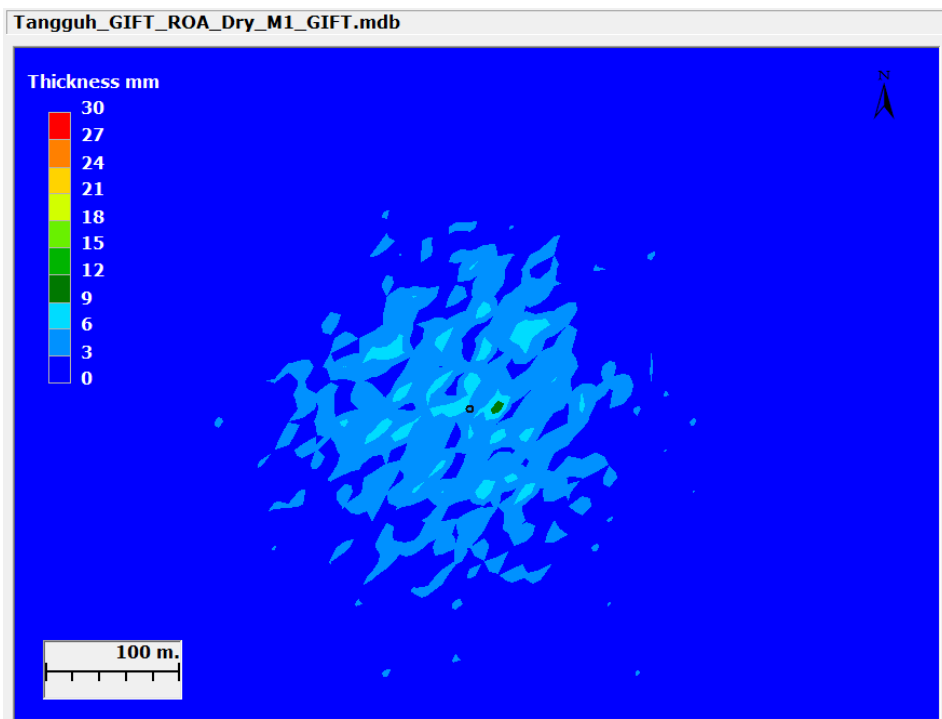


Figure 11.7 Maximum Sediment Thickness during Drilling at ROA under Dry Season Conditions

11.3.2 Drilling at TTB

In Scenario 4W, the maximum instantaneous incremental TSS value is 2.0 mg/L. A snapshot of the TSS plume during the drilling operation at a time and vertical location when the maximum TSS occurred is shown in **Figure 11.8**. The plume is elongated and oriented towards southeast due to the shoreline orientation. The TSS values drop quickly below 0.25 mg/L at distances greater than 250 m from the drilling location. The maximum instantaneous sedimentation rate was 937 mg/cm²-d and the maximum sediment thickness was 15 mm, both of which occurred at the drill site. **Figure 11.9** and **Figure 11.10** show the snapshot of sedimentation rate and sediment thickness at times when maximums occurred. Both sedimentation rate and sediment thickness drop to less than 100 mg/cm²-d and 3.0 mm, respectively, within 150 m from the drilling location. These results clearly show that the resulting TSS and sedimentation due to the drilling at TTB are a localized phenomenon, a result similar to that obtained at ROA.

In Scenario 4D, the incremental TSS, sedimentation rates and sediment thickness are comparable to its wet season counterpart. The maximum incremental TSS was predicted to be 7.2 mg/L, and maximum sedimentation rate and sediment thickness were predicted to be 799 mg/cm²-d and 14.9 mm, respectively. **Figure 11.11**, **Figure 11.12** and **Figure 11.13** show the maximum instantaneous incremental TSS plume, sedimentation rate and sediment thickness resulting from the drilling at TTB under wet seasons conditions.

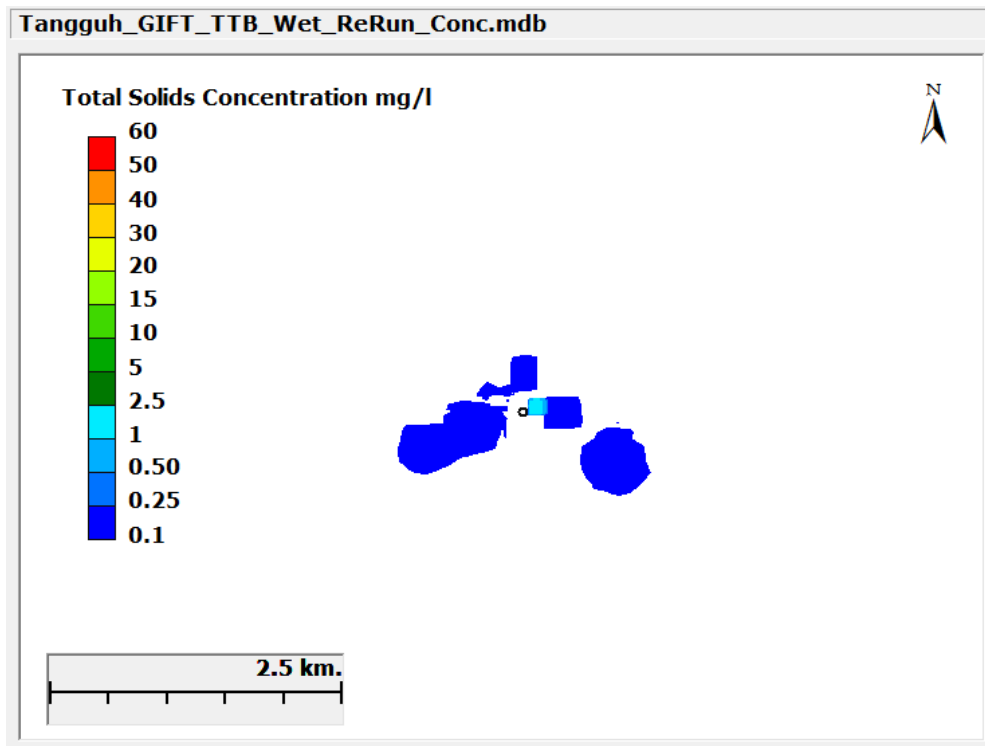


Figure 11.8 Maximum Incremental TSS Concentrations during Drilling at TTB under Wet Season Conditions

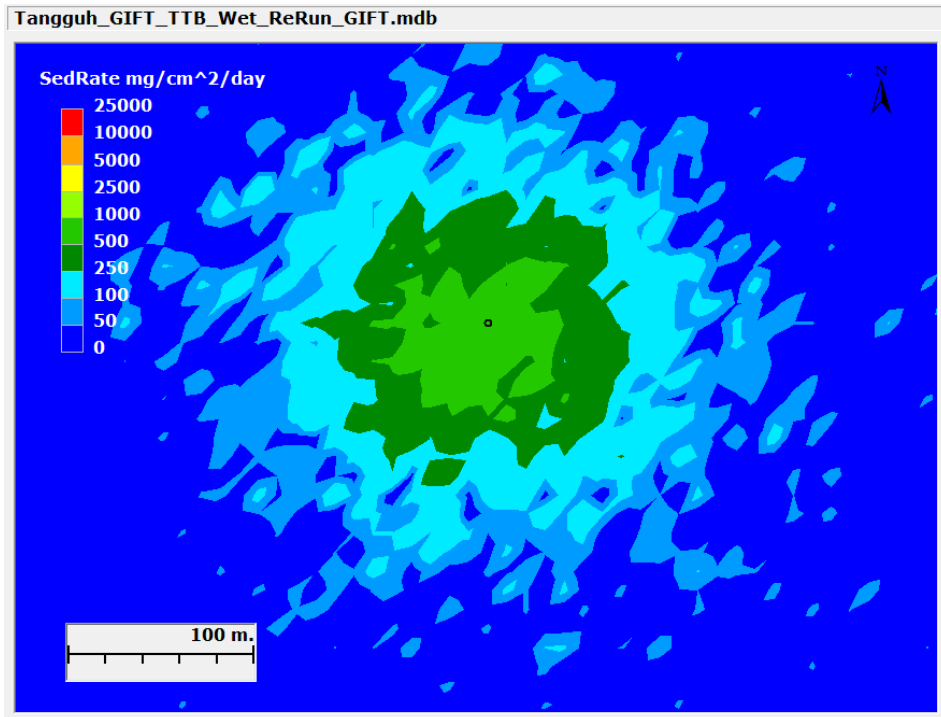


Figure 11.9 Maximum Sedimentation Rate during Drilling at TTB under Wet Season Conditions

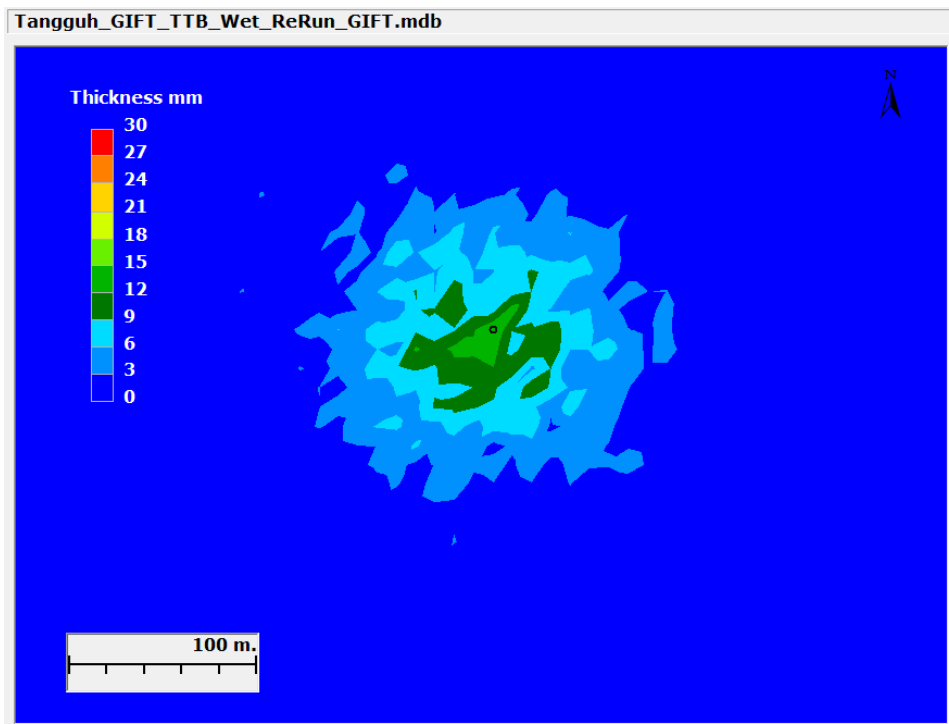


Figure 11.10 Maximum Sediment Thickness during Drilling at TTB under Wet Season Conditions

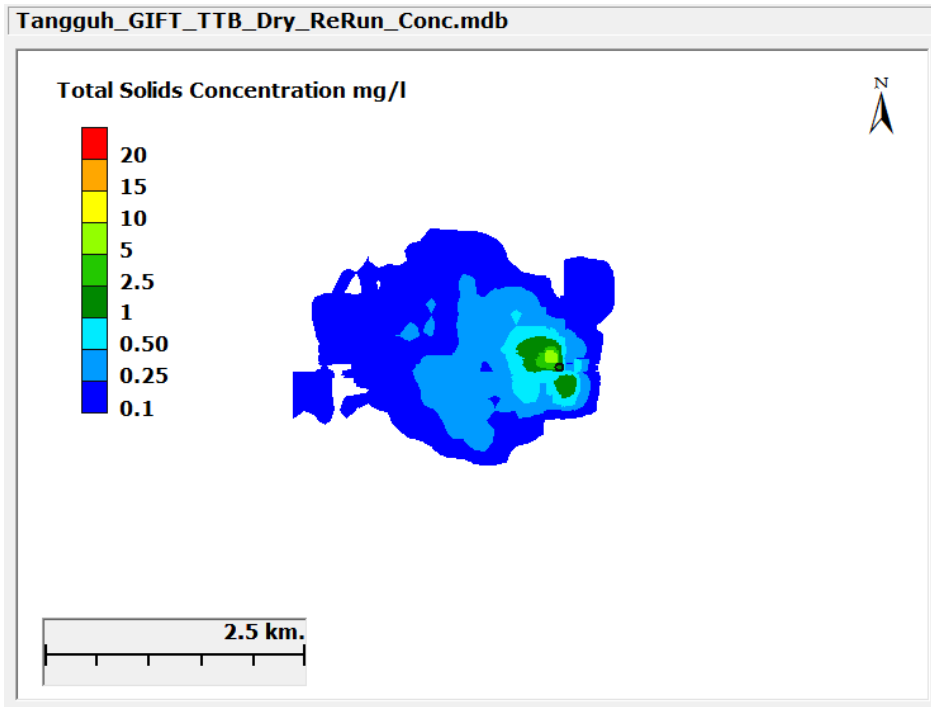


Figure 11.11 Maximum Incremental TSS Concentrations during Drilling at TTB under Dry Season Conditions

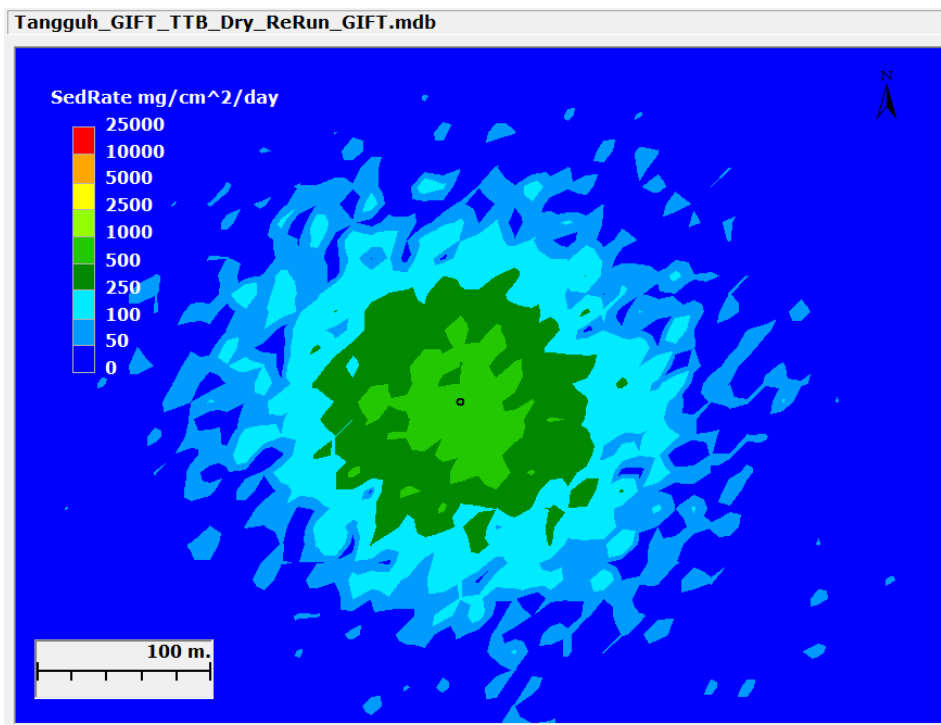


Figure 11.12 Maximum Sedimentation Rate during Drilling at TTB under Dry Season Conditions

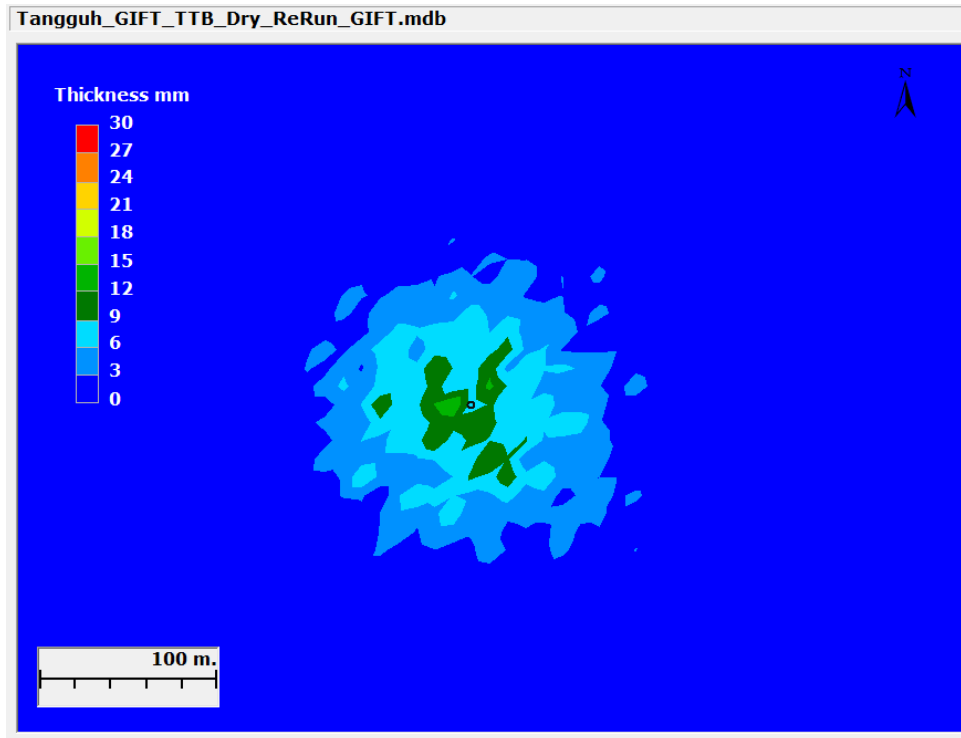


Figure 11.13 Maximum Sediment Thickness during Drilling at TTB under Dry Season Conditions

11.3.3 Drilling at WDA

In Scenario 5W, the maximum instantaneous incremental TSS value was calculated to be 6.8 mg/L. A snapshot of the TSS plume during the drilling operation at a time and vertical location when the maximum TSS occurred is shown in **Figure 11.14**. The plume is elongated and oriented towards northeast following the shoreline and the dominant tidal current direction. The TSS values drop quickly below 0.25 mg/L at distances greater than 1.5 km from the drilling location. The maximum instantaneous sedimentation rate was 382 mg/cm²-d and the maximum sediment thickness was 7.8 mm, both of which occurred at the drill site. The sedimentation rate and sediment thickness are lower than the values computed for ROA and TTB. They are lower because WDA is deeper (62 m deep) than ROA (36 m) and TTB (28 m). Larger waterbody depth allow the drill cuttings and muds to have to travel a greater vertical distance which results in additional plume spreading and dilution before sedimentation occurs. **Figure 11.15** and **Figure 11.16** show the snapshot of the sedimentation rate and sediment thickness at times when maximums occurred. Both sedimentation rate and sediment thickness drop to less than 100 mg/cm²-d and 3.0 mm, respectively, within 150 m from the drilling location.

In Scenario 5D, the incremental TSS, sedimentation rates and sediment thickness are comparable to its wet season counterpart. The maximum incremental TSS was predicted to be 5.9 mg/L, and maximum sedimentation rate and sediment thickness were predicted to be 344 mg/cm²-d and 6.3 mm, respectively. **Figure 11.17**, **Figure 11.18** and **Figure 11.19** show the maximum instantaneous incremental TSS plume, sedimentation rate and sediment thickness resulting from the drilling at WDA under wet seasons conditions.

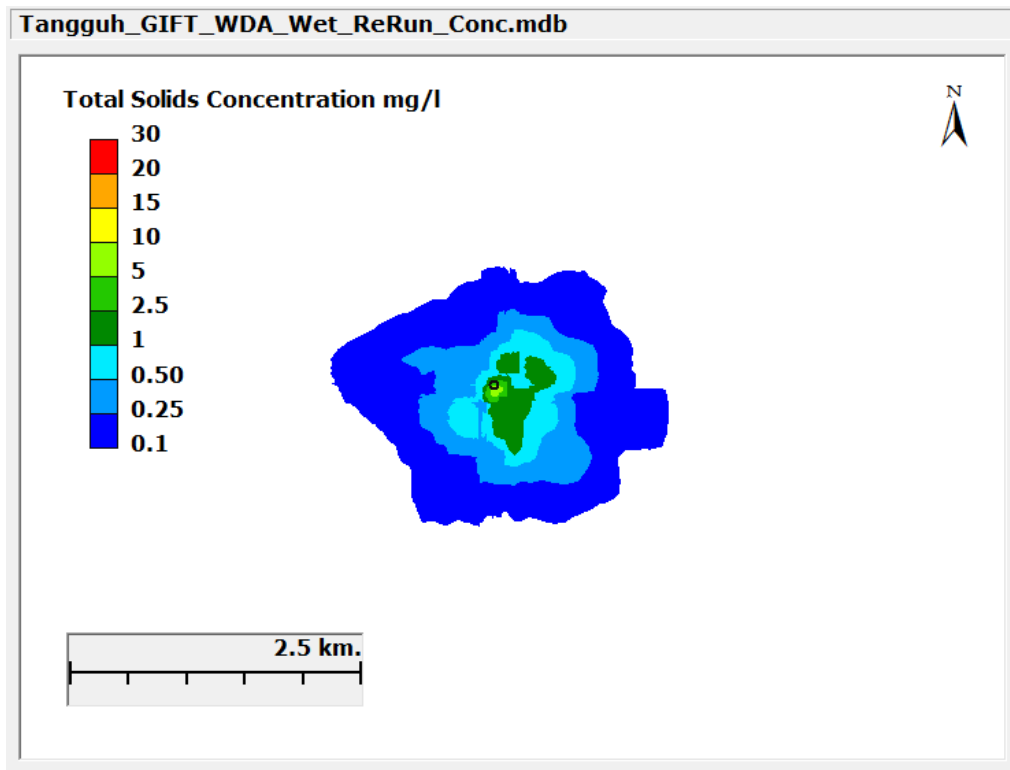


Figure 11.14 Maximum Incremental TSS Concentrations during Drilling at WDA under Wet Season Conditions

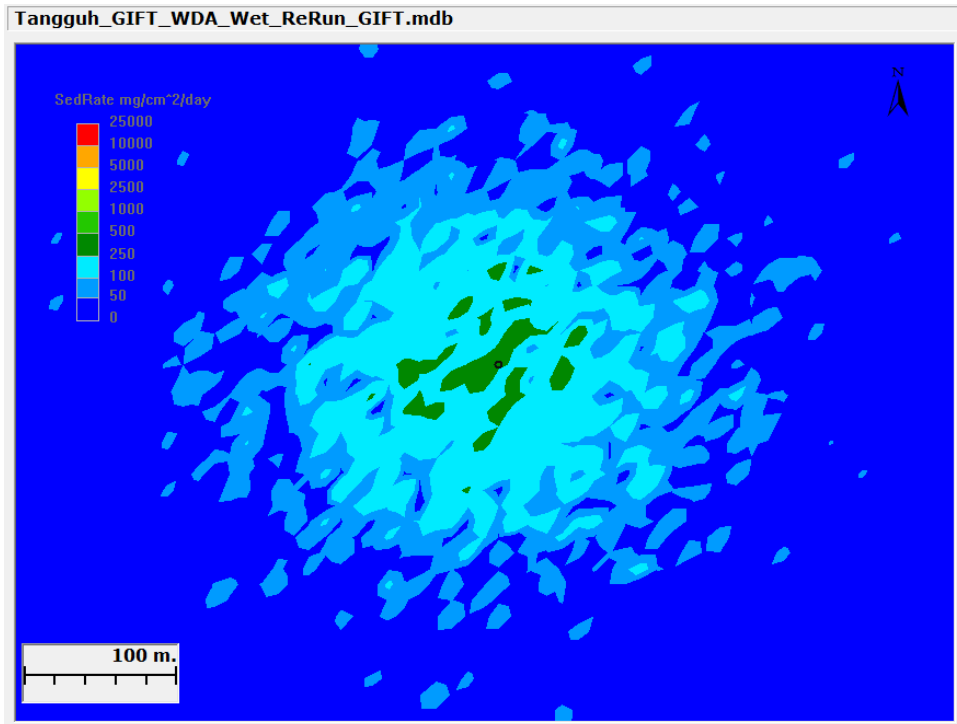


Figure 11.15 Maximum Sedimentation Rate during Drilling at WDA under Wet Season Conditions

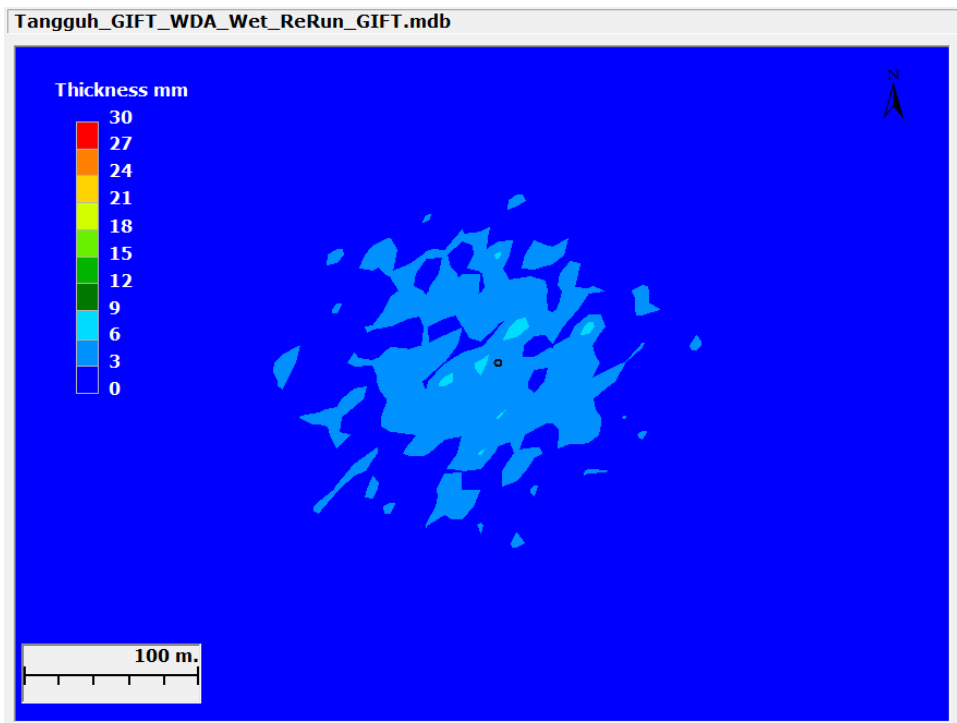


Figure 11.16 Maximum Sediment Thickness during Drilling at WDA under Wet Season Conditions

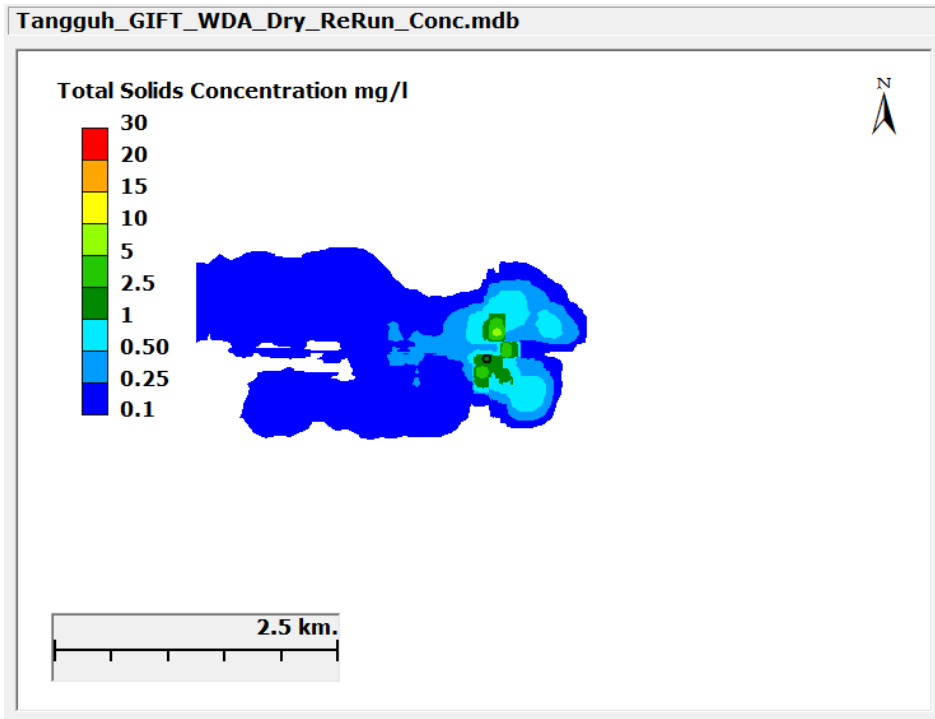


Figure 11.17 Maximum Incremental TSS Concentrations during Drilling at WDA under Dry Season Conditions

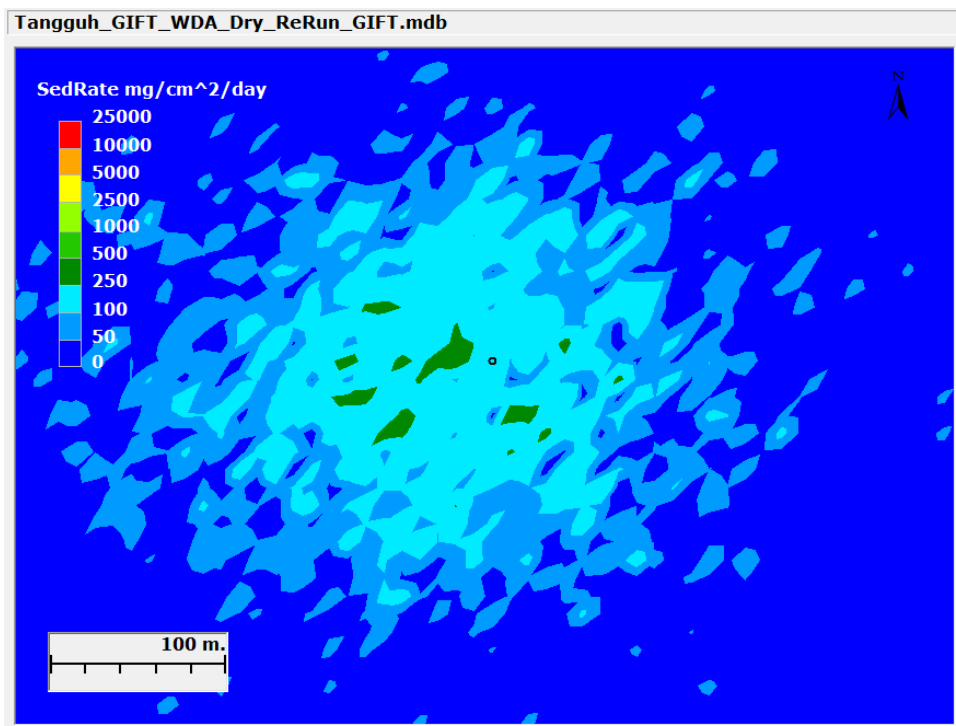


Figure 11.18 Maximum Sedimentation Rate during Drilling at WDA under Dry Season Conditions

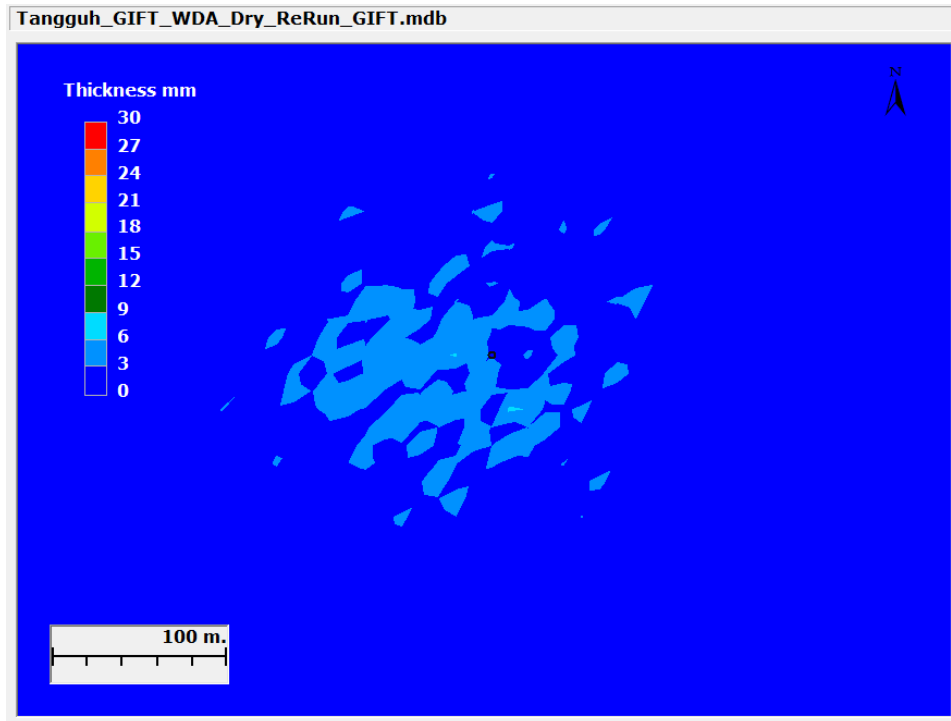


Figure 11.19 Maximum Sediment Thickness during Drilling at WDA under Dry Season Conditions

11.3.4 Drilling at UBA

In Scenario 6W, the maximum instantaneous incremental TSS value was calculated to be 21.1 mg/L. A snapshot of the TSS plume during the drilling operation at a time and vertical location when the maximum TSS occurred is shown in **Figure 11.20**. The plume is elongated and oriented towards northeast following the dominant tidal current direction. The TSS values drop quickly below 1 mg/L at distances greater than 1.0 km from the drilling location. The maximum instantaneous sedimentation rate was 1199 mg/cm²-d and the maximum sediment thickness was 21.2 mm, both of which occurred at the drill site. **Figure 11.21** and **Figure 11.22** show the snapshot of sedimentation rate and sediment thickness at times when maximums occurred. Both sedimentation rate and sediment thickness drop to less than 100 mg/cm²-d and 3.0 mm, respectively, within 150 m from the drilling location.

In Scenario 6D, the incremental TSS, sedimentation rates and sediment thickness are comparable to its wet season counterpart. The maximum incremental TSS was predicted to be 7.0 mg/L, and maximum sedimentation rate and sediment thickness were predicted to be 1021 mg/cm²-d and 17.2 mm, respectively. **Figure 11.23**, **Figure 11.24** and **Figure 11.25** show the maximum instantaneous incremental TSS plume, sedimentation rate and sediment thickness resulting from the drilling at UBA under wet seasons conditions.

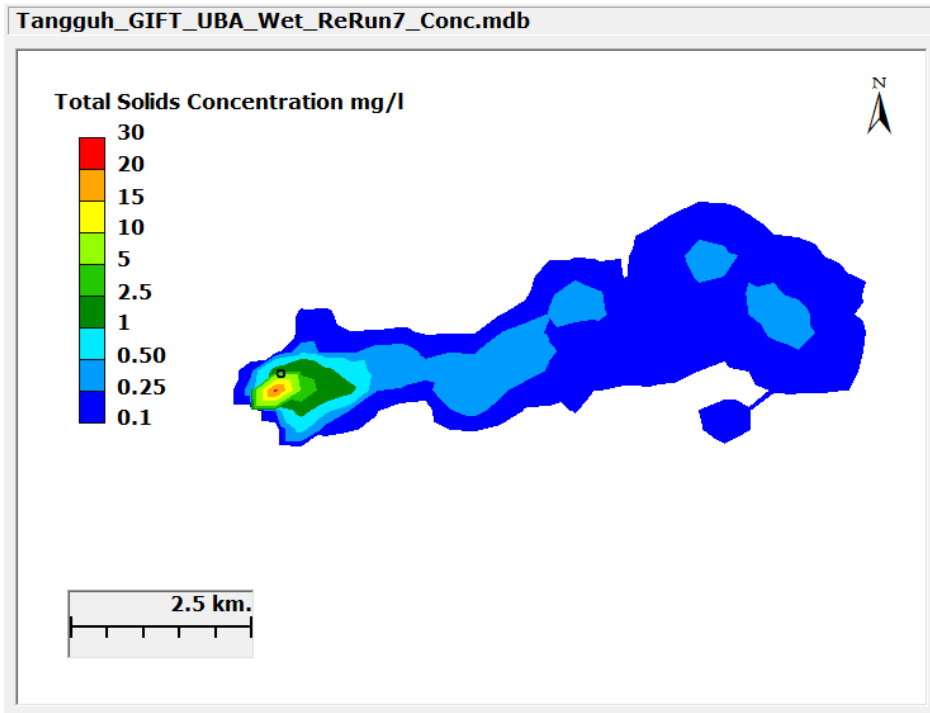


Figure 11.20 Maximum Incremental TSS Concentrations during Drilling at UBA under Wet Season Conditions

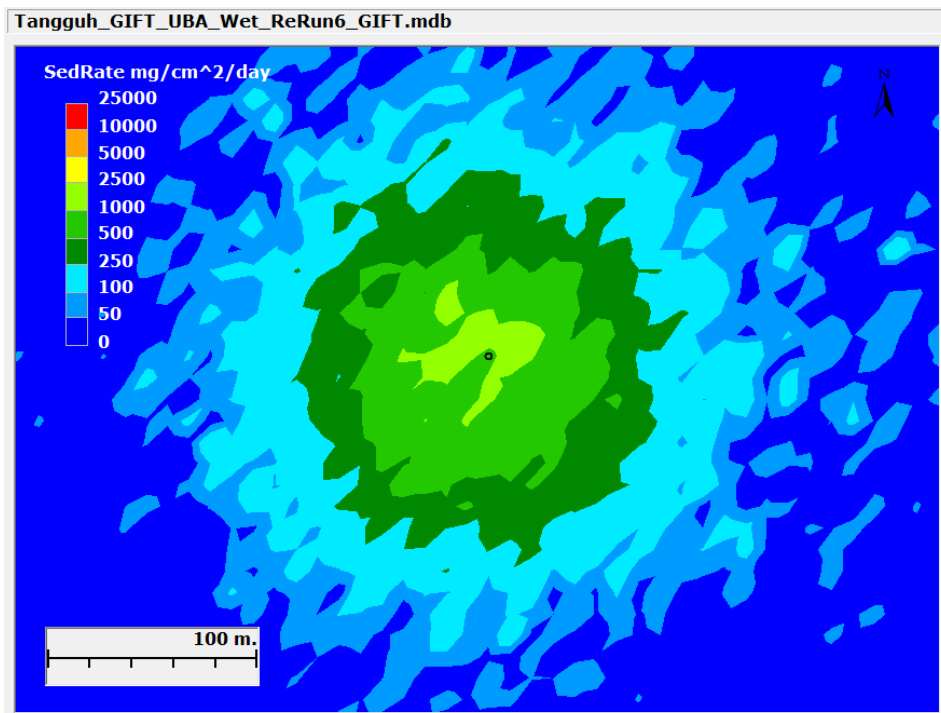


Figure 11.21 Maximum Sedimentation Rate during Drilling at UBA under Wet Season Conditions

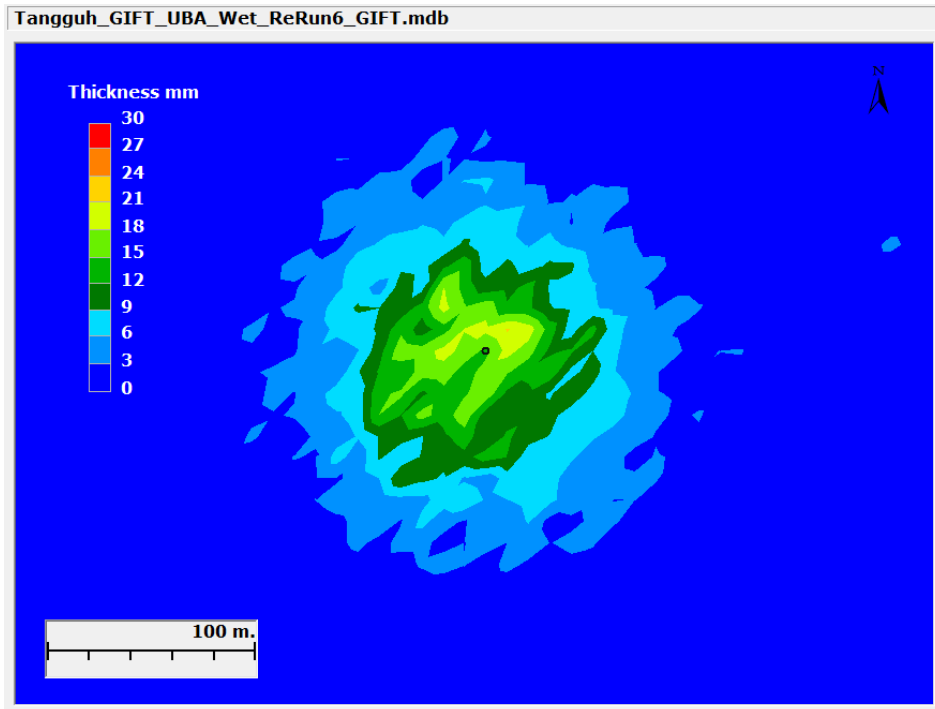


Figure 11.22 Maximum Sediment Thickness during Drilling at UBA under Wet Season Conditions

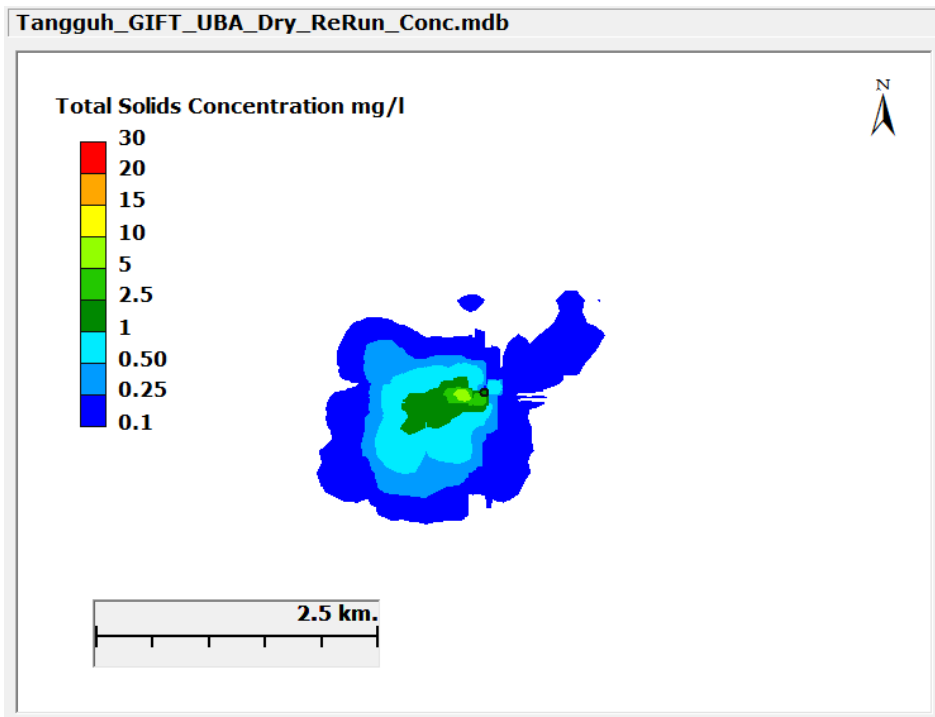


Figure 11.23 Maximum Incremental TSS Concentrations during Drilling at UBA under Dry Season Conditions

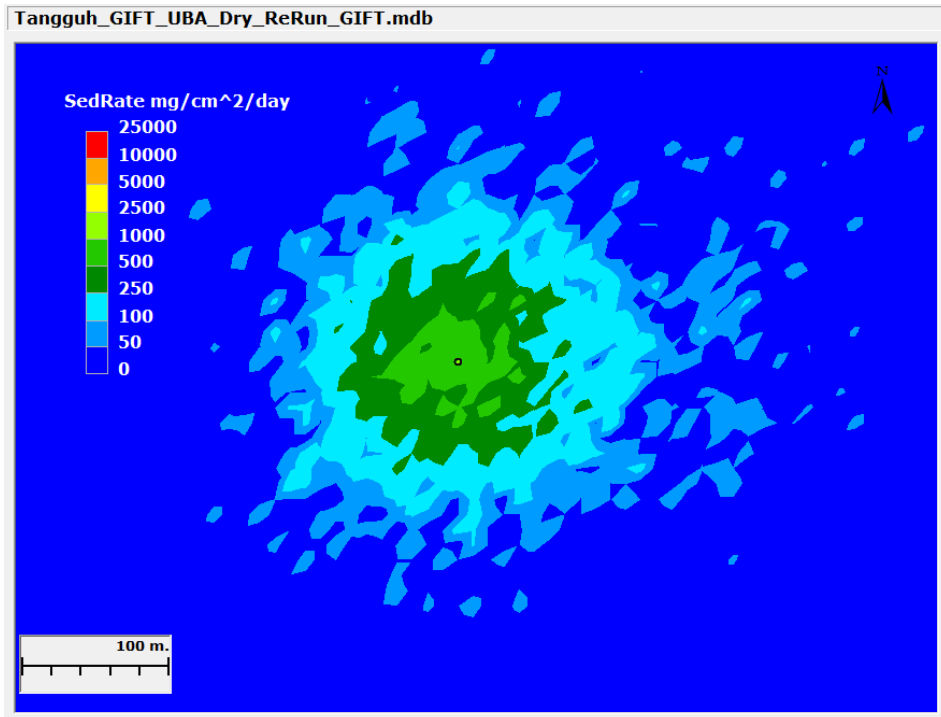


Figure 11.24 Maximum Sedimentation Rate during Drilling at UBA under Dry Season Conditions

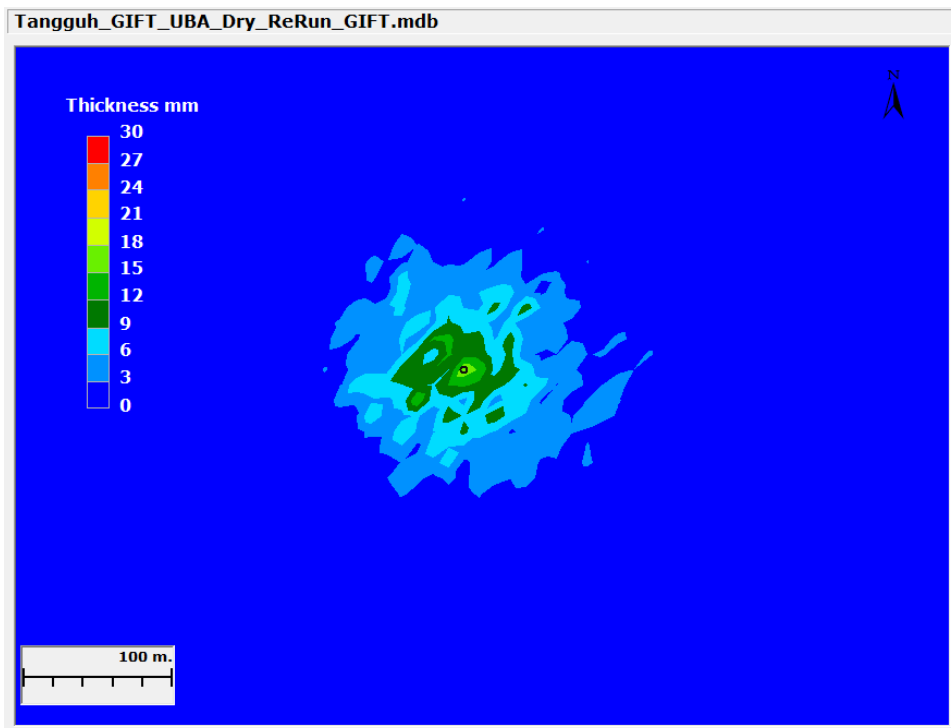


Figure 11.25 Maximum Sediment Thickness during Drilling at UBA under Dry Season Conditions

11.4 CONCLUSION

The results of the modelling and the plots presented indicate for all scenarios indicate that the deposition of drill cuttings and muds only occurs in the vicinity of the drilling location, mostly within 150 m. The results shown are maximums predicted during the drilling operation. These maximums only occur for a short period of time as the ambient conditions are transient and the plume quickly spreads or settles to the bottom. The TSS plume spreads farther than the extent where sedimentation is predicted. However, the maximum incremental TSS above ambient seawater quality is predicted to be only 21.1 mg/L. The maximum predicted extent of the 1.0 mg/L TSS threshold is 1.5 km. The maximum baseline TSS during dry period is 27 mg/L which when added to the incremental maximum TSS due to drilling results in a TSS value of 48.1 mg/L, well below the ambient seawater quality standard for mangrove-lined water bodies of 80 mg/L. Additionally, the maximum predicted TSS concentration is transient in nature and dissipates to a lower value quickly. **Figure 11.26** shows the TSS concentrations during the first four days of continuous release. These predicted results show that the proposed drilling operations are unlikely to result in exceedance of applicable environmental standards or create any significant impacts. **Table 11.5** shows the summary of resulting TSS above ambient seawater quality, sedimentation rate, sediment thickness, and area of depositional thickness exceeding 5 cm.

Table 11.5 Summary of Predicted Results for All Drilling Operation Scenarios

Scenario	Maximum TSS Above Ambient Seawater Quality (mg/L)	Maximum Sedimentation Rate (mg/cm ² -day)	Maximum Depositional Thickness (mm)	Area of Thickness > 5 cm (m ²)
3W	3.0	594	10.1	0
3D	3.0	608	11.4	0
4W	2.0	937	15.0	0
4D	7.2	799	14.9	0
5W	6.8	382	7.8	0
5D	5.9	344	6.3	0
6W	21.1	1199	21.2	0
6D	7.0	1021	17.2	0

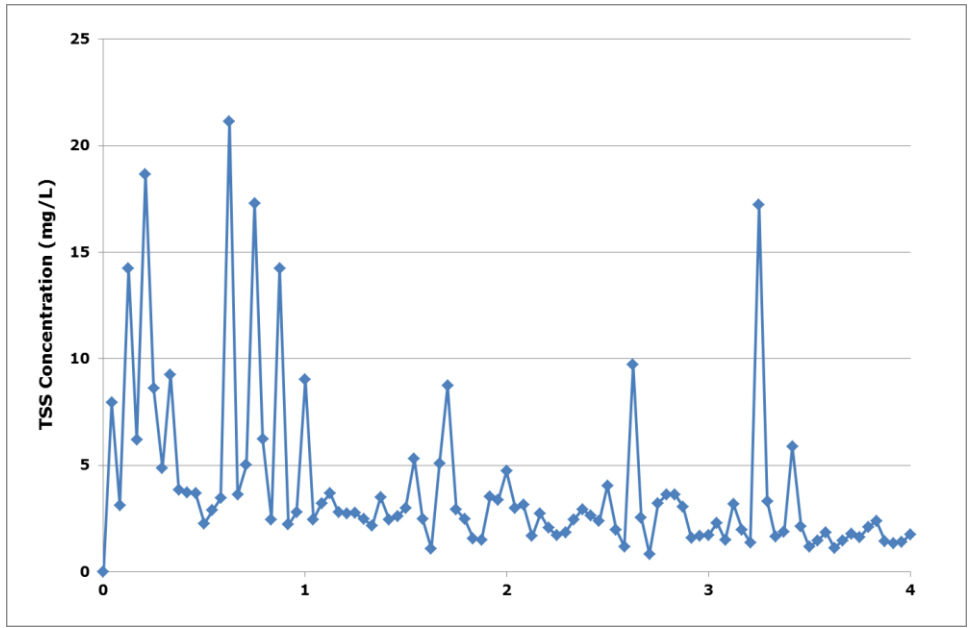


Figure 11.26 Maximum TSS Concentration at UBA under Wet Season Drilling

ACRONYMS

ADDAMS:	Automated Dredging and Disposal Alternatives Modelling System
BOF:	Bulk Offloading Facility
CAD:	Computer Aided Design
CORMIX:	Cornell Mixing Zone Model
FF:	Far Field
GEMSS:	Generalized Environmental Modelling System for Surfacewaters
GIFT:	Generalized Integrated Fate and Transport
HDM:	Hydrodynamic Module
LAT:	Lowest Astronomical Tide
LNG:	Liquefied Natural Gas
NF:	Near Field
OSU:	Oregon State University
OTPS:	OSU Tidal Prediction Software
RMSE:	Root Mean Square Error
STFATE:	Short Term Fate
TLNG:	Tangguh LNG Coordinates
TGU:	Turbidity Generation Unit
TSS:	Total Suspended Solids
TTB:	Teteruga Prospect - B
UDC:	User-Defined Constituent
USACE:	United States Army Corps of Engineers

Adenekan, A.E., V.S. Kolluru, and J.P. Smith. 2009. Transport and Fate of Chlorination By-Products Associated with Cooling Water Discharges. Proceedings of the 1st Annual Gas Processing Symposium pp. 1-13.

Alberson, S., A. Ahmed, M. Roberts, G. Pelletier, and V. Kolluru. 2009. "Model-Derived Hydrodynamics of Inlets in South Puget Sound." Proceedings of the Eleventh Annual Conference on Estuarine and Coastal Modeling. American Society of Civil Engineers. pp. 128-136, 2009.

Asian Development Bank, 2005. "Summary Environmental Impact Assessment: Tangguh LNG Project in Indonesia" June 2005.

BP 2013a. 2013-05-01 email from O. Dewanti

BP 2013b. 2013-06-11 email from O. Dewanti

Buchak, E. M. and J. E. Edinger. 1984. Generalized, Longitudinal-Vertical Hydrodynamics and Transport: Development, Programming and Applications. Prepared for U.S. Army Corps of Engineers Waterways Experiment Station, Vicksburg, Miss. Contract No. DACW39-84-M-1636. Prepared by J. E. Edinger Associates, Wayne, PA. Document No. 84-18-R. June.

Edinger J.E., J. Wu and E.M. Buchak. 1997. Hydrodynamic and Hydrothermal Analyses of the Once-through Cooling Water System at Hudson Generating Station. Prepared for Public Service Electric and Gas (PSE&G). Prepared by J. E. Edinger Associates, Inc., June 1997.

Edinger, J. E. and E. M. Buchak. 1980. Numerical Hydrodynamics of Estuaries in Estuarine and Wetland Processes with Emphasis on Modeling, (P. Hamilton and K. B. Macdonald, eds.). Plenum Press, New York, New York, pp. 115-146.

Edinger, J. E. and E. M. Buchak. 1980. Numerical Hydrodynamics of Estuaries in Estuarine and Wetland Processes with Emphasis on Modeling, (P. Hamilton and

Edinger, J. E. and E. M. Buchak. 1985. Numerical Waterbody Dynamics and Small Computers. Proceedings of ASCE 1985 Hydraulic Division Specialty Conference on Hydraulics and Hydrology in the Small Computer Age. American Society of Civil Engineers, Lake Buena Vista, FL. Aug. 13-16.

Edinger, J. E. and E. M. Buchak. 1995. Numerical Intermediate and Far Field Dilution Modelling. Journal Water, Air and Soil Pollution 83: 147-160, 1995. Kluwer Academic Publishers, The Netherlands.

Edinger, J. E., E. M. Buchak, and M. D. McGurk. 1994. *Analyzing Larval Distributions Using Hydrodynamic and Transport Modelling*. Estuarine and Coastal Modeling III. American Society of Civil Engineers, New York.

Edinger, J. E., V. S. Kolluru, 1999. "Implementation of Vertical Acceleration and Dispersion Terms in an Otherwise Hydrostatically Approximated Three-Dimensional Model." In Spaulding, M.L, H. L. Butler (eds.). *Proceedings of the 6th International Conference on Estuarine and Coastal Modeling*. pp. 1019 - 1034.

El-Dessouky, H. T. and H. M. Ettouney, 2002. *Fundamentals of Salt Water Desalination, Technology & Engineering*.

Ellis D., C. Heim, 1985. Submersible surveys of benthos near a turbidity cloud. *Marine Pollution Bulletin*, 16(5), 197-203.

Febbo E., V. Kolluru, S. Prakash, A. Adenekan. 2012. "Numerical Modeling of Thermal Plume and Residual Chlorine Fate in Coastal Waters of the Arabian Gulf". SPE-156813-PP. Presented at the SPE/APPEA International Conference on Health, Safety, and Environment in Oil and Gas Exploration and Production. Perth, Western Australia. 11-13 September 2012.

Fichera, M.J., V.S. Kolluru, C. Buahin, C. Daviau, and C.A. Reid. 2013. "Comprehensive Modeling Approach for EIA Studies in the Oil and Gas Industry." IAIA 2013.

Hawker D.W. & D.W. Connell. 1992. *Standards and Criteria for Pollution Control in Coral Reef Areas*. Chapter 7 of *Pollution in Tropical Aquatic Systems*. Connell DW & Hawler DW ed. CRC Press.

Hayes, D.F. and C.H. Je. 2000. *DREDGE Module User's Guide*. Department of Civil and Environmental Engineering. University of Utah. July 2000.

HGL and Aqua Terra. 1999. *Selection of Water Quality Components for Eutrophication-Related Total Maximum Daily Load Assessments*. Task 4: Documentation of Review and Evaluation of Eutrophication Models and Components EPA Contract Number 68-C6-0020 Work Assignment No. 2-04. Prepared by HydroGeoLogic, Inc. Herndon, VA 20170 and AQUA TERRA Consultants, Mountain View, CA. June.

ITB and BP, 2012. "Drilling Cutting and Mud Dispersion Simulation". January 2012.

Johnson, B. H., D.N. McComas, D.C. McVan and M.J. Trawle. 1994. Development and verification of numerical models for predicting the initial fate of dredged material disposed in open water. Report 1, Physical model tests of dredged material disposal from a split-hull barge and a multiple bin vessel. Draft Technical Report, U.S. Army Engineer Waterways Experiment Station, Vicksburg, MS.

Koh, R.C.Y. and Y.C. Chang. 1973. Mathematical model for barged ocean disposal of waste. Environmental Protection Technology Series EPA 660/2-73-029, U.S. Army Engineer Waterways Experiment Station, Vicksburg, MS.

Kolluru, V. S., E. M. Buchak and J. E. Edinger, 1998. "Integrated Model to Simulate the Transport and Fate of Mine Tailings in Deep Waters," in the Proceedings of the Tailings and Mine Waste '98 Conference, Fort Collins, Colorado, USA, January 26-29.

Kolluru, V. S., E. M. Buchak, J. Wu, 1999. "Use of Membrane Boundaries to Simulate Fixed and Floating Structures in GLLVHT." In Spaulding, M.L, H.L. Butler (eds.). Proceedings of the 6th International Conference on Estuarine and Coastal Modeling. pp. 485 - 500.

Kolluru, V. S., J. E. Edinger, E. M. Buchak and P. Brinkmann 2003. "Hydrodynamic Modeling of Coastal LNG Cooling Water Discharge." Journal of Energy Engineering. Vol. 129, No. 1, April 1, 2003. pp 16 - 31.

Kolluru, V.S. and Mike Fichera, 2003. "Development and Application of Combined 1-D and 3-D Modeling System for TMDL Studies." Proceedings of the Eighth International Conference on Estuarine and Coastal Modeling. American Society of Civil Engineers. pp. 108-127, 2003.

Kolluru, V.S. and S. Prakash. 2012. "Source Water Protection: Protecting our drinking waters". India Water Week 2012. April 10-14. New Delhi, India.

Kolluru, V.S., E. Buchak, J.E. Edinger, and P.E. Brinkmann. 2005. "Three-Dimensional Thermal Modeling of the RasGas Cooling Water Outfall." 2005.

Kolluru, V.S., M. J. Fichera, and S. Prakash. 2006. SETAC.

Kolluru, V.S., S. Prakash and E. Febbo. 2012. "Modeling the Fate and Transport of Residual Chlorine and Chlorine By-Products (CBP) in Coastal Waters of the Arabian Gulf". The Sixth International Conference on Environmental Science and Technology 2012. June 25-29. Houston, Texas, USA.

Kolluru, V.S., S. R. Chitikela and M. J. Fichera. 2009. "Watershed Water Quality Attainment Using TMDL - A Delaware USA Review." International Conference "Water, Environment, Energy and Society" (WEES-2009), New Delhi. 12-16 January.

Kruk, M., M. Kempa, T. Tjomsland, D. Durand. 2011. "Vistula Water Quality Modeling." pp. 165-180.

Mapstone B.D., J. H. Choat, R. L. Cumming and W. G. Oxley. 1989. The fringing reefs of Magnetic Island: benthic biota and sedimentation - a baseline study. A report to the Great Barrier Reef Marine Park Authority.

Marine Life Information Network (MarLIN). 2011. Benchmarks for the Assessment of Sensitivity and Recoverability. The Marine Biological Association of the UK, Citadel Hill, Plymouth, Devon, U.K. URL: <http://www.marlin.ac.uk/sensitivitybenchmarks.php> (Accessed April 2011).

Meteorological Data Collection Program, 2000

Palermo, M. R., P. R. Schroeder, T. J. Estes, N. R. Francingues, 2008. "Technical Guidelines for Environmental Dredging of Contaminated Sediments". ADA488763.

Pastorok, R.A. and G.R. Bilyard. 1985. Effects of sewage pollution on coral-reef communities. *Marine Ecology Progress Series* 21: 175-189.

Pertamina, 2002. "Tanggung LNG, ANDAL: Integrated ANDAL Activities Gas Exploitation, Gas Transmission, LNG Plant, Sea Port, Airfield, and Resettlement, Tangguh LNG Project, Manokwari, Sorong, and Fak-Fak Regencies, Papua Province ". October 2002.

Prakash, S. and V.S. Kolluru. 2006. "Implementation of higher order transport schemes with explicit and implicit formulations in a 3-D hydrodynamic and transport model." Published in the 7th International Conference on Hydrosience and Engineering (ICHE 2006), Sep 10 - Sep 13, Philadelphia, USA

Prakash, S., J.A. Vandenberg and E. Buchak. 2011. "*The Oil Sands Pit Lake Model - Sediment Diagenesis Module.*" MODSIM 2011. Modelling and Simulation Society of Australia and New Zealand, December 12-16, 2011. Perth, Australia.

Prakash, S., J.A. Vandenberg and E. Buchak. 2012. "*CEMA Oil Sands Pit Lake Model.*" CONRAD 2012 Water Conference. April 20-22. Edmonton, Alberta.

Prakash, S., V. S. Kolluru, and P. Tutton. 2012. "*Semi-Lagrangian Approach to Studying Grassing Issue on a Nuclear Power Plant Cooling Water Intake.*" Proceedings of the 10th Intl. Conf.on Hydrosience & Engineering, Nov. 4-7, 2012, Orlando, Florida, U.S.A.

PT Calmarine, 2000. "Meteorological Data Collection Program (0N-4) Report (Part-1) Tanah Merah". 900-SDY-151. 12 April 2000.

Schroeder, P.R. and M.R. Palermo. 1990. Automated dredging and disposal alternatives management system, User's Guide. Technical Note EEDP-06- 12, U.S. Army Engineer Waterways Experiment Station, Vicksburg, MS.

U. S. Army Engineer Waterways Experiment Station, Environmental Laboratory, Hydraulics Laboratory. 1986. CE-QUAL-W2: A Numerical Two-Dimensional, Laterally Averaged Model of Hydrodynamics and Water Quality; User's Manual. Instruction Report E-86-5. Prepared for Department of the Army, U.S. Army Corps of Engineers, Washington, DC. Final Report. August.

Vandenberg, J.A., S. Prakash, N. Lauzon and K. Salzsauler. 2011. *"Use of water quality models for design and evaluation of pit lakes."* Australian Center for Geomechanics. Mine Pit Lakes: Closure and Management. Page 63-81.

Water Environment Federation. 2001. Water Quality Models: A Survey and Assessment. Order No.: D13209WW (Electronic Media).